MIMO/Beamforming for Multicast services in 4G scenario

Emanuele De Carolis - Quentin Berder

Supervisor:
Persefoni Kyritsi - Haibo Wang

9th and 10th semester
September 2007 to June 2008

THIS PAGE IS INTENTIONALLY LEFT BLANK

Contents

THIS PAGE IS INTENTIONALLY LEFT BLANK

Ålborg university
E-Studyboard
Mobile Communications 9^{th} and 10^{th} semesters

TITLE:

MIMO/Beamforming for Multicast services in 4G scenario

THEME:

Communication, Signals and Systems

PROJECT PERIOD:

3^{rd} September 2007 - 4^{th} June 2008

PROJECT GROUP:

08-gr-1111

GROUP MEMBERS:

Berder Quentin
De Carolis Emanuele

SUPERVISORS:

Kyristi Persefoni
Wang Haibo

ABSTRACT:

Broadband and wireless are the most common adoption in the communication market during the past ten years. Users want to be able to access to multimedia applications, data and voice while still using wireless mobility. To do so a high data rate is required. Moreover, multicasting is a tool used in networking which allows a selected group of users to receive the same information, and it is particularly useful for multimedia traffic. Obviously the research on the possible techniques to obtain such connection is a challenging topic in the field of mobile communication. The most analyzed techniques to achieve this optimization have been beamforming and multiple-input-multiple-output. Furthermore in order to properly handle such applications and services it is necessary to choose a suitable technology. WiMAX was primarily designed for this reason: to deliver different types of data in both fixed and mobile environments. Mobile WiMAX is an amendment this technology with improved performance and capacity while adding full mobility. This report will present beamforming and MIMO, simulate them in a realistic environment fitting for a Mobile WiMAX transmission and conclude on their efficiency in optimizing the connection between a base station and a mutlicast group of users.

THIS PAGE IS INTENTIONALLY LEFT BLANK

Acknowledgement

We would like to express our gratitude to our supervisors Persefoni Kyristi and Haibo Wang for their help throughout this project, for their constant or complementary availability. Also we would like to thanks all the people who directly and indirectly helped us in the different steps of this project during our last year.

I, Quentin Berder, will also like to express all my gratitude to my mother Gisèle Berder and my father Yves Berder that permit me to be who i am today. I will also thanks my brothers Stefan and Ronan Berder for their support and acceptance throughout the years. Kathrin Olesen that supports my sleepless nights of work. My flat mates Yamil Hasbun and Alex Kalinke for the help brought in my daily life. Milan for taking care of my health and shape. My friends to bring me the fun and joy needed. And finally Georges for her wild but true behavior.

I, Emanuele De Carolis, would like to thanks my wonderful family because is thanks to them that I was able to reach this point of my life and that I grew up the way I did. Germana, because she supported me in every single moment of the last years. Thanks also to all my old friends which kept on growing with me though the distance, and thanks to the new friends which were able, in a small period of time, to give me something important for my personal knowledge and my personality.

THIS PAGE IS INTENTIONALLY LEFT BLANK

Chapter 1

Introduction

In the telecommunication market most of the traffic is changing from speech-oriented communication to multimedia communications. Thus the actual communication system 3G needs to evolve to be able to handle this change. The next generation of communication system 4G can be defined as the total convergence of wireless mobile and wireless access communications that permits to handle the various multimedia applications. Furthermore, nowadays most of the users equipped with a mobile device such as "*iPhone*" or "*Blackberry*" want to enjoy Internet and all its multimedia applications. However those type of applications, such as high-definition television, require a higher data rate than the one needed by standard data or voice traffic. In order to optimize the transmission to achieve a higher data rate, several techniques can be applied either at the transmitter or receiver side. Nowadays the most challenging techniques are beamforming and multiple-inputs-multiple-outputs. Moreover, the multimedia traffic is usually requesting multicast services for a better optimization of the resources *i.e.* the users are served as part of a group instead as a unique user. The WiMAX is offering all those requirements and has been chosen for the evaluation of this report.

This project analyzes a cell in which a number of users within a group will be modelized. Beamforming and multiple-inputs-multiple-outputs techniques will be applied to this group. All the effects inherit in this type of environment such as obstacles, buildings or trees, users' positions and user's movements, will be simulated in order to obtain a simulation as close as possible to the reality. Several techniques for beamforming and multiple-inputs-multiple-outputs will be analyzed and their interactions discussed. Other aspects of the problem, such as the size of the cell, the number of users within the group or the dropping of the user, will be investigated and compared in term of efficiency for the multicast group.

This report will give an overview of the theory needed to understand the problem and its various parameters. The problem is to delimit and design our beamforming and MIMO solutions in a multicast model for an implementation purpose in MATLAB®. Finally the simulation are described and the results analyzed. A brief description of the different parts of this report is given next page.

1.1 Project questions

A first analysis of the project topic leads us to the following questions:

- What is the definition of the 4^{th} generation technologies?
- What are the advantages of the multi-carrier transmission and the specificities of the orthogonal frequency division multiplexing?
- What is Multicast? Which are the specifications for the wireless Multicast?

Taking into account this knowledge it is possible to focus on the technology:

- How can beamforming and MIMO improve the transmission?
- What are the characteristics of mobile WiMAX?
- What are the characteristics of the channel model?

The understanding of those technologies leads us to the main technical questions:

- What are the possible beamforming and MIMO solutions to optimize the connection for multicast services?
- What technology between beamforming and MIMO is achieving the best performance in our delimitations?

1.2 Report outline

This report is divided in the following parts:

- **Introduction:** this chapter is introducing our work, an exhaustive list of the questions treated in this project and the outline of the report.
- **Theory:** this chapter is presenting the necessary theoretical aspects of this project such as multicast, beamforming, MIMO, the wireless model or the technology used are presented.
- **Delimitation:** this chapter is stating the project goal and the target metric. It also submitting the choice of the values used for the simulation. Furthermore the performance metrics and the project aim are presented.
- **Model design:** this chapter is presenting the mathematical models used to implement the beamforming algorithms, the MIMO techniques and the channel model.
- **Simulation and Results:** this chapter introduces our simulation and the verifications of the already existing and implemented MIMO and beamforming algorithms. Besides it introduces our results taking into account our contributions.
- **Conclusion and future work:** this chapter concludes the project and proposes some subjects that can be investigated for a future work.
- **Appendix:** this chapter contains the appendix necessary for this project such as the needed OFDM background, the test of the channel model or the mobility model.

Chapter 2

Theory

This chapter presents the theory background necessary for this project. Firstly a description of the 4G technology will be provided , which leads us to a description of the wireless channel and its components. Then the OFDM technology and its principal characteristics will be introduced before acquainting the notion of multicasting. Next the beamforming and MIMO models are submitted and the WiMAX technology and its features described. Finally a description of the chosen channel model is proposed.

2.1 4G technologies

The acronym 4G stands for Fourth-Generation Communications System (4G), which is an updating of the already existing 3G (Third- Generation Communication System). In the mobile communications market, the number of subscribers has increased much faster than predicted, especially for the terrestrial use, and the majority of the traffic is changing from speech-oriented communications to multimedia communications [1]. There is no formal definition regarding the features of 4G, but the aim of this system is to provide the total convergence of wireless mobile and wireless access communications. A system where forthcoming applications like wireless broadband access, Multimedia Messaging Service, video chat, mobile TV, High definition TV content, digital video broadcasting (DVB), minimal service like voice and data can be served to any user using a higher data rate compared to the previous generation.

4G is based on two main concepts. Some features are based on the old 3G system and they are an EVOLUTION of it. Other aspects involves new approaches to wireless mobile and they are more REVOLUTIONARY (e.g., OFDM technology), looking further providing wide band multimedia services.

The convergence of broadband wireless system is, nowadays, the most important topic related to the wireless industry. Such kind of system will be extremely important in developing countries for the improvement of the wireless communication infrastructures.

2.1.1 From 1G to 4G

Within thirty years a big step in communication systems has been done. Going from the First Generation (1G) to the fourth made possible more and more services available on the mobile phones. This evolution has been obtained due to the digitalization of the information and the updating of the used technology.

The first Generation was implemented around 1970s and followed the invention of the microprocessors and it was launched in United States as First Generation of mobile system. It was based on frequency division multiple access (FDMA) technology and it was a system which allowed users to make voice call within one country. No data traffic was available yet, the voice itself was the main traffic.

At the end of 1980s the Second Generation (2G) was developed. Digitalization of the control link between mobile and base station and digitalization of the voice signal were the most advanced characteristics. The new system provided better quality and higher capacity. Global system for mobile communications (GSM) and general packet radio service (GPRS) were the services available and time division multiple access (TDMA) the technology used.

The first Third Generation (3G) network was deployed in Japan in 2001. The systems in this standard are an update from 2G, going from circuit switched nodes to packet oriented nodes. The advantages of 3G systems are mainly the increase of available bandwidth per single user and the possibility to have multimedia entertainment services on the mobile phones. A lot of technology are being standardized for the 3G system all around the World, but the most important change comparing with the 2G is the use of code division multiple access (CDMA) as access technology. Regarding the 3G, some of the services have been standardized are enhanced data rates for global evolution (EDGE) and universal mobile telecommunications system (UMTS).

Looking forward for the 4G Communication System, its services are the advanced version of the 3G services. The 4G services are expected to be broadband, with large capacity, with high-speed transmission and to provide optimum services everywhere and anywhere. Going from 3G to 4G the infrastructure will have only packet switched traffic also named as all-IP. Voice, data and multimedia application all on the same Communication System.

The 4G systems are OFDM-based system, which is a technology that increase the system capacity and the spectrum utilization in order to have a wide band communication. The technologies which are considered to be pre-4G are WiMax and 3GPP LTE [2][3].

2.2 Wireless channel

A wireless transmission is a link between devices in which no wires is connecting the various devices. If a device is fixed it is called Base Station (BS) and if a device is moving it is called Mobile Station (MS).

The antenna of the MS is usually close to the ground, at the height of the user, and often not in the line-of-sight (LOS) of the BS due to obstacles (shadowing). It is also possible to notice the presence of propagation phenomena such as diffraction, absorption and diffusion. Moreover a lot of ways for the signal to arrive at the receiver antenna which brings the multipath phenomenon. Those occurrences are shown on picture 2.1.

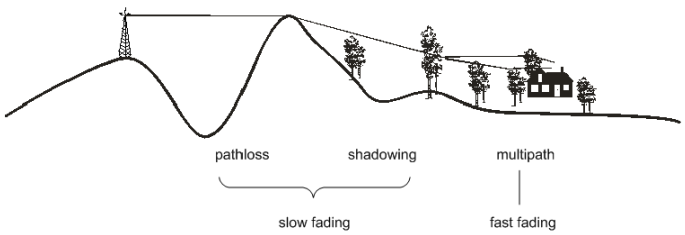

Figure 2.1: Channel model

2.2.1 Path loss

The path loss is the amount of energy of the signal that gets lost during the transmission through a channel. It is due to many effects such as diffraction, reflection, refraction, absorption and free-space loss. Furthermore the path loss depends of the environment (rural, urban, suburban or heavy urban), the distance between the BS and the MS, the height and location of the antennas and the propagation medium (dry or humid air).

To describe the behavior of the channel a channel model is used and depends on the environment. The most common models are the Okumura-Hata model, the COST-231 Hata or the Lee's propagation model [4]. The path-loss equation will be analyzed in a further chapter depending on the channel model chosen.

2.2.2 Shadow fading

Shadow fading or shadowing is a phenomenon that occurs when the wireless signals are obstructed by large obstacles such as buildings, trees, hills, etc. These obstacles cause attenuation and reflection of the signal. The level of shadowing depends of the frequency of the signal, the structure of the obstacle and the size of the object.

The common characterization for the shadow fading is a log-normal distribution [5].

2.2.3 Multipath fading

Multipath, also called small scale fading, is due to the reflection of wireless signals by objects in the way between the transmitter and the receiver. Due to the fact that all the signals are following different paths to reach the receiver, the signals arrive at the receiver with different phase. The resulting signal is randomly suffering of fading as the reflections constructively or destructively add. The fading depends on the relative power and phases of the various signals that are reaching the receiver. A common method to describe the multipath effect is to use a Rayleigh distribution.

The time delay spread of the signal can have two consequences depending on the bandwidth of the symbol: flat fading or frequency selective fading. Before going further it is important to define the coherence bandwidth. If the frequency separation of two frequency components $\Delta f = |f_2 - f_1|$ is greater than B_c, the fading of those frequencies is said to be uncorrelated. The correlation function is expressed as

$$\begin{aligned} R_H(f, f+\Delta f) &= \frac{cov(H(f),H(f+\Delta f))}{\sigma_{H(f)}\sigma_{H(f+\Delta f)}} \\ &= \frac{E[(H(f)-\mu_{H(f)})(H(f+\Delta f)-\mu_{H(f+\Delta f)})]}{\sigma_{H(f)}\sigma_{H(f+\Delta f)}} \end{aligned} \tag{2.1}$$

with $\mu_{H(f)}$ the expected value of $H(f)$, $\sigma_{H(f)}$ the standard deviation and $H(f)$ the Fourier transform of the channel impulse response $h(t)$ defined as

$$H(f) = \int_{-\infty}^{+\infty} h(\tau) e^{-j2\pi f\tau} d\tau \tag{2.2}$$

Assuming $\mu_{H(f)} = E[H(f)]$ and $\sigma^2_{H(f)} = E[H(f)^2] - E[H(f)]^2$, equation 2.1 can be rewritten as

$$R_H(f, f+\Delta f) = \frac{E[H(f)H^*(f+\Delta f)] - E[H(f)]E[H^*(f+\Delta f)]}{\sqrt{E[H(f)^2] - E[H(f)]^2}\sqrt{E[H(f+\Delta f)^2] - E[H(f+\Delta f)]^2}} \tag{2.3}$$

Considering $H(f)$ normalized *i.e.* $\mu_{H(f)} = 0$ and $\sigma_{H(f)} = 1$, equation 2.3 becomes

$$R_H(f, f+\Delta f) = E[H(f)H^*(f+\Delta f)] \tag{2.4}$$

It is possible to expressed the frequency correlation function as [6]

$$R_H(\Delta f) = \int_{-\infty}^{+\infty} P_h(\tau) e^{-j2\pi f\tau} d\tau \tag{2.5}$$

where $P_h(\tau)$ is the delay power density.

The coherence bandwidth B_c is defined as the smallest value of Δf for which $R_H(\Delta f)$ equals some suitable correlation coefficient, *e.g.* 0.5 or 0.9. For example, if this threshold is equal to 0.9, it is possible to approximate B_c by

$$B_c \approx \frac{1}{50\sigma_\tau} \tag{2.6}$$

with σ_τ the root mean square (RMS) delay spread equal to

$$\sigma_\tau = \sqrt{\overline{\tau}^2 - (\overline{\tau})^2} \tag{2.7}$$

with $\overline{\tau}$ the mean excess delay expressed as

$$\overline{\tau} = \frac{\sum_k P(\tau_k)\tau_k}{\sum_k P(\tau_k)} \tag{2.8}$$

where $P(\tau_k)$ is the power of the kth tap.

Flat fading

If the delay spread of the channel is smaller that the symbol's time duration, the channel is said to be flat fading [7]. In a flat fading channel the inter-symbol interference (ISI) is absent; indeed, such a channel has a constant gain and a linear phase response over a bandwidth that is greater than the bandwidth of the transmitted signal as shown in picture 2.2. The characteristics of a flat fading channel are shown in figure 2.3.

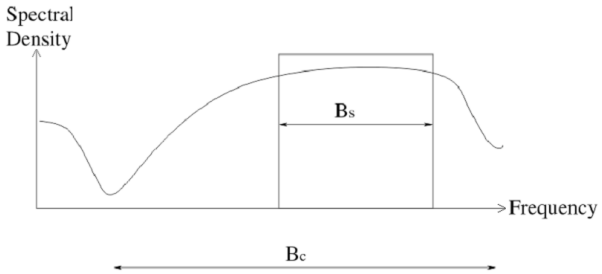

Figure 2.2: Spectral density of a flat fading channel [8]

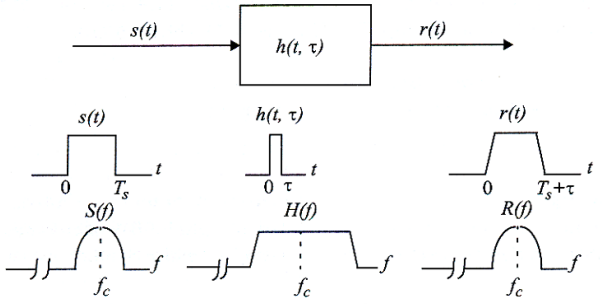

Figure 2.3: Characteristics of a flat fading channel [8]

A flat fading channel is characterized by

$$B_s << B_c \quad \text{or} \quad T_s >> \sigma_\tau \tag{2.9}$$

with B_s the bandwidth of the transmitted signal, B_c the coherence bandwidth of the channel, T_s the period of the symbol and σ_τ the RMS delay spread.

Frequency selective fading

On the other hand, if the bandwidth of the transmitted signal is greater than the coherence bandwidth of the channel, this channel cause frequency selective fading as shown in picture 2.4. Thus the received signal includes multiple versions of the same symbol, each one delayed and attenuated. The received signal is distorted which brings ISI. In the frequency domain, this means that certain frequency components in the received signal spectrum have larger gains than others [7]. The characteristics of a frequency selective channel are shown in figure 2.5.

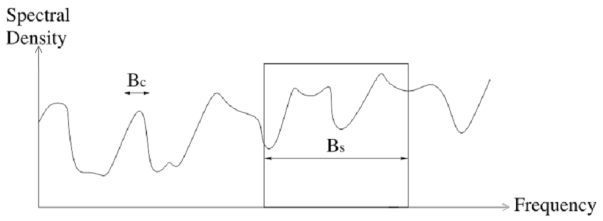

Figure 2.4: Spectral density of a frequency selective channel [8]

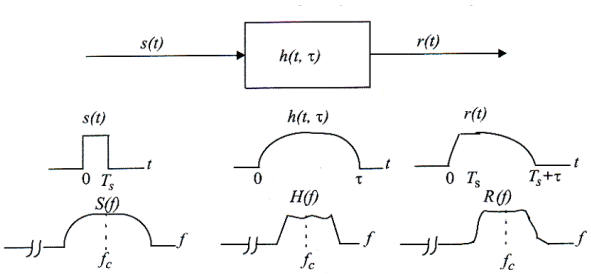

Figure 2.5: Characteristics of a frequency selective channel [8]

A frequency selective channel is characterized by

$$B_s > B_c \quad \text{or} \quad T_s < \sigma_\tau \tag{2.10}$$

2.2.4 Doppler effect

Doppler effect is caused by the relative movement of the transmitter and the receiver. It can be described as the effect produced by a moving source of waves in which there is an apparent shift in frequency for observers toward whom the source is approaching and an apparent downward shift in frequency for observers from whom the source is receding [9]. When the receiver speed is high, if it is located in a train or a fast moving car for example, the Doppler shift will be very high too and thereby the receiver may not be able to detect the transmitted signal.

2.3 Frequency division multiplexing

Frequency division multiplexing (FDM) is a technology that permits to transmit multiple signals concurrently on a unique channel. Each baseband signal is modulated on different carrier waves. Orthogonal frequency division multiplexing (OFDM) is a FDM technique which distributes the data over a large amount of carriers spaced at particular frequencies. The orthogonality is provided by the spacing between the several carriers. This technology will permit to limit the fading and the interference. This chapter will provide an overview of the OFDM technology; for a deeper analysis refer to appendix A.

Before going further, it is useful to define the term bandwidth. The bandwidth of an analogue signal is the difference between the highest and lowest frequencies contained in the signal.

2.3.1 Multi-carrier transmission

In this section the multi carrier approach will be investigated and compared to the single carrier in term of numbers of symbols suffering from ISI.

Single carrier approach

As defined in [10], in a single carrier modulation the transmitted symbols are pulse shaped by a transmitter filter $g(t)$ as shown in picture 2.6.

Figure 2.6: Single carrier system [11]

This approach is characterized by the following conditions:

- Transmission rate: $R = \frac{1}{T_s}$
- Maximum channel delay: τ_{max}

with T_s the symbol time.

Those two conditions permit to find the number of symbols suffering from ISI [11]:

$$number\_of\_interfered\_symbols = \frac{\tau_{max}}{T_s} \tag{2.11}$$

The bandwidth of the system equals to R and is shown in 2.7.

Multi-carrier approach

In a multi carrier modulation the available channel bandwidth W is divided into a certain number (N) of sub channels.[10] Such a division of the signal

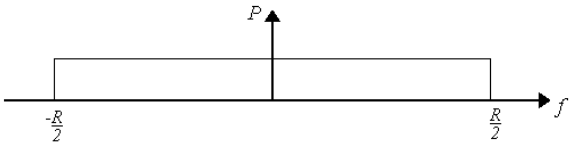

Figure 2.7: Bandwidth of a single carrier system

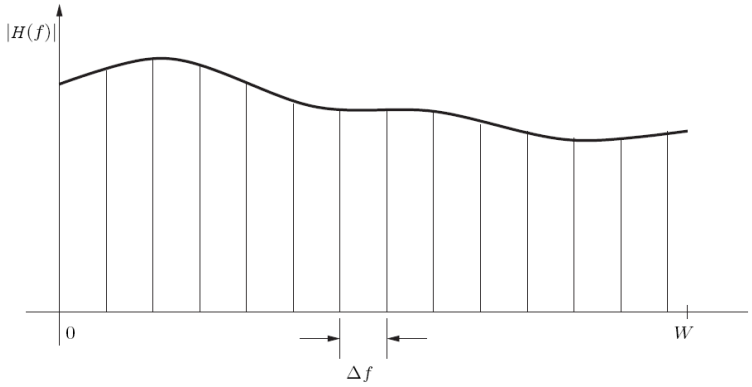

Figure 2.8: Subdivision of the channel bandwidth W into narrowband subchannels of equal width Δf [12]

bandwidth is illustrated in figure 2.8. with $|H(f)|$ the Fourier transform of the channel The original data stream of rate R is divided into N parallel data streams of rate $R_{sub} = \frac{1}{T_{sub}} = \frac{R}{N}$. Each of the data streams is modulated with a different frequency and the resulting signals are transmitted together in the same band as shown in picture 2.9.

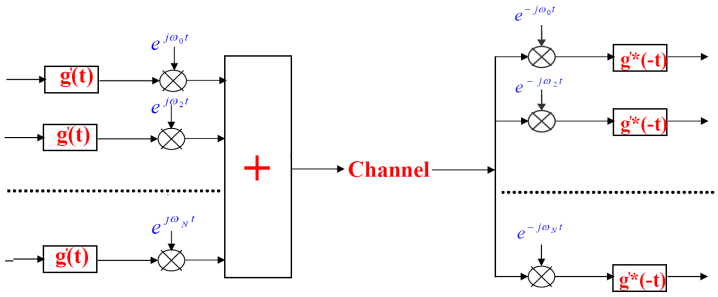

Figure 2.9: Multi carrier system [11]

This leads to the following expression of the number of symbols suffering of

ISI [11]:

$$number\_of\_interfered\_symbols = \frac{\tau_{max}}{T_{sub}} = \frac{\tau_{max}}{N.T_s} \tag{2.12}$$

It is easy to realize that number of symbols suffering of ISI for a multi carriers system is the same amount as in equation 2.11 divided by N.

The bandwidth of each subcarrier equals to R/N. An example of this is shown in figure 2.10.

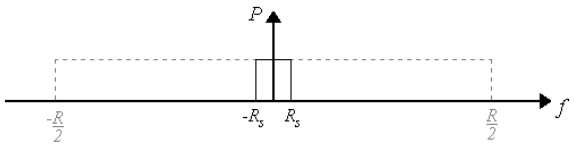

Figure 2.10: Bandwidth of one subcarrier of a multi carrier system

Thus, the bandwidth of the transmitted signal, which is the concatenation of N subcarriers, is equal to R and is shown in picture 2.11.

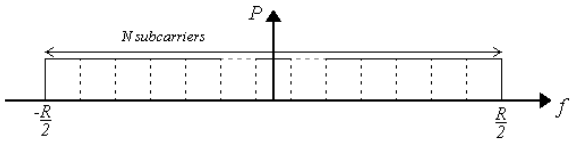

Figure 2.11: Bandwidth of a multi-carrier system

Advantage of Multi-carriers approach

As shown in this section, a single carrier system suffers from ISI when the data rate is high. Nevertheless the actual wireless applications need a high data rate. ISI occurs when $T_s < \tau_{max}$. Thus the dividing the bandwidth B into N different sub channels permits to decrease the data rate of each sub channel and, as a result, to increase the period of each symbol. Consequently, the effect of ISI is drastically reduced.

The effect of ISI in a single carrier system can be limited by using equalization techniques. However the components used to design such systems are not always linearly functioning in high frequencies. Moreover, the equalization techniques require an update of the coefficient. Also the price of such components is pretty high which leads to an expensive system design.

On the other hand, a multi carrier approach is basically to divide the bandwidth B into N different parts. For example, let's take a bandwidth $B = 1MHz$, $N = 100$ and a typical value of the delay spread for an outdoor channel of $\tau_{max} = 1\mu s$. Then the bandwidth of each sub channel is equal $10kHz$ and the symbol time for each sub channel is equal to $100\mu s$. This value is 10 times bigger

than the maximum delay spread and the effects of ISI are avoided. It is also possible to argue that, by dividing the signal in N parts, it permits to obtain more flat channel response over the subchannels and therefore to minimize the ISI.

One of the main problem in designing such a system is that by increasing the numbers of subcarriers, the spacing between each frequency is decreasing. To be able, at the receiver, to retrieve efficiently the information transmitted, the system will need a very sensitive frequency synchronization and as a consequence very accurate components.

2.4 Multicast

2.4.1 Multicast Basics

In a communication system it is possible to distinguish three main categories of "Information Delivery": Unicast, Broadcast and Multicast.

- **Unicast**: In the unicast scenario, messages are sent from the transmitting device to a receiving device. The communication is from a single host to another single host.

- **Broadcast**: As the name suggests, Broadcast is when a single device is transmitting a message to all other devices in a given address range. These messages are sent to every device on a network without exclusions. This technique is used when information needs to be communicated to everyone else on the network, or is used when the sending station needs to send to just one recipient, but does not know its address.

- **Multicast**: Multicast enables a single device to communicate with a specific set of hosts. The multicast messages are a compromise between the previous two types: they are sent to a group of stations that meet a particular set of criteria. These stations are usually related to each other in some way, such as serving a common function, or being set up into a particular multicast group.

The following pictures explain the network organization for the three different topologies.

The red circle symbolize a transmitter; the black circle symbolize a non transmitting user and the blue circle symbolize an active user which is receiving information from the transmitter.

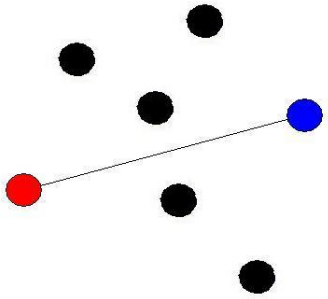

Figure 2.12: Unicast scenario

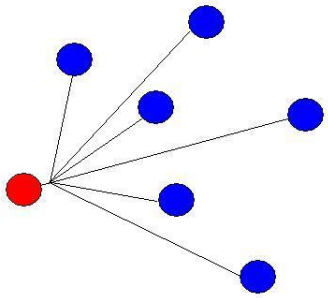

Figure 2.13: Broadcast scenario

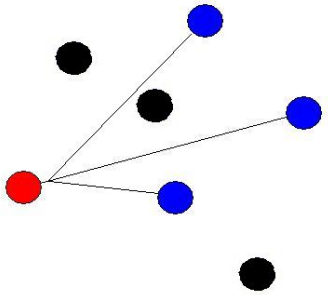

Figure 2.14: Multicast scenario

It is possible to define multicasting as particular evolution of broadcasting when the transmitter is sending information to all the devices within a network, and then the single device itself decides to listen to the source or not. Considering such communication system, it is possible to state that multicasting is not a new application in the communication systems. Multicast communications has been supported for at least the past 10 years in the Internet environment for fixed users using wired links. Radio and TV companies, for example, are broadcasting information 24h per day, but only the users who are interested in it are using the received information. Till ten years ago the data rate available in such systems was limited and the digital television systems, such as cable TV, used wireline solutions for high bandwidth transmission.

2.4.2 Problems in fixed network

Some of the problems related to a multicast transmission, which in the generic case are considered to be within a wired scenario, are: group dynamics, routing support and feedback control

Group's Dynamics:

In the fixed network when an host joins a multicast group, it has to inform the local multicast router which is in contact with the other multicast routers. Based on this it is possible to create the multicast tree trough the multicast routing protocol. All the routing communication are performed by the Internet Group Management Protocol (IGMP). There must be a logical meaning for routing the data to the group members because the network must locate all the members and arrange the routing. The difference between multicasting data to several users, and separately unicasting data to several different destinations has the point in the *host group* model: a host group is a set of receivers sharing a common identifier address. They are all receiving any data packets addressed to this identifier address. From the sender's point of view this model reduces the multicast transmission to a unicast transmission where the sender is sending data to just one address. An important specification related to the group model is that the sender may or may not be a member of the group and may have no knowledge of the group's membership. If the sender is a member of the group, the group is called closed; otherwise it is called open. It is easy to imagine that the behavior of the group is changing over time. It does not have restricted dimensions, it could be transient or persistent in time and it could have constant or varying number of members.

Multicast Routing:

Since the group is dynamically changing the members, the network has to keep track of the group's membership during the entire communication session. It is possible to imagine a multicast route as a tree rooted at the sender with a receiver at each leaf. The way of designing the tree can follow two different ways: resource sharing (how to split the resources fairly among all the users), and what the cost is, which is a matter also in unicast communications. Traditional unicast-routing decision is intended to minimize the path length from the sender to the receiver in order to minimize transmission cost and delay. The comparable multicast solution could be based on the shortest path tree as well, cutting off any branches that do not lead to any receiver in the group, anyway, different algorithms for the tree's implementation can be used.

Feedback control:

Another important requirement is related to the feedback control in communication systems. Whether a network provides a simple connection or a complicated one there are several requirements that have to be satisfied in order to have a reliable connection. Feedback mechanisms of the unicast protocols, for example, are protocols which control the flow, the congestion and the error control.

Flow control assures that the sender does not cause overflow on the receiver with data that cannot be decoded in a determined period of time (e.g. symbol time). Congestion control deals with the available resources for the communication and it controls sender and receiver status. Error control ensure that the packets transmitted by the sender are received correctly at the receiver. While flow control is an end-to-end issue, error control and congestion control depend on the network status and need constant update within the connection status.

In a unicast communication there is a constant exchange of information between the sender and the receiver which permits to have the channel estimation and the reports that describe reception statistics. This will permit to the sender to change its behavior according to the system properties in that moment. But this feature in multicast communications can have feedback implosion as a result of the reports when several receivers are transmitting to only one sender. [13]

2.4.3 Wireless Multicast

Also in the wireless communication, multicast is a efficient method of supporting group communication. In military environments, for example, tactical information may be multicast to users, tanks, and planes; such applications demand minimal delay and secure and reliable connection. Distance education and entertainment services can be offered to mobile or remote users; such applications require high bandwidth and near-real-time connection for quality viewing [14].

The existing multicast support for fixed users can be extended to the wireless environment but not without difficulties. The easiest example could be the mobility of any single user which leads to multicast tree problems, loss of packets, incorrect routing. In a wireless network the communication with a node can be disrupted because of interference, noise or signal attenuation. Moreover, talking about strict request of quality of service (QoS), the transmission has to be performed respecting a certain delay.

Infrastructure-based Network

The infrastructure-based network involves the use of a central base station linked by a fixed network. The users, of course, are associated to different mobile station which are able to move within the scenario.

The two antennas (which represent Base Station antennas, collocated or not) are dividing the area within their cell coverage and are connected to each other through the wired connection (connection not included in the picture). All the users are receiving the requested information from their associated BSs; depending on the network configuration, each user can receive information from the BS the user is associated with, or it is possible to have communication with more than just this single BS.

Existing multicast protocol can be modified for the wireless network in order to manage the packet routing and the users mobility. The Core-Based Tree (CBT)[1] and the Protocol Independent Multicast-Sparse Mode (PIT-SM)[1]

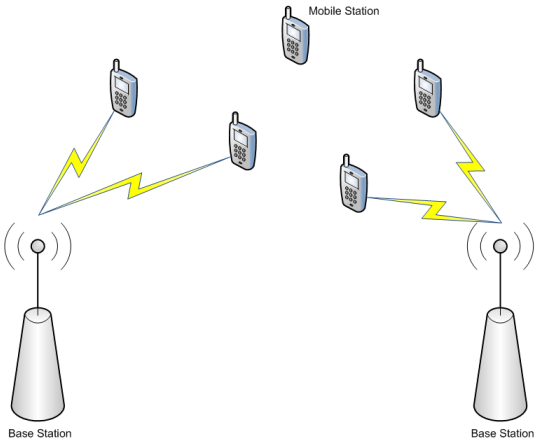

Figure 2.15: Infrastructure Network organization

can both be used as the routing protocol as they are based only on the destination which permits to reach every mobile station to receive the multicast packet within any point of the network.

Ad-Hoc Network

A Mobile Ad-hoc network (MANET) is an autonomous system of mobile devices which are connected by wireless link with no supporting central administration.[15]

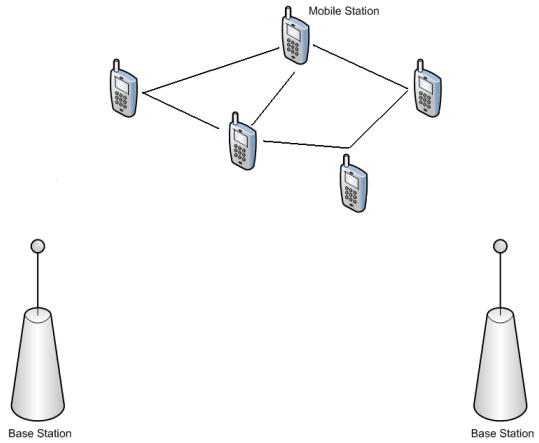

Figure 2.16: Ad-Hoc Network organization

Because of this infrastructure, if two hosts are not directly covered by their own transmission range, the communication between them must pass trough other hosts. Such topology could also be referred as multi-hop network, where each host may serve as router. In a multi-hop network the transmission of the information is hoping from host to host till it reaches the desired destination. For example: the source sends the Route Request Message to its neighbors. If the neighbor has no information on the destination, it will send the message to

its neighbors as well. When the request reaches a hosts that has information about the destination (or either the destination itself), the path is identified and the information can be sent from the source. In a multicast scenario the ad-hoc network can be used in order to save network bandwidth consumption and the hosts power. As said before, a multicast group is composed by one or multiple hosts, which should receive and handle any information sent to that group. Due to the high degree of mobility, at any time each host can join a multicast group, and each group member can leave its group. In a MANET, the group member can randomly have grown in the network, which causes more difficulty in packet delivery and group maintenance. Since there is no fixed infrastructure in an ad hoc network, all nodes may be required to compute, maintain and store the routing information.

2.4.4 Problems in wireless network

Security and reliability of the service are the main issues required by the wireless multicast. Reliability requires detection of packet loss and error recovery. Different approaches can be used for packet loss detection depending on different protocol organization:

- *sender-initiated*: the receiver is usually sending acknowledgments for correctly received data. A timer can be used on the transmitter side in order to detect packet losses at its side. However, if every receiver sends an acknowledgment for a received packet, the implosion at the transmitter can occur.
- *receiver-initiated*: negative acknowledgments are used by the receiver to inform the transmitter about packet loss.

The choice of the approach depends on the number of users which are requesting the information. A large number of mobile station which are sending the acknowledgment to the transmitter, can cause the feedback implosion with the overload of information.

Error recovery can be performed by retransmitting the information to the receiver which did not receive it correctly. It can be achieved in different way depending on the network architecture: group retransmission, cluster head responsible for retransmission, or cooperation between the users.

Security in the wireless network depends on the wireless link status, it includes complete loss of service or information stealing. Encrypted communications, group authentication and the usage of secure key can bring more robustness to the connection but, on the other hand, can bring significant processing complexity and network overhead. More complex data processing can also bring delayed transmission which is, for the multimedia content multicast of this project, a risky problem in terms of QoS.

In order to contrast those problems, the cross layer design has been studied with different approaches.[16] The cross layer design means that different layers of the communication model are taken into count during the transmission organization. In wireless multicast there is a strong interaction between network,

medium access and physical layer. This interaction adds significant complexity to the system which motivates its optimized performance with the efficient support of different QoS requirements.

The next table it is a resume of the differences between wired and wireless infrastructures for a multicast communication system.

Issue	**Current "wired" multicast**	**Wireless and mobile multicast**
Type and properties	Symmetrical and fixed characteristics Broadcast links in LANs	Possibly asymmetrical and/or unidirectional links of varying performance and point-to-point links in cellular and PCS
Bandwidth	Plentiful	Limited and variable amount
Topology	Fixed	Fixed in infrastructure-based, dynamic in ad hoc networks
Loss of packets	Infrequent (<1%)	Frequent and variable (1%-30% based on links)
Membership changes	Only when a user leaves or joins a group	When a user leaves or join a group and also when a user moves to another location
Routing	Fixed routing structure throughout the multicast session	Routing structure subject to change due to user mobility
Security Issues	Less complex due to fixed users and wireless links	More complex due to wireless links and possible use of broadcasting
Quality of service	Individual routes can use resource reservation protocol (RSVP)	Due to user mobility, RSVP may cause excessive overhead
Reliability	Possible use of a transport-layer protocol (such as the Multicast File Transfer Protocol)	More complex due to user mobility; possible unwanted interaction of protocols at transport and link layers

Table 2.1: Qualitative comparison of wired and wireless multicast [14]

2.5 Beamforming/MIMO

The need of a better wireless communication, in terms of higher data rate, fewer dropped calls, QoS and network capacity, brought the scientist to focus on different approach for the communications organization. The number of transmitter/receiver antennas is one of the parameters which has been analyzed over time.

Usually the radiation pattern of a single element antenna is relatively wide and provides low value of gain, and so, directivity. For long distance communication, a very directive antenna needs to be designed. This can be done by increasing the electrical size of the antenna. To enlarge the dimensions of the antenna, without increasing the size of each element, it is possible to gather several radiating elements in a geometrical and electrical configuration. The elements are often identical, which is simpler and more practical. Moreover, a particular case of multiple antennas is the Multiple Input Multiple Output (MIMO) which refers to a system that uses antenna arrays at both transmitter and receiver side and promises a better spectral efficiency and a more reliable wireless connection.

2.5.1 Beamforming

One of the system which is using multiple antennas for the transmission is the Beamforming. The vector addition of the fields radiated by the individual elements of an antennas array permits to obtain the total field of the array. To obtain very directive patterns, it is necessary that the field from the elements of the array interfere constructively in the desired directions and destructively in the remaining space. To shape the overall pattern of the antenna, supposing an array of identical elements, there are five controls that can be used to shape the overall pattern of the array. These are:

- the geometrical configuration of the overall array (linear, circular, rectangular, spherical, etc.)
- the relative displacement between the elements
- the excitation amplitude of the individual elements
- the excitation phase of the individual elements
- the relative pattern of the individual elements

The easiest and most practical arrays is formed by placing the elements along a line. A two-element array will first be analyzed in term of array factor then a N-element array will be considered.

Two-element array

As described in [17] " *the total field of the array is equal to the field of a single element positioned at the origin multiplied by a factor which is widely referred to as the array factor (AF)*". Assuming far-field observations, for the two-element

array of constant amplitude, shown in figure 2.17, the array factor, in normalized form, is given by

$$(\mathrm{AF})_{normalized} = cos[\frac{1}{2}(kdcos\theta + \beta)] \tag{2.13}$$

with $k = \frac{2\pi}{\lambda}$ the angular wavenumber, d the maximum length of the antenna,

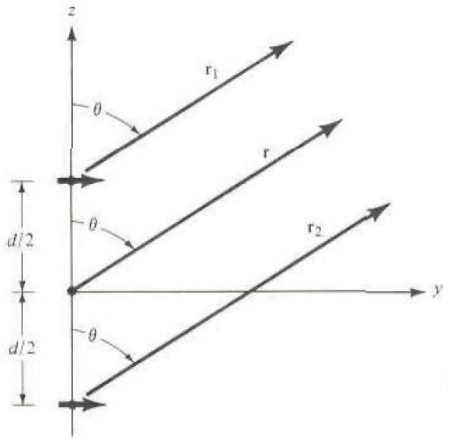

Figure 2.17: Two-element array positioned along the z-axis [17]

θ the angle between the arrays and the point of observation as shown in picture 2.17 and β the difference in phase excitation between the elements.

Thus by varying the separation d and/or the phase β between the elements, it is possible to control the total field of the array and the characteristics of the array factor. Let us consider some examples to illustrate these principles.

Considering $d = \lambda/4$ and $\beta = 0$, it is possible to find the nulls of the array factor by

$$(\mathrm{AF})_{normalized\_nulls} = 0 \Rightarrow cos\left(\frac{\pi}{4}cos\theta_{nulls}\right) = 0, \tag{2.14}$$

which leads to

$$\frac{\pi}{4}cos\theta_{nulls} = \pm\frac{\pi}{2} \Rightarrow \theta_{nulls} \text{ does not exist.} \tag{2.15}$$

Thus the AF will not add any additional nulls to the far-zone field of the two-element array. Indeed the separation between the elements is not large enough to lead to a phase difference of π between the elements.

Let us now consider $d = \lambda/4$ and $\beta = +\pi/2$, it is possible to find the nulls of the array factor by

$$(\mathrm{AF})_{normalized\_nulls} = 0 \Rightarrow cos\left(\frac{\pi}{4}(cos\theta_{nulls} + 1)\right) = 0, \tag{2.16}$$

which leads to

$$\frac{\pi}{4}(cos\theta_{nulls} + 1) = \pm\frac{\pi}{2} \Rightarrow \theta_{nulls} = 0, \tag{2.17}$$

Thus the AF will add an additional null to the far-zone field of the two-element array. Indeed, the element in the negative z-axis as shown in figure 2.17 has an initial phase lag of $\pi/2$ from the other element. Considering the propagation of a wave from this element toward the positive z-axis, it suffers an additional $\pi/2$ phase retardation when it reaches the other element on the positive z-axis. It leads to a total phase difference of π between the waves of the two elements. Nevertheless, if the wave is propagating towards the negative z-axis, the waves of the two elements are in phase.

It is also possible to consider $d = \lambda/4$ and $\beta = -\pi/2$. It is the same calculation then previously however it leads to $\theta_{nulls} = \pi$. Figure 2.18 shows a plot of those examples.

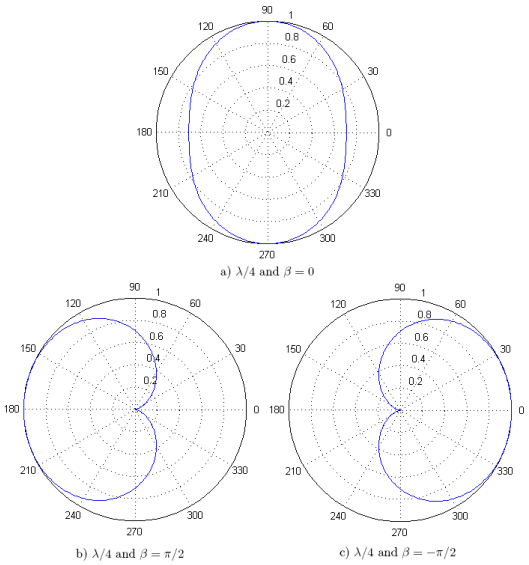

Figure 2.18: Plots of the array factor

Figure 2.19 shows that the spacing affect the number of side lobes that appear on the array factor. Precisely, while d is increasing above $\lambda/2$, the number of side lobes that appear increases. Whereas while d is decreasing below $\lambda/2$, the array factor tends to a circular shape.

Figure 2.20 shows the effect of the phase β between the elements of the antenna on the array factor.

N-element array

It is possible now to generalize to N elements as shown in figure 2.21(a), assuming that all the elements are excited with currents of identical amplitudes and with a progressive phase shift β . As described in [17] "*An array of identical elements all of identical magnitude and each with a progressive phase is referred to as a uniform array*". Thus it is possible to obtain the generalized equation

$$\mathrm{AF} = \sum_{n=1}^{N} e^{j(n-1)\psi} \tag{2.18}$$

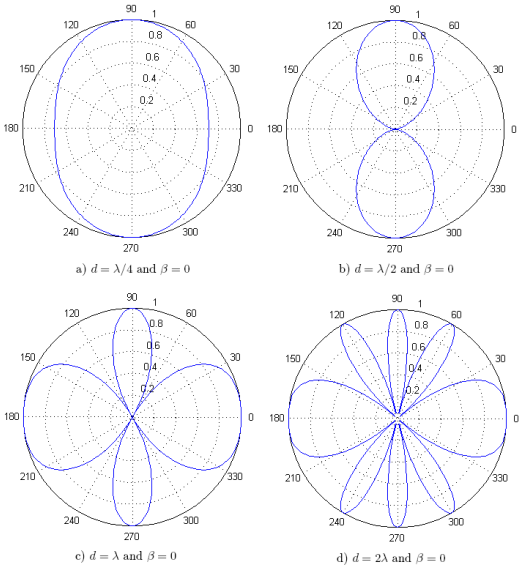

Figure 2.19: Effect of the variation of the length d of the antenna on the array factor

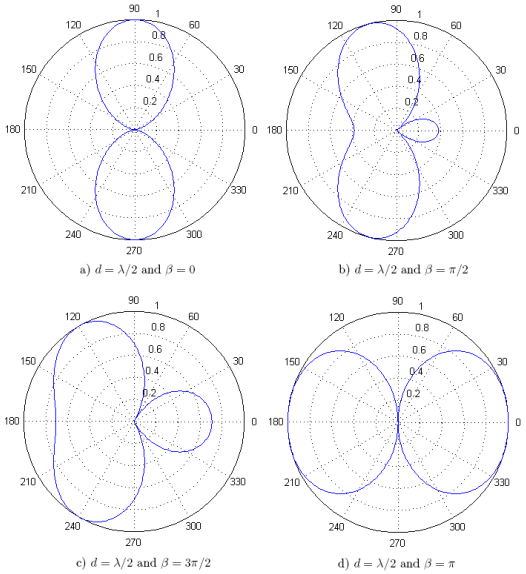

Figure 2.20: Effect of the variation of the phase β between the elements of the antenna on the array factor

with $\psi = kdcos\theta + \beta$.

The total AF is a summation of exponentials *i.e.* it is a sum of N phasors each of unit amplitude and a progressive phase ψ relative to the previous one. As shown in picture 2.21(b), the amplitude and the phase of the array field can

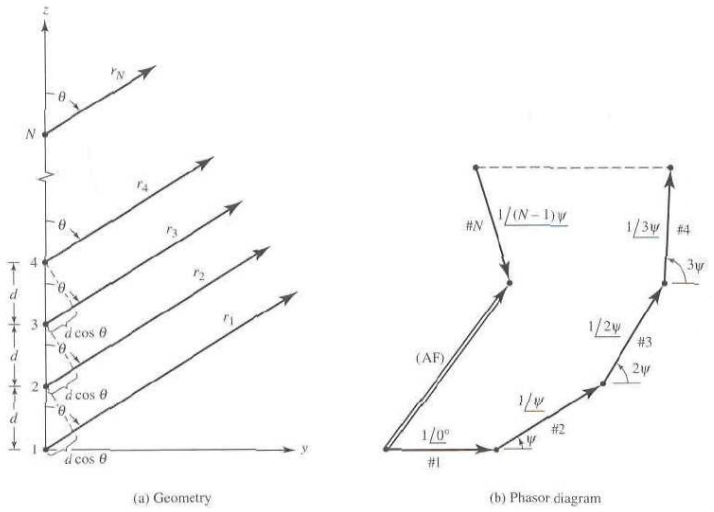

Figure 2.21: Far field geometry and phasor diagram of N-element array of isotropic sources positioned along the z-axis [17]

be managed by a right choice of the relative phase ψ between the elements.

2.5.2 MIMO

It is known that the signal sent by an antenna, due to multipath fading, is arriving at the receiver over different paths. MIMO is taking advantage of the multipath characteristics of the signal and is sending data over those multiple paths, thereby increasing the amount of information the system carries. The data are received by multiple antennas and recombined properly by some of the available MIMO algorithms, which will be discussed in following section of this report.

Background

MIMO was originally born in Bell Labs: its engineers were trying to address the bandwidth limitations that signal interference caused in large, high-capacity cable. But it was too expensive at that time to be practical. Nowadays, after fixing the problems with the wired infrastructure, the improvement of the wireless systems leads MIMO to be reconsidered as a useful technology. [18]

Right now, the MIMO technology is used in the IEEE 802.16 WiMax standard and it has been promoted also for the coming up IEEE 802.11n wireless network standard. In addition, the Third Generation Partnership Project (3GPP)is evaluating MIMO for the next generation of cellular phone networks.[18]

The main difference between MIMO and Beamforming is related to the number of antennas on the receiver side. Both the technologies are based on multiple antenna on the transmitter side; but while MIMO refers to a connection between one BS and one MS both with multiple antennas, beamforming refers

to a connection between on BS with multiple antennas and one MS with a single antenna. More details regarding the scenario of this project will be discussed in chapter 3.

How MIMO works

MIMO takes advantage from the multiple bouncing of the signal over many paths going from the transmitter to the receiver. The transmission based on two or more antennas at the transmitter permits to put data on multiple signal paths and, consequently, increases the amount of information the system can carry and the number of users it can serve. In addition, with this approach it is possible to divide the data in different parts and send it over different paths. The nature of the signal over each path changes depending on the antennas' spacing, the interference and the channel characteristics, and at the receiver side there is a manipulation of the signal in order to reconstruct the original message properly.[19]

Advantages and disadvantages

Based on what it has been presented, it is possible to list different advantages:

- The wireless rate of a MIMO system is higher than a normal system and there is possibility to handle multimedia data which requires high-data-rate.
- The increased available bandwidth also lets wireless network to serve higher number of user at the same time with a given data-rate than they could do without MIMO.
- This technology is also decreasing the amount of interference. It is then possible to focus only on a better-quality signal during the transmission in order to save transmitting power.
- There is less power consumption and less chance of interference to or from other systems.
- Reliability is also one of the important advantages of MIMO system. Dividing the data to send over multiple paths, makes more difficult for hackers to find a way of receive and understand the signals that have been divided at the transmitter side.

Despite these advantages, MIMO is still facing challenges:

- Designing MIMO system, which send signals using multiple paths, is a challenge because the engineers focused in the past in sending the information only on a single path.
- MIMO has worked well in laboratories, but is still not well known its behavior in a real cellular network where the users are free to move within and over the network.
- The MIMO's greatest technical problem may be the processor-energy consumption caused by the complexity of the algorithms required for handling the transmitted data over the multiple path

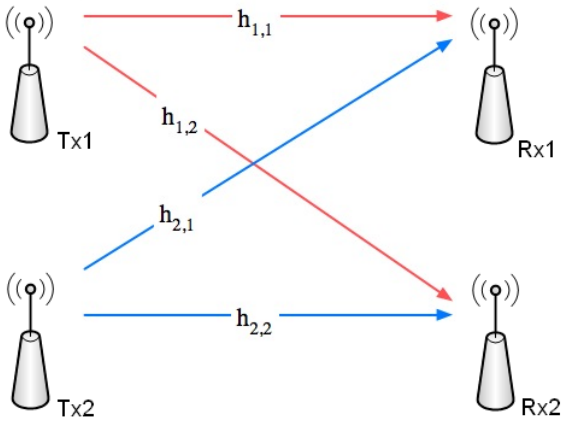

Figure 2.22: MIMO structure

The picture 2.22 shows how a MIMO system is working. Different antennas at the transmitter side are transmitting the information to different antennas on the receiver side through different channels.

In a simplest communication system with one antenna at the transmitter, one channel and one antenna at the receiver the received signal is usually stated in the form:

$$y(t) = h(t) * x(t) + n(t) \tag{2.19}$$

where $h(t)$ is the channel impulse response ($h(t) = h * \delta(t)$), $x(t)$ is the transmitted signal and $n(t)$ is the noise. In the MIMO case, as it is possible to notice by the picture, all the multiple signals arriving at the receiver side have the same composition:

$$y_1 = h_{11}x_1 + h_{12}x_2 + \ldots + h_{1M}x_M + n_1 \tag{2.20}$$

$$y_i = h_{i1}x_1 + h_{i2}x_2 + \ldots + h_{iM}x_M + n_i \tag{2.21}$$

and it is possible to use a matrix form of the above's equations which give us:

$$\underline{y}_{N\times 1} = \mathbf{H}_{N\times M}\underline{x}_{M\times 1} + \underline{n}_{N\times 1} \tag{2.22}$$

The channel transfer function is expressed as a matrix $N \times M$ where N is the number of antennas at the receiver and M is the number of transmitter antennas.

Capacity

Range extension MIMO is also used in order to increase the transmission range of a wireless communication. By using clearer signals and minimizing the effect of interference, the signals can be sent over longer distance than simpler

technologies which are penalized by channel fading and multipath fading. This characteristic can bring to a very useful conclusion because, for example in a cellular network, the cell size is very important in determining the number of BS needed for the coverage of a given area. Having a larger coverage for each BS means less money for the deployment of the entire infrastructure.

It is generally understood that, in a wireless system, the capacity and the coverage range are inversely proportionated factors. Increasing the capacity usually means a decrease of range and vice versa. For a MIMO system, it has been surprisingly discovered that it is possible to have an increase of capacity and, in specific cases, have at the same time better range.[18] The range increase is larger for outage capacity, which refers to the slow fading environments, and is smaller for the average capacity, which refers to the fast fading environments that are more important for the mobile communications.

Capacity increase through spatial multiplexing Comparing system with single antenna at both sides of the network with multiple antennas system, spatial multiplexing leads to a linear capacity increase. The gain is made available by the simultaneous transmission of independent data streams in the same frequency band. In a MIMO system the system capacity is defined as follows:

$$C = log_2 \left[det \left(I + \frac{\rho}{M} \underline{H} \underline{H}^H \right) \right] \tag{2.23}$$

where M is the rank of the previous explained $\underline{H}$ channel matrix, ρ is the signal to noise ratio and I is a $M \times M$ identity matrix. It was demonstrated in [20] that in real-word propagation conditions, multipath propagation (which leads to frequency-selective fading) can be highly beneficial in terms of spatial multiplexing gain. Multipath propagation increases the angle spread on both the transmitter and receiver side, which increases the rank of the channel matrix and hence the spatial multiplexing gain. This has as a result the higher complexity of the receiving process managed by the receiver station.

Improved link reliability using diversity gain Diversity leads to improvement of link reliability by adding more redundancy to information going trough the channel. Diversity gain is obtained by transmitting a certain data signal over different paths from the transmitter to the receiver which are independent with each other in time, frequency and space. MIMO itself refers naturally to the space diversity because of its nature. Multiple antenna sending the same information over multiple paths is a condition which increases the communication reliability.

MIMO and OFDM

In OFDM-based MIMO system, the communication is performed by transmitting independent data streams using different sub-carriers. The division of the different sub-carriers is made using a tone-to-tone base. The use of OFDM eliminates ISI during the transmission but it gives more complexity to the system architecture. The number of available tone changes depending on the scenario between 48 (IEEE 802.11) and 1728 (IEEE 802.16)[20] and spatial separation has to be performed for any single tone. Different algorithms are still a work

in progress for the reduction of the computational complexity. Referring to the diversity gain, using MIMO-OFDM system the frequency diversity can be accomplished as well as the basic spatial diversity. As a result a system with two sources of diversity is available: space diversity and frequency diversity. It is then a matter of code and modulation to organize how those sources of diversity can work concurrently.

2.6 Mobile WiMAX

The Worldwide Interoperability for Microwave Access (WiMAX) is a telecommunication technology based on the Institute of Electrical and Electronics Engineers 802.16 standard (IEEE). The first 802.16 standard was approved in December 2001. It is a standard for point to multipoint broadband wireless transmission in the frequency band between 10 GHz to 66 GHz, with exclusively line-of-sight (LOS) capability [21].

The evolution of this standard led to various amendment including the 802.16e-2005 one, also called Mobile WiMAX. Mobile WiMAX implementations can be used to deliver both fixed and mobile services. In opposition the fixed WiMAX, amendment 802.16-2004, does not provide handoff between BSs, thus the service provider cannot propose mobility.

The Mobile WiMAX Air Interface adopts Orthogonal Frequency Division Multiple Access (OFDMA) in order to improve the multipath performance in non-line-of-sight environments. OFDMA is a multi-user OFDM that allows multiple access on the same channel. OFDMA distributes the subcarriers among users so all users can transmit and receive at the same time within a single channel on subchannels. OFDMA subcarrier-group subchannels can be matched to each user to provide the best performance *i.e.* less influence with the interference and fading of the signal. OFDMA also permits to change the modulation and/or coding for each subcarrier depending on the received SNR. This modulation based on the received SNR can provide the data rate as shown in tables 2.2 and 2.3.

Channel bandwidth	5MHz
PHY mode	512 OFDMA
Oversampling	28/25
Modulation Code rate	**PHY-Layer Data Rate (kbps)**
QPSK, 1/2	2520
QPSK, 3/4	3780
16-QAM, 1/2	5040
16-QAM, 3/4	7560
64-QAM, 2/3	10080
16-QAM, 3/4	11340

Table 2.2: PHY-Layer Data Rate [22]

Modulation	Coding rate	Received SNR (dB)
QPSK	1/2	9.4
	3/4	11.2
16-QAM	1/2	16.4
	3/4	18.2
64-QAM	2/3	22.7
	3/4	24.4

Table 2.3: IEEE 802.16 PHY assumptions [22]

The Mobile WiMAX layer is based on Scalable Orthogonal Frequency Division Multiple Access (sOFDMA). Scalability is supported by adjusting the size of the FFT while fixing subcarrier frequency spacing to 10.94 kHz. Thus it supports channel bandwidths ranging from 1.25 MHz to 20 MHz. It is important to notice that the subcarrier spacing is independent of the bandwidth while the number of subcarriers scale with the bandwidth.

The key advantages of Mobile WiMAX are:

- tolerance to multipath and self-interference,
- scalable channel bandwidth,
- orthogonal uplink multiple access,
- fine quality of service,
- advance antenna technology.

The OFDM parameters used for Mobile WiMAX are shown in table 2.4.

Parameter	**Fixed WiMAX OFDM-PHY**	**Mobile WiMAX Scalable OFDMA-PHY**			
FFT size	256	128	**512**	1024	2048
Number of used data subcarriers	192	72	**360**	720	1440
Number of pilot subcarriers	8	12	**60**	120	240
Number of null subcarriers	56	44	**92**	184	368
Cyclic prefix (Tg/Tb)	1/32, 1/16, **1/8**, 1/4				
Channel bandwidth (MHz)	3.5	1.25	**5**	10	20
Subcarrier frequency spacing (kHz)	15.625	**10.94**			
Useful symbol time (μs)	64	**91.4**			
Guard time assuming 12.5 % (μs)	8	**11.4**			
OFDM symbol duration (μs)	72	**102.9**			
Number of OFDM symbol in 5ms frame (μs)	69	**48.0**			

Table 2.4: OFDM parameters used for Mobile WiMAX [22]

THIS PAGE IS INTENTIONALLY LEFT BLANK

Chapter 3

Delimitation

This chapter presents the delimitation of our project. Firstly the project goal and the target metric of this project are stated. Then the simulation process is described and the choice of our simulation values discussed explaining the chosen performance metrics.

3.1 Project goal and target metric

This project is dealing with the implementation of beamforming and MIMO techniques in order to improve multicast services in a 4G scenario. The main goal of the project is to increase the efficiency of the user in the worst condition within a multicast group. Indeed in a multicast group the main destructive contribution is brought by the user in the worst condition. Thus by optimizing the efficiency of the worst user it is possible to reach a better average efficiency among all the users within the multicast group.

The beamforming and MIMO techniques will be analyzed by the following results:

- *SNR for an increasing number of users:* the size of the multicast group has an impact on the group efficiency. Indeed the efficiency of the beamforming algorithms depends on the group size as discussed in section 4.1. To show the impact of the multicast group size on the performance of the various techniques, the minimum SNR for an increasing number of users will be presented. Notice that it is the minimum SNR that can be presented due to the nature of the algorithms of section 4.1 and the fact that a multicast algorithm is limited by the worst user. It also important to highlight the fact that the MIMO algorithms are not developed specifically for the multicast case. Furthermore the implemented MIMO algorithms are just a way to send the data symbols from the BS to the multicast users to improve the single user transmission efficiency.

- *Channel capacity:* from an application point of view, where the requirements are in term of bits per second (bps), it is necessary to look at the channel capacity. It permits to visualize if the multicast group is able to reach the desired application requirements in term of rate of transmission.

- *Complete CSI and partial CSI:* a large amount of feedback from BS to MS in a wireless communication can cause overload on the BS side. As explained in section 2.4 a wireless multicast system is even more sensitive to the feedback due to the possibility of congestion at the BS. In order to limit this problem, a partial CSI approach has been proposed. A deeper explanation of this process is explained in the further section 5.3.

3.2 Simulation process

The simulation process is the following:

1. A circular shaped cell of the desired radius is created and the shadowing map is then applied to this created cell.

2. The desired amount of users is placed in initial positions in the cell. Those users are then moving within the cell along different trajectories with the created mobility model as presented in appendix D.

3. Throughout those position the path loss, which depends of the distance between the MS and the BS, is calculated. The shadowing values at those positions are then added along with the various parameters taken into account such as the intercept factor, the correction factor for the operating frequency or the correction factor for the MS antenna height. All these parameters permit us to obtain the total path loss of the users in the different positions.

4. Based on those parameters it is possible to obtain the pre-processing SNR of each user along their respective positions. With this pre-processing SNR, the dropping of the worst user can be applied to the multicast groups.

5. The beamforming or the MIMO algorithms are applied.

6. With the results of the algorithms it is possible to determine the post-processing SNR of all the users in the various positions. The channel capacity for each multicast group is then determined using the minimum post-processed SNR within the multicast group, with or without the dropping of users. This is due to the fact that the rate is determined by the worst user performance within the group.

The results obtained in the next section are coming from several iterations of the same simulation process as previously described. Indeed to respect our statistical approach of the problem it is necessary to take the mean value over various realizations of our model. Nevertheless, as explained in appendix C it is possible by running enough simulations on the same shadowing map to respect our statistical approach.

It is important to highlight the fact that, in the future work of this report, a workspace will be defined as a result of one iteration of the process proposed before and with the following values:

- 20 independent initial placements of the users within the cell,
- users are moving along 10 positions,
- group sizes analyzed are 2, 4, 6, 8 and 10 users,

Those steps are realized for different cell sizes: 500m, 800m and 1400m.

3.3 Simulation values

This section will explain and discuss the choice of our simulation values.

- **Antenna correlation:** this value is taken accordingly to the SUI model [23] and defined in section 4.3.1,
- **Frequency:** the frequency band selection is based on the available WiMAX spectrum ranges as defined in the WiMAX standard [24],
- **Type of channel model:** the choice of the channel model is based on two issues: is the choice made in the WiMAX certifications tests [24], and is the choice of the empirical model has been made because it is closer to the reality as stated in section 4.3,
- **Number of users within the cell:** the amount of users has been kept to 10 or less in order to achieve a respectable simulation time (refer to section 5.1.1),
- **Mean velocity of the users:** this value is taken for a user in a urban scenario accordingly to [25],
- **Minimum distance between the BS and MS:** this value is defined in the WiMAX standard [24],
- **Cell size:** the maximum value of the cell size is the maximum value stated in the WiMAX standard [24],
- **BS height:** this value is based on the value of the SUI model [23],
- **MS height:** this value is based on the value of the SUI model [23],
- **Shadowing:** the standard deviation of the shadowing is taken to fit to a urban macro cell as stated in table 4.2,
- **Available power at the BS:** the choice of this value is based on the lecture [26],
- **Noise power:** the noise power level is taken as suggested in the WiMAX forum,
- **Number of taps of the Doppler filter:** this value is taken according to the SUI model [23],

- **Accuracy of resampling process:** this value is taken according to the SUI model [23],
- **Doppler resolution of SUI parameter:** this value is taken according to the SUI model [23],
- **Observation rate:** this value is taken according to the SUI model [23],
- **Number of antenna at the BS:** the number of antennas is taken based on paper [27],
- **Number of antenna at the MS:** the number of antenna is taken to fit to the reality for the beamforming and MIMO cases.

In order to have an easy access to the parameters used for the simulations, table 3.1 summarizes the various elements and their respective values.

Parameter	**Value**	**Unit**
Antenna correlation	0.3	
Frequency	2.3	GHz
Channel model		
Type of channel model	SUI-4	
Number of users within the cell	2 to 10	
Mean velocity of the users	1.36	$m.s^{-1}$
Minimum distance between BS and MS	36	m
Cell size	500, 800 or 1400	m
BS height	50	m
MS height	7	m
Shadowing	8	dB
Available power at the BS	34	dBm
Noise power	-120	dBm
Small scale fading		
Number of taps of the Doppler filter	256	
Accuracy of resampling process	20	
Doppler resolution of SUI parameter	0.1	Hz
Observation rate	4	Hz
Beamforming simulations		
Number of antennas at the BS (M)	4	
Number of antennas at the MS (N)	1	
MIMO simulations		
Number of antennas at the BS (M)	2 or 4	
Number of antennas at the MS (N)	1 or 2	

Table 3.1: List of the parameters

3.4 Performance metrics

This section will present the main formulas used to calculate the results. The formulas will be given in the beamforming and MIMO cases. The formulas are the following

- **Beamforming case**
  The SNR for the beamforming case in linear form is calculated using equation (4.2). It is expressed as:

$$SNR_{bf} = \frac{E\{||\mathbf{H}\mathbf{w}s||^2\}}{E\{||\mathbf{n}||^2\}} \tag{3.1}$$

  with, as explained in section 4.1, $E\{.\}$ expectation operator, $||.||$ the Euclidean norm of a vector, $\mathbf{H}$ the channel matrix, $\mathbf{w}$ the beamforming weight vector, s the data symbol and $\mathbf{n}$ the additive white gaussian noise.

- **MIMO** 2×1
  The SNR for the MIMO 2×1 case in linear form is calculated using equations (4.16) and (4.17). It is expressed as:

$$SNR_{2\times1} = \frac{(|h_1|^2 + |h_2|^2).\frac{E_{tr}}{2}}{E[|n|^2]} \tag{3.2}$$

  with, as explained in section 4.2, h_1 and h_2 the coefficients of the flat fading channel, E_{tr} the available transmit power and n an additive gaussian white noise. Here the stream power is equal to $\frac{E_{tr}}{2}$ because we are sending a symbol on each of the two antennas.

- **MIMO** 2×2
  The SNR for the MIMO 2×2 case in linear form is calculated using equations (4.19), (4.20), (4.21) and (4.22). It is expressed as:

$$SNR_{2\times2} = \frac{(|h_{11}|^2 + |h_{12}|^2 + |h_{21}|^2 + |h_{22}|^2).\frac{E_{tr}}{2}}{E[|n|^2]} \tag{3.3}$$

  with, as explained in section 4.2, h_{11}, h_{12}, h_{21} and h_{22} the coefficients of the flat fading channel, E_{tr} the available transmit power and n an additive gaussian white noise. As said before, the stream power is equal to $\frac{E_{tr}}{2}$ because we are sending a symbol on each of the two antennas.

- **MIMO** 4×1
  The SNR for the MIMO 4×1 case in linear form is calculated using equation (4.26). It is expressed as:

$$SNR_{4\times1} = \frac{|h^2|^2.\frac{E_{tr}}{4}}{|h^2|^2.|X|^2.\frac{E_{tr}}{4} + E[|\mathbf{H}^H.n|^2]} \tag{3.4}$$

  with, as explained in section 4.2, h^2 the channel gain, X the channel dependent real-valued random variable (equation 4.28), E_{tr} the available transmit power, $\mathbf{H}^H$ and n an additive gaussian white noise. Here the stream power is equal to $\frac{E_{tr}}{4}$ because we are sending a symbol on each of the four antennas.

- **Channel capacity**
  The channel capacity can be obtained based on the SNR using the following formula:

$$C = Blog_2(1 + SNR) \tag{3.5}$$

  where C is the capacity in bps, B is the channel bandwidth in Hz and SNR is the SNR in linear. The channel capacity for a group is calculated using the minimum SNR within the studied group.

Chapter 4

Model design

This chapter presents the design of the model used for our simulations. First the beamforming algorithms and their solutions are submitted. Second the MIMO techniques are showed. Finally the channel model is developed.

4.1 Beamforming model for a multicast scenario

For a multicast scenario the MIMO technology can be used but, based on what the definition says, the network structure changes a little. MIMO is supposed to be a point-to-point communication system, but a multicast scenario is a point-to-multipoint scenario. Therefore a different user configuration need to be defined. The users in a multicast scenario are divided into groups, and each user belonging to a group requests the same information at the same time. This means that the user group can be seen as a single user with a multiple antennas. Having at the transmitter side an array of antennas and this configuration at the receiver side makes possible the association of MIMO system in a multicast scenario.

This section will focus on the application of adaptive beamforming to multicast services and is based on the paper [28],[29] and [30].

The BS is equipped with an M-element antenna array and the N mobile stations with single-antenna devices. Considering a vector $\mathbf{d} \in \mathbb{C}^N$ with N data symbols, modulated by a matrix $\mathbf{M} \in \mathbb{C}^{M \times N}$, transmitted over the radio channel $\mathbf{H} \in \mathbb{C}^{N \times M}$, with the addition of a white Gaussian noise $\mathbf{n} \in \mathbb{C}^N$, and demodulated by a matrix $\mathbf{D} \in \mathbb{C}^{N \times N}$, the N downlink estimates $\hat{\mathbf{d}} \in \mathbb{C}^N$ of the N transmitted symbols $\mathbf{d}$ may be written as

$$\hat{\mathbf{d}} = \mathbf{DHMd} + \mathbf{Dn} \tag{4.1}$$

Is is possible to see the multicast scenario as a particular case of MIMO multiuser system, for which all users expect the same symbols *i.e.* $\mathbf{d} = s\mathbf{1}$, where $\mathbf{1}_{N \times 1}$ is a vector of ones and s is the data symbol. Thus 4.1 can be rewritten as

$$\hat{\mathbf{d}} = \mathbf{DHw}s + \mathbf{Dn} \tag{4.2}$$

where $\mathbf{w}_{M\times 1} = \mathbf{M1}$ is the resulting weight vector *i.e.* the sum of the weight vectors of the individual users contained within $\mathbf{M}$.

The aim of the following algorithms is to properly determine the transmit weight vector $\mathbf{w}$ in equation 4.2. In the case of multicast, where independent single are considered, the demodulation matrix $\mathbf{D}$ is diagonal. Thus the system equation can be expressed for each user i as

$$\hat{d_i} = D_{ii}\mathbf{H}_i\mathbf{w}s + D_{ii}n_i, \tag{4.3}$$

In order to maximize the SNR, the optimization problem for determining each element of $\mathbf{D}$ is

$$\begin{aligned} D_{ii,opt} &= \underset{D_{ii}}{\text{argmax}} \frac{E|D_{ii}\mathbf{H}_i\mathbf{w}s|^2}{E|D_{ii}n_i|^2} \\ \text{subject to: } &\begin{cases} ImD_{ii}\mathbf{H}_i\mathbf{w} = 0 \\ |D_{ii}|^2 = 1 \end{cases} \end{aligned} \tag{4.4}$$

where D_{ii} is the i^{th} element of the main diagonal of $\mathbf{D}$, $|.|$ is the absolute value of a scalar and $\mathbf{H}_{i1\times M}$ corresponds to the channel of user i *i.e.* the i^{th} row of matrix $\mathbf{H}$.

The solution of the problem for each user and the corresponding matrix form are expressed as

$$D_{ii,opt} = |\mathbf{H}_i\mathbf{w}|^{-1}(\mathbf{H}_i\mathbf{w})^* \tag{4.5}$$

$$\mathbf{D}_{opt} = diag(|\mathbf{H}_1\mathbf{w}|, ..., |\mathbf{H}_N\mathbf{w}|)^{-1} diag(\mathbf{H}\mathbf{w})^H \tag{4.6}$$

where $diag(.)$ is a diagonal matrix with the arguments on the diagonal.

The following subsection *matched filter*, *max-min algorithm* and *user selective matched filter* are presented.

4.1.1 Matched filter

In the case of a single user scenario, the matched filter optimization consists of finding the weight vector maximizing the SNR perceived at the receiver. In the case of multicast, the optimization consists of finding the weight vector maximizing the sum, or average, SNR perceived by users within the multicast group. Therefor the optimization system can be written as

$$\begin{aligned} \mathbf{w}_{opt} &= \underset{\mathbf{w}}{\text{argmax}} \frac{E||\mathbf{H}\mathbf{w}s||^2}{E||\mathbf{n}||^2} \\ &\text{subject to:} ||\mathbf{w}s||^2 \leq E_{tr}, \end{aligned} \tag{4.7}$$

where $\mathbf{w}_{opt}$ is the optimal weight vector, E_{tr} is the available transmit energy and $||.||$ is the Euclidean norm of the vector. This leads to an eigenvalue problem, with solution

$$\mathbf{w}_{opt} = \beta.(\text{principal eigenvector of } \mathbf{H}^H\mathbf{H}), \tag{4.8}$$

where $\beta = \sqrt{E_{tr}/\sigma_s^2}$ and σ_s^2 is the average symbol energy.

4.1.2 Max-min algorithm

The following optimization technique try to introduce fairness among the users by maximizing the minimum SNR within the group. It can be written as

$$\begin{aligned} \mathbf{w}_{opt} &= \underset{\mathbf{w}}{\text{argmax}} minSNR_i \\ \text{subject to:} &||\mathbf{w}s||^2 \leq E_{tr}, \end{aligned} \tag{4.9}$$

where $SNR_i = |\mathbf{H}_i\mathbf{w}s|^2/\sigma_n^2$ for $i = 1, ..., N$ and σ_n^2 is the noise power.

This problem is a quadratically constrained quadratic programming problem and does not have a quadratic solution as stated in [29]. To solve this problem the MATLAB toolbox *SeDuMi* [31] has been chosen. It doest so by removing one of the constraints of an equivalent optimization problem [32]. A deeper explanation of the implementation of this algorithm is given in section 5.1.

4.1.3 User selective matched filter

The user selective matched filter (USMF) is a heuristic algorithm which tries to improve the performance of the matched filter in the multicast scenario.

Assuming a point-to-point connection for each user i, to maximize the SNR, the ideal solution is the use of a matched filter *i.e.* $\mathbf{w} = \mathbf{H}_i^H$. The USMF stack these individual weight vectors within a matrix $\mathbf{H}^H$, but disregarding the weight vectors within it that do not positively contribute to the goal of maximizing the lowest SNR. Thus the algorithm can be written as

$$\mathbf{w}_{USMF} = \beta.\mathbf{H}^H\mathbf{P1} \tag{4.10}$$

where $\beta = \sqrt{(E_{tr}/\sigma_s^2).tr(\mathbf{P}^T\mathbf{H}\mathbf{H}^H\mathbf{P}\mathbf{1}\mathbf{1}^T)}$ and $\mathbf{P}_{N\times N}$ is a non-zero diagonal matrix, with elements $p_{ii} \in 0, 1$, for $i = 1, ..., N$.

There is N users and the diagonal elements of $\mathbf{P}$ are restricted to binary values, therefore there is a total of $2^N - 1$ possibilities. For a small group sizes, it is possible to evaluate all possible $\mathbf{P}$ matrices. From this evaluation, the one providing the highest minimum SNR can be chosen. Nevertheless, the complexity grows exponentially while the number of users increase. To make it computationally efficient, only a limited number of possibilities will be compute. The selection of those matrices is obtained by randomization.

4.2 MIMO techniques

An adaptive array with N antennas can provide different benefits to the system:

- A higher antenna gain for extended range and higher throughput.
- Multipath diversity gain for improved reliability.
- Interference suppression.
- Higher link capacity through the use of MIMO with spatial multiplexing.

Two of the mentioned MIMO advantages which can be exploited for this system are diversity gain and spatial multiplexing, but in this system analysis only diversity techniques will be explored and simulated.

The pre-processed SNR for this model is defined as

$$SNR = \frac{|h|^2.E_{tr}}{|n|^2} \tag{4.11}$$

with h the channel gain, E_{tr} the available transmit energy and n a Gaussian white noise.

4.2.1 MIMO 2x1

Using a simple transmission scheme with two antennas at the transmitter and one antenna at the receiver, the Alamouti scheme provides a communication system with diversity order equal to two. The most important point of this scheme is that it does not require any bandwidth expansion neither feedback from the MS, so it keeps the user's mobile station simple while applying diversity at the transmitter side.

Explaining the narrowband case, when the technique is applied for a single subcarrier, at a symbol period two signals are simultaneously transmitted from the two antennas. The symbols are transmitted using a combination of negation and complex conjugation. The technique could be represented as follows:

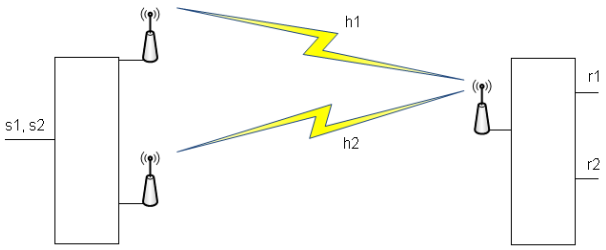

Figure 4.1: Alamouti's diagram

Suppose that (s_1,s_2) represent two consecutive symbols in the data to send; and the time is divided in two parts: t_1 for the first symbol time and t_2 for the second one. During t_1 the antenna Tx_1 transmits symbol s_1 and Tx_2 transmits symbol s_2. Next, during the second symbol time, Tx_1 transmits s_2* and Tx_2 transmits $-s_1$*. Assuming h_1 and h_2 the channel gain to the receiver from Tx_1 and Tx_2 respectively and that it is the same for both time slots t_1 and t_2, the received signal could be written as:

$$r_1 = h_1 s_1 + h_2 s_2 + n_1 \tag{4.12}$$

$$r_2 = h_1 s_2^* - h_2 s_1^* + n_2 \tag{4.13}$$

where n_1 and n_2 are the additive noise terms.

Based on this computation, the received vector r is formed by stacking the two consecutive samples $[r_1, r_2]^T$ in time $\mathbf{r} = \mathbf{Sh} + \mathbf{v}$ where the symbol block S and the channel matrix h have been introduced,

$$\mathbf{S} = \begin{bmatrix} s_1 & s_2 \\ s_2^* & -s_1^* \end{bmatrix} \tag{4.14}$$

$$\mathbf{h} = \begin{bmatrix} h_1 \\ h_2 \end{bmatrix} \tag{4.15}$$

The receiver computes the following signals to estimate the symbols s_1 and s_2:

$$x_1 = h_1^* r_1 - h_2 r_2^* = \left(|h_1|^2 + |h_2|^2\right) s_1 + h_1^* n_1 - h_2 n_2^* \tag{4.16}$$

$$x_2 = h_2^* r_1 + h_1 r_2^* = \left(|h_1|^2 + |h_2|^2\right) s_2 + h_2^* n_1 + h_1 n_2^* \tag{4.17}$$

These expression show that x_1 can be sent to a threshold detector to estimate symbol s_1 without interference from the other symbol. The post detection SNR, in order to show diversity's performance, is analyzed using the following formula:

$$SNR_{2\times1} = \frac{(|h_1|^2 + |h_2|^2).\frac{E_{tr}}{2}}{E[|n|^2]} \tag{4.18}$$

It is possible to notice the introduction of the diversity by looking at the difference between this SNR formulation and the one for the pre-processed SNR 4.11.

4.2.2 MIMO 2x2

Alamouti's transmit diversity scheme can be also used when two antennas are used at the mobile station side. The procedure has the same flow as the previous one and its received signal can be evaluated in the following way:

$$r_{11} = h_{11} s_1 + h_{12} s_2 + n_{11} \tag{4.19}$$

$$r_{12} = h_{11} s_2^* - h_{12} s_1^* + n_{12} \tag{4.20}$$

This is the representation for the first receive antenna. But in this case we have the same representation also for the second receive antenna.

$$r_{21} = h_{21} s_1 + h_{22} s_2 + n_{21} \tag{4.21}$$

$$r_{22} = h_{21} s_2^* - h_{22} s_1^* + n_{22} \tag{4.22}$$

This computation does not give any spatial multiplexing but it has 4^{th} order diversity that can be fully recovered at the receiver side without adding any big complexity to the receiver structure. The post detection SNR, for this technique, is analyzed using the following formula:

$$SNR_{2\times2} = \frac{(|h_{11}|^2 + |h_{12}|^2 + |h_{21}|^2 + |h_{22}|^2).\frac{E_{tr}}{2}}{E[|n|^2]} \tag{4.23}$$

4.2.3 MIMO 4x1

The Alamouti space-time code for transmit diversity can also be extended to the case of $2^k \times 2^k$ antenna elements (where k is any integer) as well as to asymmetrical arrays of the size $m \times n$ [33]. A 4×1 scheme is here analyzed in order to have a fair comparison with the beamforming algorithm analyzed in the report.

This scheme is implemented using the Alamouti's approach and the different variables are the following:

- Symbol block:

$$\mathbf{S} = \begin{bmatrix} s_1 & s_2 & s_3 & s_4 \\ s_2^* & -s_1^* & s_4^* & -s_3^* \\ s_3^* & s_4^* & -s_1^* & -s_2^* \\ s_4 & -s_3 & -s_2 & s_1 \end{bmatrix} \tag{4.24}$$

- Channel matrix:

$$\mathbf{H} = \begin{bmatrix} h_1 & h_2 & h_3 & h_4 \\ -h_2^* & h_1^* & -h_4^* & h_3^* \\ -h_3^* & -h_4^* & h_1^* & h_2^* \\ h_4 & -h_3 & -h_2 & h_1 \end{bmatrix} \tag{4.25}$$

- Receiver matrix:

$$\mathbf{z} = h^2 \begin{bmatrix} s_1 & + & Xs_4 \\ s_2 & - & Xs_3 \\ s_3 & - & Xs_2 \\ s_4 & + & Xs_1 \end{bmatrix} + \mathbf{H}^H \mathbf{v} \tag{4.26}$$

The 4.24 shows the space-time block word organization for transmitting four symbols. The element $[S]_{ik}$ is transmitted over the k-th antenna in the i-th time step. The result of this scheme has the equivalent form of the previous schemes but an interference term X is added due to the multiple transmission over different antenna of the symbols. Moreover, a matched filter $\mathbf{H}^H$is adopted at the receiver side in order to decouple the channel and have a full 4^{th} order diversity.
The fundamental assumption is to have a flat fading channel with channel gain equal to

$$h^2 = |h_1|^2 + |h_2|^2 + |h_3|^2 + |h_4|^2 \tag{4.27}$$

and the channel dependent real-valued random variable X which brings the partial interference among different channels. This means that X should be as small as possible in order to have a reliable communication.

$$X = 2Re\left(h_1 h_4^* - h_2 h_3^*\right)/h^2 \tag{4.28}$$

The post detection SNR is then analyzed:

$$SNR_{4\times1} = \frac{|h^2|^2 . \frac{E_{tr}}{4}}{|h^2|^2 . |X|^2 . \frac{E_{tr}}{4} + E[|\mathbf{H}^H . n|^2]} \tag{4.29}$$

It is important to notice that for different analyzed MIMO techniques, the energy of the transmitted symbol varies depending on the number of transmitted antennas. Moreover, halving the power of the transmitted symbol it is suppose to bring a difference of 3dB in the post detection SNR for the different MIMO techniques.

4.3 Channel Model

As described in section 2.2 to make an accurate model of our environment it is important to consider three main aspects that contribute to change the received power at the MS in a downlink connection: path loss, shadow fading and short scale fading.

Propagation models can be categorized in three types in respect to their approach: deterministic, stochastic and empirical. The deterministic models use the laws governing electromagnetic wave propagation to determine the received power at a particular location. Those models frequently involve a complete three dimensional map of the propagation environment. On the other hand, stochastic models model the environment as a series of random variables. Thus they need less information about the environment but are the least accurate model. The empirical models are based on observations and measurements. They permit to obtain a model closer to the reality.

It is possible to divide the empirical models into two subcategories: time dispersive and non-time dispersive. Time dispersive channels are defined for wide band systems and is based on the power delay profile of the channel. It permits to characterize the time dispersive characteristics of the channel *i.e.* the multipath delay spread of the channel. On the other hand non-time dispersive channels are defined for narrow band systems.

4.3.1 SUI model

The Stanford University Interim (SUI) models were selected for the design, implementation and testing of WIMAX technologies in six different scenarios SUI-1 to SUI-6[34]. The SUI model is an empirical and time dispersive model. The SUI models are divided in three types of terrains: A, B and C. Terrain A is appropriate for hilly terrain with moderate heavy foliage density. Terrain B characterizes either mostly flat terrains with moderate to heavy tree densities or hilly terrains with light tree densities. Terrain C suits for flat terrain with light tree densities.

Path loss and shadowing

The basic path loss equation with correction factors is

$$PL_{dB} = A + 10\gamma log_{10}\left(\frac{d}{d_0}\right) + X_f + X_h + s \quad \text{for } d > d_0 \tag{4.30}$$

where

- d is the distance between the BS and the MSs in meters,
- d_0 is a reference distance, usually $d_0 = 36$m,
- A is the intercept factor expressed as

$$A = 20log_{10}\left(\frac{4\pi d_0}{\lambda}\right) \tag{4.31}$$

- γ is equal to the pass loss exponent expressed as

$$\gamma = a - bh_b + c/h_b \tag{4.32}$$

where the parameter h_b is the BS height above ground in meters and should be between 10 m and 80 m. The constant used for a, b and c are given in table 4.1.

Model Parameter	**Terrain A**	**Terrain B**	**Terrain C**
a	4.6	4.0	3.6
b (m^{-1})	0.0075	0.0065	3.6
c (m)	12.6	17.1	20

Table 4.1: Numerical values for the SUI model parameters

Thus, for a given terrain type the pass loss exponent is determined by the BS height h_b.

- X_f is the correction factor for the operating frequency expressed as

$$X_f = 6.0log_{10}\left(\frac{f}{2000}\right) \tag{4.33}$$

with f the frequency in MHz.

- X_h is the correction factor for the MS antenna height expressed as

$$\begin{array}{rcll} X_h & = & -10.8log_{10}\left(\frac{h_r}{2000}\right) & \text{for Terrain types A and B} \\ & = & -20.0log_{10}\left(\frac{h_r}{2000}\right) & \text{for Terrain type C} \end{array} \tag{4.34}$$

where h_r is the MS antenna height above ground in meters.

- s is a lognormally distributed factor that is used to account for the shadow fading. According to [35] the probability density function is

$$p(s) = \frac{1}{\sigma_s\sqrt{2\pi}}e^{-\frac{s^2}{2\sigma_s^2}} \tag{4.35}$$

where σ_s is the deviation of the local mean (in dB) due to the location variability, the shadowing of the signal. The value of σ_s depends on the type of the terrain. According to [36] it is possible to obtain table 4.2.

Environment	σ_s ***(dB)***
Urban micro cell	2.3
Urban micro cell - Manhattan layout	3.1
LOS fixed station (rooftop to rooftop)	3.4
Urban macro cell	8
Sub-urban macro cell	8.2-10.6
Indoor small office	12

Table 4.2: Some typical values for the standard deviation σ_s of the shadowing [36]

Tapped delay line

The tapped delay line permits to represent the multipath fading of the channel. It is modeled as a tapped-delay line with 3 taps with non-uniform delays. Each gain associated with each tap is characterized by a Ricean distribution. In the absence of any dominant paths, $K = 0$ and the Ricean distribution reduces to a Rayleigh distribution.

The delay spread for each tap and their respective power are represented in tables 4.3 and 4.4.

Channel model	**Tap 1**	**Tap 2**	**Tap 3**	**RMS delay spread**
	μs			
SUI-1	0	0.4	0.9	0.111
SUI-2	0	0.4	1.1	0.202
SUI-3	0	0.4	0.9	0.264
SUI-4	0	1.5	4	1.257
SUI-5	0	4	10	2.842
SUI-6	0	14	20	5.240

Table 4.3: Delay spread of SUI channels

Channel model	**Tap 1**	**Tap 2**	**Tap 3**
	dB		
SUI-1	0	-15	-20
SUI-2	0	-12	-15
SUI-3	0	-5	-10
SUI-4	0	-4	-8
SUI-5	0	-5	-10
SUI-6	0	-10	-14

Table 4.4: Tap power of SUI channels

K-factor

The narrow band received signal fading can be characterized by a Ricean distribution. The key parameter of this distribution is the K-factor, defined as the ratio of the fixed component power and the scatter component power.

As defined in [37] and [23], the K-factor decreases as the distance between the MS and the BS increases, and as the antenna bandwidth increases. The analysis of K-factors that meet the requirement that 90% of all locations within a cell have to be services with 99.9% has been accomplished by [23]. The calculation of K-factors for this scenario is complex due to the numerous parameters involved. However it is possible to obtain approximate values which are summarize in table 4.5.

Channel model	**Tap 1**	**Tap 2**	**Tap 3**
SUI-1	4	0	0
SUI-2	2	0	0
SUI-3	1	0	1
SUI-4	0	0	0
SUI-5	0	0	0
SUI-6	0	0	0

Table 4.5: 90% K factor of SUI channels

Antenna Correlation

In scenarios where multiple antenna are transmitting/receiving data, an antenna correlation has to be considered within the SUI channel model. Antenna correlation parameter is defined as the correlation coefficient between signals received at different antenna elements. The received baseband signals are modeled as two complex random processes X(t) and Y(t) with an envelope correlation coefficient of:

$$\rho_{env} = \left| \frac{E\left\{(X - E\left\{X\right\})(Y - E\left\{Y\right\})*\right\}}{\sqrt{E\left\{|X - E\left\{X\right\}|^2\right\} E\left\{|Y - E\left\{Y\right\}|^2\right\}}} \right| \tag{4.36}$$

Since the envelope correlation coefficient is independent of the mean, only the random channel components can be considered for its calculation.

As said before, the channel is modeled as tapped-delay system. The number of taps into the SUI model is three and they are composed by different tap coefficients and delays. The antenna correlation can be then related to the individual tap correlation. First, a set of channel coefficient are created and then it is possible to correlate the coefficients with each other and correlate them with the antenna correlation parameter.

Doppler Spectrum

Following the Ricean power spectral density (PSD) model, it is possible to define the scatter and fixed doppler spectrum component. Usually in wireless communication system the PSD of the scatter is distributed around f=0 Hz. A rough approximation of it, is coming from:

$$S\{f\} = 1 - 1.72f_0^2 + 0.785f_0^4 \tag{4.37}$$

$$where|f_0| \leq 1 \tag{4.38}$$

The parameter f_0 is coming from the maximum Doppler frequency f_m and is equal to: $f_0 = f/f_m$. In order to generate the correct set of channel coefficients, a filter which amplitude frequency response is deriver from the previous formula.

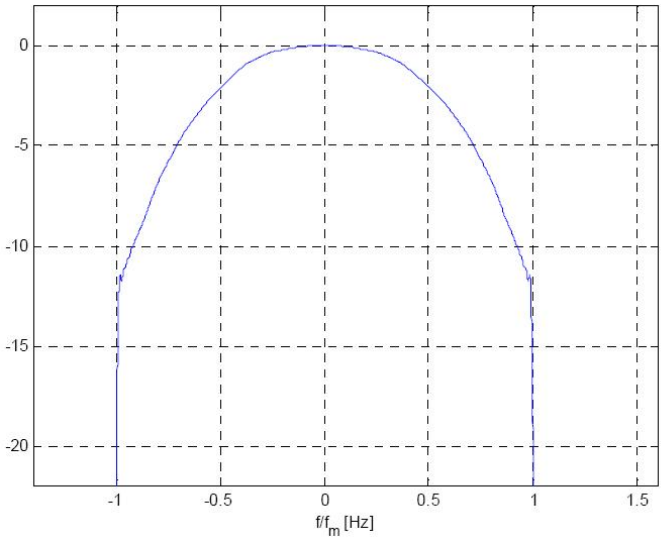

Figure 4.2: Rounded Doppler PSD model

THIS PAGE IS INTENTIONALLY LEFT BLANK

Chapter 5

Simulation and Results

This chapter presents the results of our implemented model. First the implementation of the existing beamforming algorithms will be tested. Then the proposed complete CSI and partial CSI analysis will be investigated using the most efficient beamforming technique. Furthermore, in order to improve the multicast performance, the proposed temporary dropping of the worst users will be analyzed. At last, existing MIMO techniques will be adopted, studied and compared with the beamforming algorithms.

5.1 Verification of the existing beamforming algorithms

As described in section 4.1, the beamforming algorithms used in this project are the *matched filter*, *max-min* and *USMF*. This section will provide an analysis of these simulated algorithms. First the implementation of those algorithms will be discussed. Second a narrowband analysis will be made in order to compare our code with the reference paper [29]. Finally a wideband analysis will permit to see the result of the extension of the analysis of those algorithms to the model we analyzed.

5.1.1 Implementation issues for the beamforming algorithms under consideration

The implementation of the *matched filter* and *USMF* is pretty simple thus it will not be explained in detail in this section. However the implementation of the *max-min* algorithm is more complex. It is divided in two parts: a semidefined programming problem (SDP) [28],[29],[30] and a randomization part. The SDP problem is defined as the *max-min* problem with one of the constraints relaxed. This SDP problem is solved using SeDuMi [31] a MATLAB toolbox for optimization over symmetric cones. If the rank of the solution of this SDP problem is one then the principal component will be the optimal solution to the original problem. If not then the trace of the solution of the SDP problem is a lower bound on the power needed to satisfy the power constraints of our problem. A way to generate good solutions of the original *max-min* problem

using the solution of the SDP problem is to use randomization. This process generates a set of candidate vectors from the solution of the SDP problem, from which the best solution is selected [32]. Considering $\mathbf{X}_{opt}$ as the solution of the SDP problem given by SeDuMi thus the eigendecomposition of this solution is $\mathbf{X}_{opt} = \mathbf{U}\mathbf{\Sigma}\mathbf{U}^H$. Where $\mathbf{U}$ is a diagonal matrix of eigenvalues and $\mathbf{\Sigma}$ columns are the corresponding eigenvectors so that $\mathbf{X}_{opt} * \mathbf{\Sigma} = \mathbf{\Sigma} * \mathbf{U}$. The candidates will be chosen as $\mathbf{w}_l = \mathbf{U}\mathbf{\Sigma}^{\frac{1}{2}}\mathbf{e}_l$ where $\mathbf{e}_l$ are independent random variables, uniformly distributed on the unit circle in the complex plane *i.e.* $[\mathbf{e}_l]_i = e^{j\theta_{l,i}}$, where the $\theta_{l,i}$ are independent and uniformly distributed on $[0, 2\pi]$. The number of those candidates is fixed to 10000.

The first step of the simulation, in order to manage the time spent to simulate, is to analyze the run time of each algorithm for each number of users analyzed. The results are shown in figure 5.1.

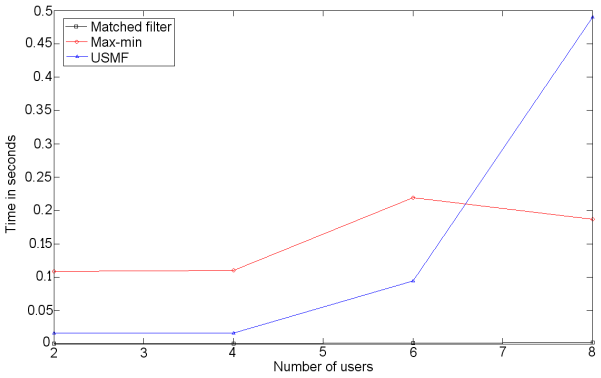

Figure 5.1: Run time of the various algorithms

It is possible to notice that the run time of the *USMF* algorithm is increasing exponentially with the number of users. This is due to the creation of the $2^N - 1$ possibilities for the matrix P.

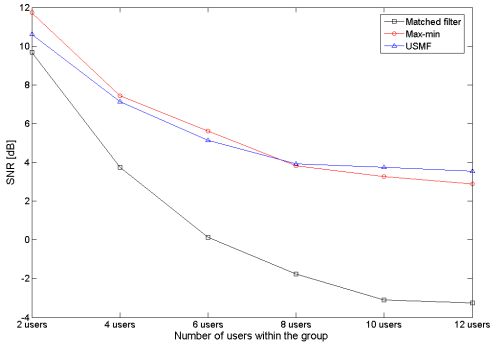

Figure 5.2: Minimum SNR for 20 repetitions

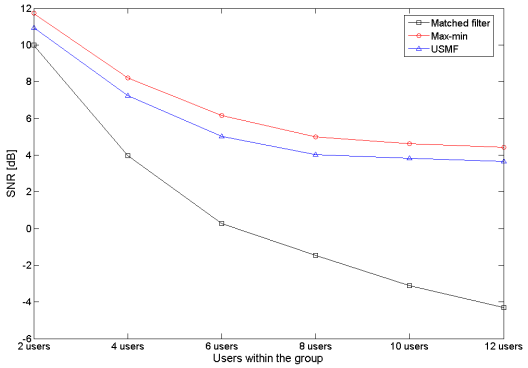

Figure 5.3: Minimum SNR for 500 repetitions

The second step of this simulation is to look at the mean of 20 repetitions of the algorithms. Thus it is possible to see their respective behaviors and to verify that the algorithms are working fine without spending to much time in computation. The results are shown in figure 5.2.

It is possible to see that our main idea, that the *max-min* algorithm is more efficient than the *USMF* one which is also more efficient than the *matched filter* one. Nevertheless the results shown are not very accurate but permit to have an idea of the behavior of the algorithms. It is also interesting to notice that for 12 users and for this amount of repetitions, the *USMF* algorithm is more efficient than the *max-min* one. This is due to the few amounts of repetitions.

To obtain more reliable information it is necessary to increase the number of repetitions. The results shown below are based on 500 repetitions and thus are more representative. Such results are shown in figure 5.3.

It is shown in figure 5.3 that the more users there are in a group, the lower the optimized SNR is. It is important to notice that the *matched filter* algorithm maximizes the average SNR whereas the *max-min* and *USMF* algorithms try to provide fairness among the users. This explains the poor performance of the *matched filter*. Indeed the eigendecomposition of the channel matrix $\mathbf{H}$ as described in 4.1 of $\mathbf{H}^H\mathbf{H}$ leads to a large ratio of the largest to the smallest singular values. It means that more energy is concentrated on the principal eigenmode. It results on that some users will achieve a very low SNR in order to let other users achieving a high SNR. On the other hand, the *max-min* and *USMF* algorithms achieve a better SNR by including fairness among the users *i.e.* some users will not achieve a very low SNR to permit to some users to achieve a high SNR. It is shown that it leads to a better performance in a multicast scenario.

Thus in a multicast scenario the *max-min* algorithm is the most efficient and fair one. The *USMF* algorithm permits to obtain a close approximation of the optimum solution of the *max-min* problem.

5.1.2 Narrowband analysis

In order to simulate a narrowband system we analyzed just a single tap of the SUI-4 model. In this way the channel under consideration is sufficiently narrow that its frequency response can be considered flat.

◇ The first step for a fair analysis is the comparison of the narrowband with the one from the reference [29] used in section 4.1. The first part of the narrowband analysis is to observe the results with the users at the same SNR. The specifications for this comparison are:

- narrowband system,
- 1 cell of 1400m,
- 4 antennas at the BS,
- 1 antenna at the MS,
- all users with the same initial SNR of 10 dB,
- no shadowing map.

In order to have the same approach than the reference paper, the users have been forced to be on a circle around the BS and the shadowing map has been omitted. In this way only the fast fading is changing the value of channel gain and our scenario is comparable with the one from the analyzed paper.

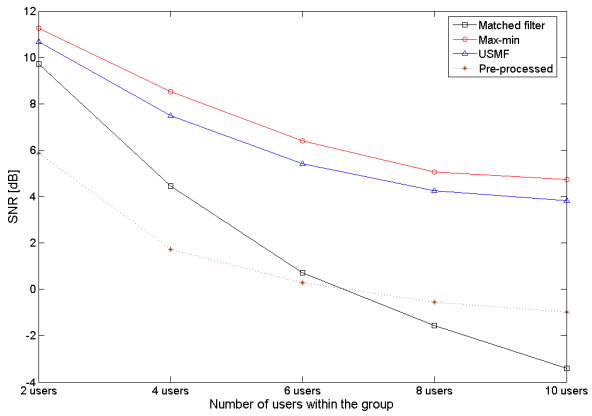

Figure 5.4: Impact of the group size on the minimum SNR over all the users for the same initialized SNR of 10 dB in a cell of 1400m without shadowing for a narrowband system

The curves represented in figure 5.4 have the same characteristics as the one proposed in the reference [29]. Thus this is a proof that the algorithms we are using have a similar behavior than the ones in the analyzed paper. It is important to highlight that the matched filter is decreasing the pre-processed SNR. Indeed this algorithm is not bringing fairness among the users, it is only stacking the matched filter of the different users in a single weight. For a more

detailed explanation of the implementation of those algorithms in our system refer to the previous section 5.1.1.

◇ The second part for the narrowband analysis is to add the shadowing to users with the same path-loss *i.e.* at the same distance from the BS. For this analysis the shadowing map is taken into account. The comparison specifications are now :

- narrowband system,
- 1 cell of 1400m,
- 4 antennas at the BS,
- 1 antenna at the MS,
- all users with the same initial SNR of 10 dB,
- shadowing map.

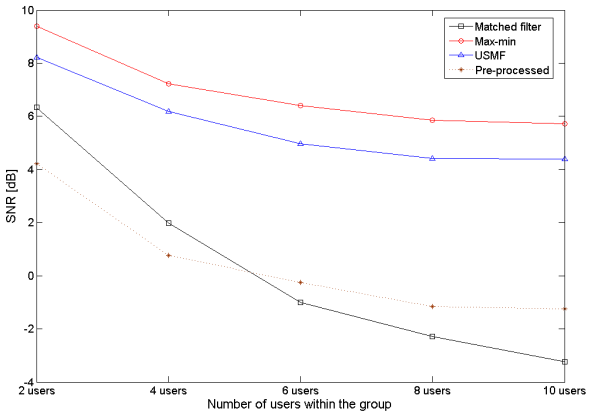

Figure 5.5: Impact of the group size on the minimum SNR over all the users for the same initialized SNR of 10 dB in a cell of 1400m with shadowing for a narrowband system

As in the previous figure 5.4 it is possible to notice that the results represented in figure 5.5 still have the same behavior of the reference paper [29]. We can also observe that due to the shadowing the performance of the beamforming algorithms are a bit worse, because in some points the channel condition are affected by a higher loss due to the shadowing.

5.1.3 Wideband analysis

In order to simulate a wideband system we analyzed the complete SUI-4 model because it refers itself to a wideband system.

◇ The second step for the analysis is the comparison of our wideband model with the one from the reference [29]. The first part of this analysis is to observe the results with the users at the same SNR. The comparison specifications are:

- wideband system,
- 1 cell of 1400m,
- 4 antennas at the BS,
- 1 antenna at the MS,
- all users with the same initial SNR of 10 dB,
- no shadowing map.

As stated previously in section 5.1.2, the users are forced to be on a circle over the BS and the shadowing map has been omitted. In this way all the users achieve the same SNR.

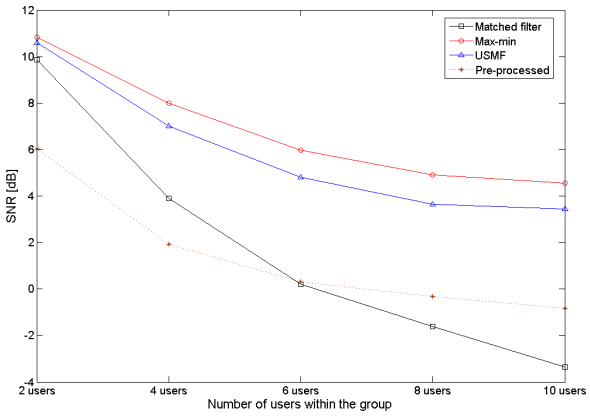

Figure 5.6: Impact of the group size on the minimum SNR over all the users for the same initialized SNR of 10 dB in a cell of 1400m without shadowing for a wideband system

The curves represented in figure 5.6 have the same characteristics as the one shown for the narrowband analysis (figure 5.4). Thus the implemented beamforming algorithms have the same behavior for the narrowband and the wideband cases.

◇ The second part for the wideband analysis is, as previously done for the narrowband case, to take the users at the same distance from the BS and include the shadowing. The comparison specifications are now :

- wideband system,
- 1 cell of 1400m,
- 4 antennas at the BS,
- 1 antenna at the MS,
- all users with the same initial SNR of 10 dB,
- shadowing map.

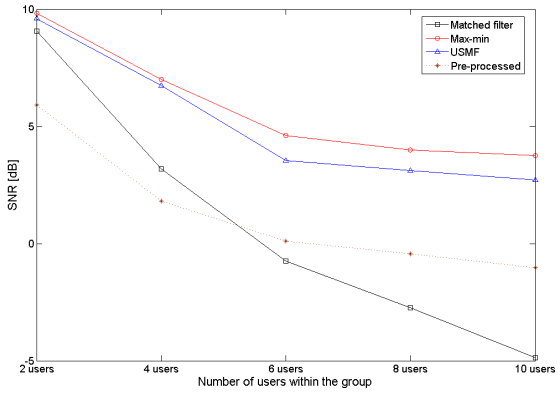

Figure 5.7: Impact of the group size on the minimum SNR over all the users for the same initialized SNR of 10 dB in a cell of 1400m with shadowing for a wideband system

As for the narrowband case, the result of the wideband case with shadowing are a bit worse than the one without. This is due to the random behavior of our implemented shadowing map.

◇ The last part for the wideband analysis is to take the users at different distances from the BS. The comparison specifications are now :

- wideband system,
- 1 cell of 1400m,
- 4 antennas at the BS,
- 1 antenna at the MS,
- all users with different initial SNR,
- shadowing map.

Those specifications will be used for the simulation of the global model including the channel model and the beamforming model. For more precision about those delimitations refer to section 3.3.

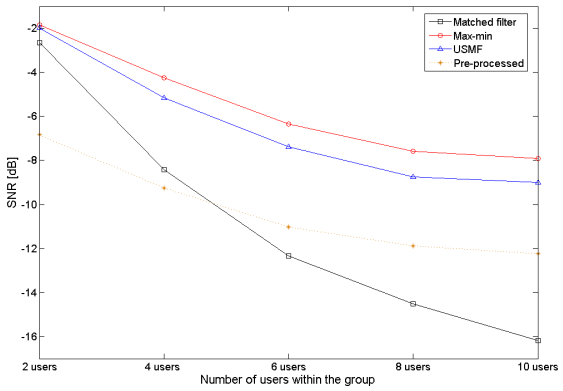

Figure 5.8: Impact of the group size on the minimum SNR over all the with different initialized SNR in a cell of 1400m for our model

The figure 5.8 has still the same behavior than the one previously presented. However the results are worse than the ones from figures 5.6 and 5.7. Indeed now that the SNR of the users is not fixed anymore to 10dB they can achieve a worse SNR. This leads to a decrease in the group performance and this for the different group sizes analyzed. An interesting figure to check the distribution of the initial SNR for the different cell sizes used in this report is its cumulative distribution function (Cdf).

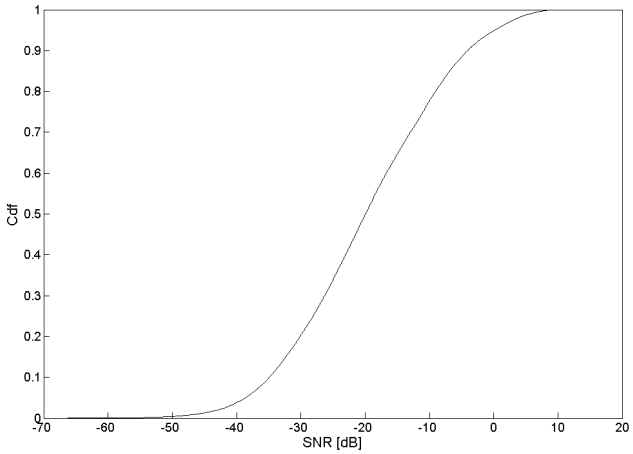

Figure 5.9: Cdf of the initial SNR for a cell size of 1400m

It is important to precise that the values presented in figure 5.10 used for this Cdf are taken in a group of 10 users. The fact that the *matched filter* is decreasing the SNR, as explained before, is due to the fact that this algorithm is not bringing fairness among the users.

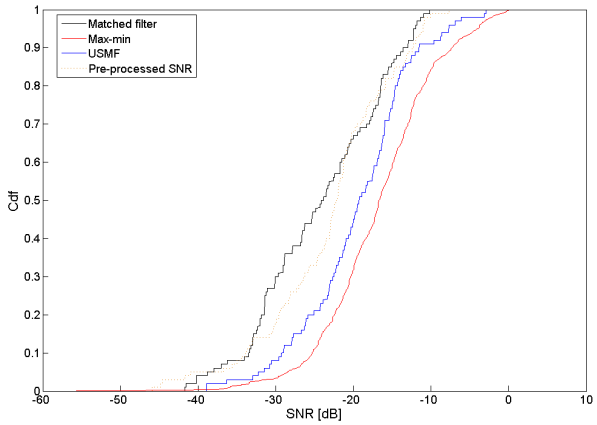

Figure 5.10: Cdf the SNR before and after the algorithms' optimization of the user in the worst condition for a cell of 1400m

As a conclusion we can state that the *max-min* algorithm is achieving the best performance. Thus for the rest of this report, only the *max-min* algorithm will be taken into account.

5.1.4 Impact of the cell size on the algorithms performances

Before analyzing the impact of the cell size on the algorithms performances, the impact of the cell size on the initial SNR is presented.

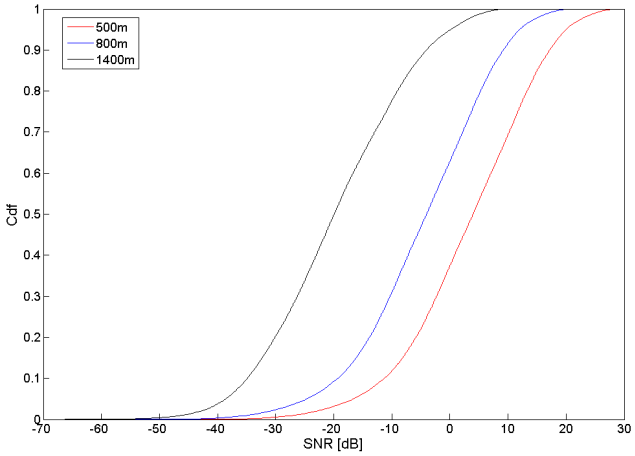

Figure 5.11: Cdf of the initial SNR for different cell sizes

We can see in figure 5.11 that for an increasing cell size the probability to achieve an initial low SNR is increasing. This is due partly due to the behavior of the path-loss. We can also look at the Cdf of the SNR before and after the algorithms' optimization of the user in the worst condition.

To analyzed the impact of the cell size on the efficiency of the *max-min* algorithm, it is interesting to look at the minimum SNR after optimization.

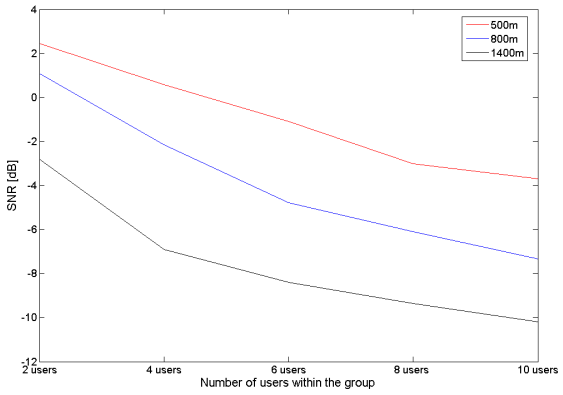

Figure 5.12: Minimum SNR after the *max-min* algorithm for different cell sizes

It is possible to see on figure 5.12 that for an increasing cell radius, the minimum SNR within the group is decreasing. Indeed increasing the cell size is increasing the possibility to obtain a user in a very bad condition. Thus the post-processed SNR is for, an increasing cell radius, decreasing, regardless to the number of users within the group.

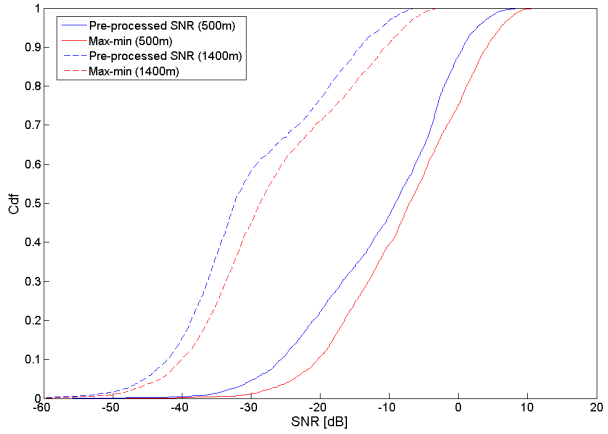

Figure 5.13: Cdf of the SNR of the user in the worst condition before and after optimization by the *max-min* algorithm for different cell sizes for a group of 10 users

Nevertheless the number of persons within a group is also a factor that is decreasing the minimum SNR within this group. This is due to the fact that the efficiency of the beamforming algorithms is depending on the group size as stated in section 4.1. It is also interesting to look at the Cdf of the SNR of the user in the worst condition in a group of 10 users before and after optimization performed by the *max-min* algorithm for different cell sizes.

Figure 5.13 shows us that the absolute efficiency of the *max-min* algorithm is not influenced by the cell size. Indeed the cell size is not taken into consideration while computing the *max-min* solution.

5.2 MIMO analysis

For a fair comparison of the multiple antenna system, also the MIMO case has been analyzed and the result are here presented and compared with the beamforming ones. Starting from the easiest way of implementation of a MIMO system which is represented by the 2x1 system, the 2x2 system is analyzed. Both system are based on the presented Alamouti technique. Moreover, for a fair comparison among the 4x1 beamforming system and the MIMO one, a MIMO 4x1 system is analyzed.

In order to have an idea on how those technique are performing, the post-MIMO SNR for the analyzed techniques are plotted and compared with the pre-MIMO SNR. In this way it is possible to get knowledge also of the relative advantage that each MIMO technique is bringing into the system and not just the overall comparison of different MIMO techniques.

The following picture shows the result of a single user analysis plotting one subcarrier's SNR variation among all the different positions:

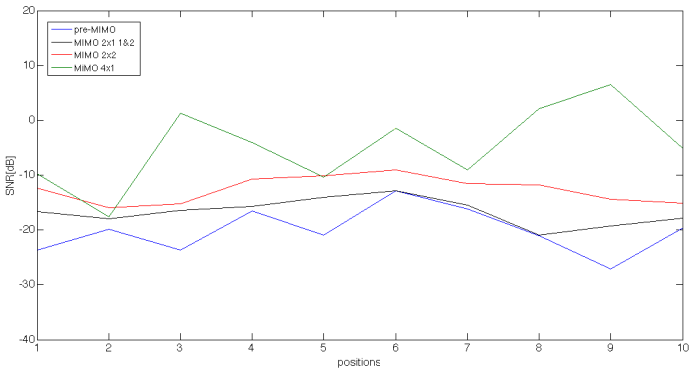

Figure 5.14: Single user's SNR analyzing one subcarrier over all the positions

It is possible to notice different performances coming out from the different MIMO techniques. The pre-MIMO SNR (blue line) shows the antenna-to-antenna connection analyzing only a single antenna at the transmitter (Trans-

mitting antenna number one) connected to the single antenna at the receiver side without any MIMO technique applied. This line is the worst one for every user's position due to the nature of the MIMO system which optimize the connection by using multiple antenna. On top of it, the other MIMO techniques take place and it is possible to notice that the increase of the performance is directly connected to the increasing number of antennas in the system.

In order to have a complete analysis of it, also the other connection components have been analyzed and the following picture shows the complete result:

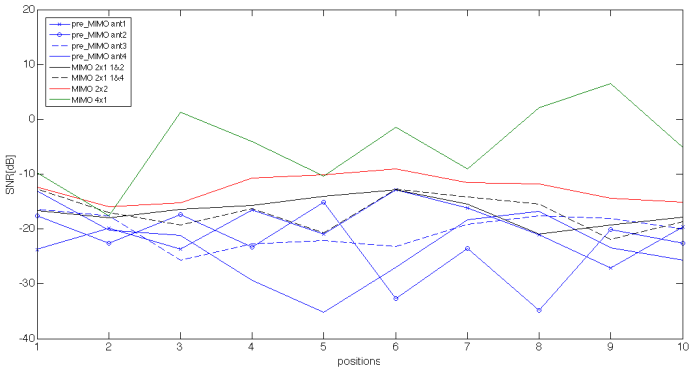

Figure 5.15: Single user's SNR analyzing one subcarrier over all the positions

In this picture it is possible to distinguish the four different line of the 1x1 connection between the BS and the MS which show the channel condition of the four different transmitting antennas. Moreover, also two of the possible combination of MIMO 2x1 technique are analyzed. By having different antenna correlation values, the case of first-second and first-fourth antennas are computed.

The best performance are reached by the 2x2 and 4x1 techniques which are the most complex analyzed in this report. It is also important to notice that this picture is not more than a snapshot of the single user's situation inside the cell. In other analyzed situation the 4x1 MIMO technique is not always better than the other techniques because of its particular composition. As it is possible to see from equation 3.4 the interference term X is affecting the SNR calculation depending on the different channels condition. Sometimes it could happen to have a particular case where the 4x1 MIMO technique has even worst result than the 1x1 connection.

In order to respect the statistical approach of this project, a large number of scenarios has been analyzed (50 workspaces) and the results plotted in pictures 5.16 and 5.17 where the minimum SNR for an increasing number of users has been analyzed among different cell sizes.

From those pictures it is possible to see that the 4x1 MIMO technique is

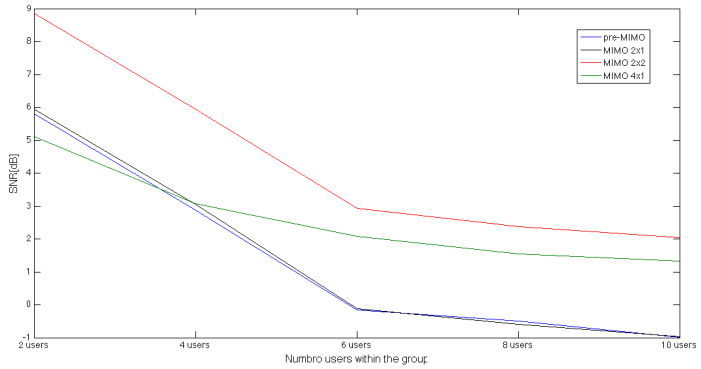

Figure 5.16: Minimum group's SNRs for cell size of 500m

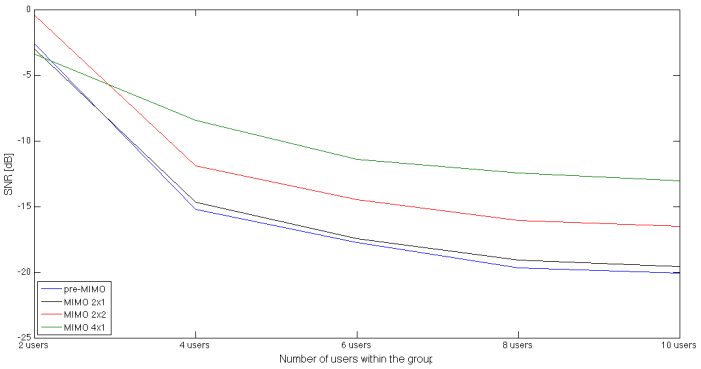

Figure 5.17: Minimum group's SNRs for cell size of 1400m

better performing for a larger number of user in a larger cell size comparing with the 2x2 technique. This is probably due to the particular behavior of the 4x1 technique explained in the above paragraph. If the multicast group is composed only of two users, there is more probability that the particular behavior affect the user in the worst condition. This is going to drastically reduces the performance of the multicast optimization. In the other case, large number of users within the group, the probability of having the worst user being affected by this event is lower.

Moreover, analyzing the distribution of the minimum SNR per group, as shown in figure 5.18, it is possible to notice that the 2x2 technique is absolutely performing better than the 4x1 technique from the multicast point of view. Nevertheless, the use of another antenna at the receiver is a very important topic nowadays for the manufacture companies. The comparison between cost/performance has to be done in a very detailed analysis because, as it is possible to see from the post detection minimum SNRs distribution 5.18, the performance are very close and comparable with each other in certain system condition.

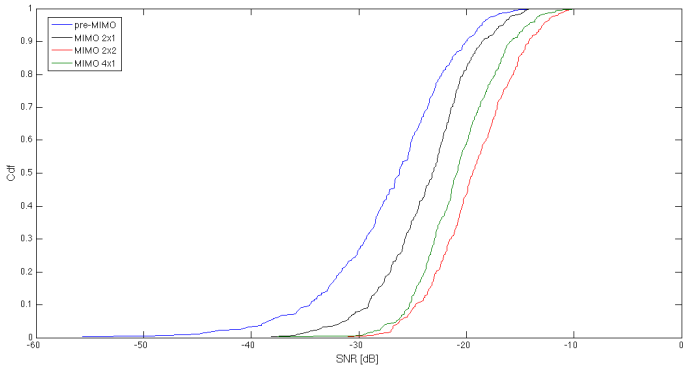

Figure 5.18: Cdf of the minimum group's SNRs for cell size of 1400m

5.2.1 Impact of the cell size in MIMO

It is important to analyze also the impact of the different cell sizes for the MIMO technique as it has been done for the beamforming analysis. Using the same approach as the beamforming case, the comparison has been done using the post detection minimum SNRs within a group us users for the different cell sizes. It is possible to notice, as the basic characteristic of wireless communications, that the SNRs values are as low as larger the cell size is.

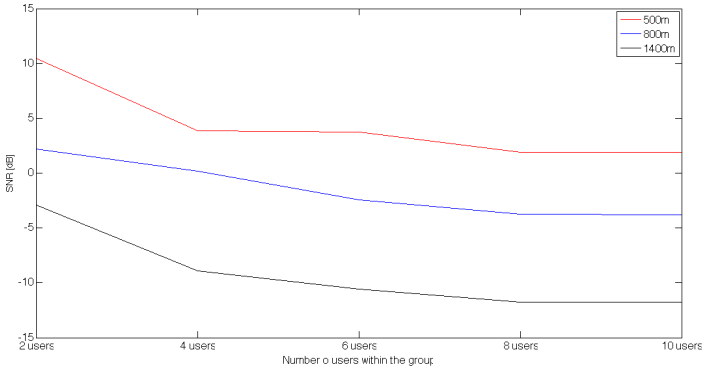

Figure 5.19: Minimum group's SNRs for different cell sizes for a 2x2 MIMO system

It is also possible to analyze the distribution of the post detection minimum SNR and the pre SNR in order to obtain a more statistical characteristic of the MIMO technique in the case of multicast services.

The picture 5.20shows two different cell size performance regarding 500m and 1400m. It is possible to see that the relative performance of the 4x1 technique and the 2x2 technique have almost the same behavior for a larger cell size. For the smaller cell size the 4x1 techniques have a very bad performance for higher

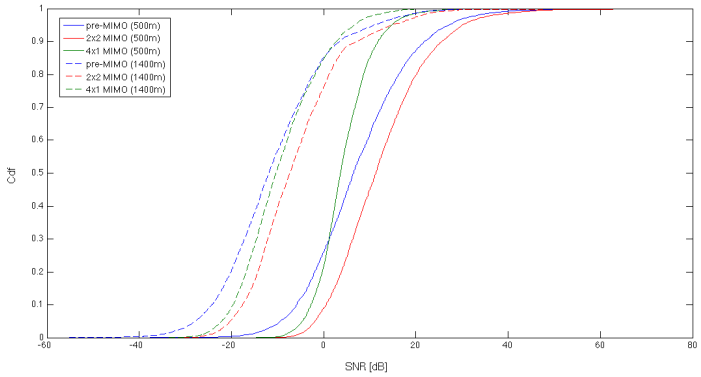

Figure 5.20: Cdf of the minimum group's SNRs for different cell sizes

SNR values. This is due to the mentioned behavior of the 4x1 which does not give stability to this technique. The comparison of the performance need also to take into account the different behavior of the 4x1 technique based on what is requested by the system: the 4x1 technique has good result for a larger cell size on the median values of the distributions. On the other hand, for small cell size, it has a good result for an outage of results (up to 30%)

5.3 Complete CSI - Partial CSI analysis

A major limiting factor in the resource allocation in wireless communications is the amount of channel state information (CSI) available at the transmitter, particularly in multiuser systems where the feedback from each user terminal must be limited. Using the CSI, the BS is able to know what the actual channel condition of the MS it wants to serve is, in order to adapt the modulation scheme in the next time/position. Also the assumption that the CSI is perfect at the pilots is made.

A balanced solution for the CSI organization could be the use of partial CSI: sending feedback along pre-specified subcarriers (pilots) instead of sending the feedback for every single subcarrier. This approach could provide sufficient information for the transmitter to efficiently utilize multiuser diversity in time, frequency, and space. Herein, we show the different performance achievable using complete CSI and partial CSI. We still consider the downlink of the same communication system we used till. The channel state information are organized over pilot subcarriers and applied to the following data-subcarriers as shown in the following pictures. This is the organization of the partial CSI, following what the WiMAX-Mobile standard states.

As shown in table 2.4 in WiMAX technology the number of pilot subcarriers is fixed to 60. The representation of the subcarriers in WiMAX technology is shown in figure 5.21.

The analysis has been made using all the previously studied beamforming

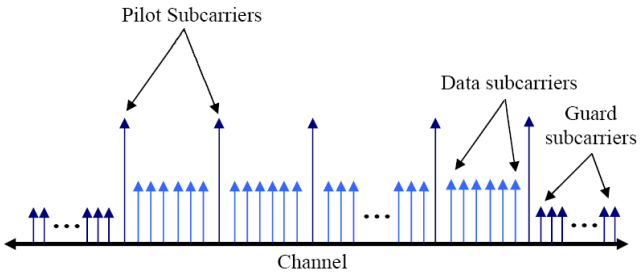

Figure 5.21: Representation of the subcarriers in WiMAX technology

algorithms in order to have a fair comparison among all the algorithms. Using exactly the same environment, both CSI configurations have been analyzed and the results are shown in figures 5.22 and 5.23.

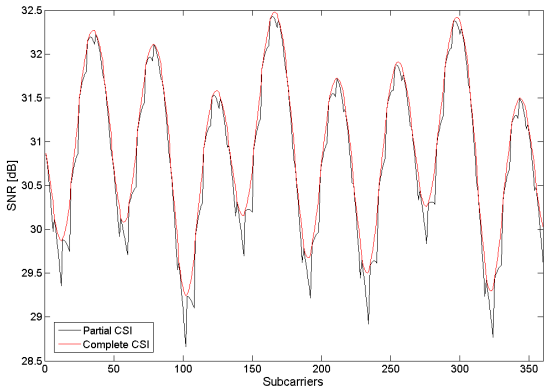

Figure 5.22: Complete CSI - partial CSI using USMF

The figures show the post-processing SNR for a group of four users within the cell. The algorithm used in this case is the USMF and it is clear that the mean value among all the subcarriers is always higher for the complete CSI. The values for the partial CSI are very close especially for subcarriers next to the pilot ones. This is due to a better approximation of the channel state while, for the subcarriers less close to the pilots ones, a more rough approximation is made. A zoom of the previous plot is shown in figure 5.23 highlighting the behavior of both curves.

The same behavior is coming out also for the Matched Filter algorithm. For the case of *max-min* algorithm, we encountered some particular behavior. The out coming values for the partial CSI are not always lower than the complete CSI one. As a matter of fact, as said in appendix 5.1.1 the *max-min* algorithm is divided in two parts: the first part finds solutions to the semi definite problem (SDP) while the second one based on randomization. With that approach, the solution which gives the weight for the tx antennas is the optimal solution over a

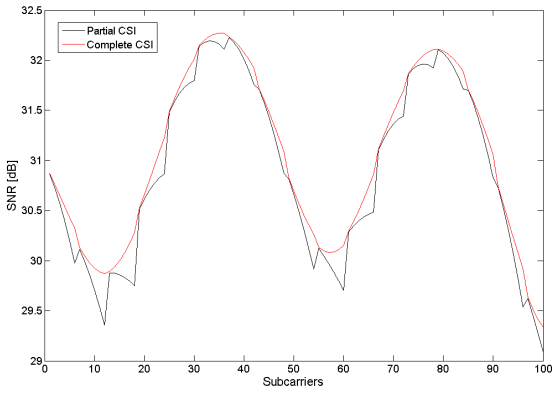

Figure 5.23: Complete CSI - partial CSI using USMF

set of produced candidate weight vectors. This means that is not "the" best solution, but the optimal among the created candidates. Because of this, different series of candidates can lead to different behavior of the beamforming algorithm.

Looking at the comparison between the complete and the partial CSI, the first one is going to be higher than the second one for some of the subcarriers. For this algorithm we are analyzing the minimum SNR among all the subcarriers. As a matter of fact the *max-min* algorithm is maximizing the minimum SNR. Indeed if the algorithm could find the true optimal, the curve representing the complete CSI will always be above the curve representing the partial CSI.

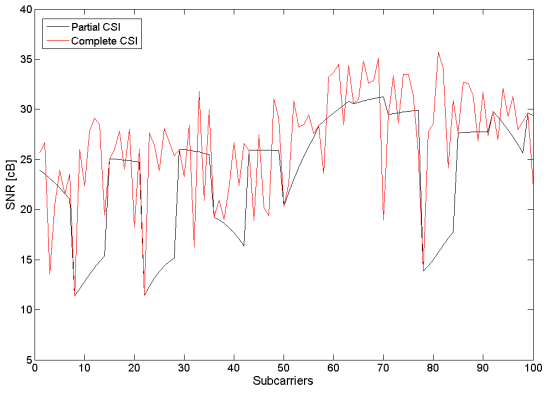

Figure 5.24: Complete CSI - partial CSI using *maxmin* algorithm

As shown in picture 5.24 some of the points calculated with the weights processed for the partial CSI are going to be higher than the complete CSI ones. This is due to the SDP solutions and the randomization as developed in appendix 5.1.1.

As a conclusion we can state that the use of partial CSI is not affecting the performance of the entire system while drastically decreasing the complexity of the calculation.

5.3.1 Pilot loss factor

In order to have a better accuracy of the model it is necessary to find the pilot loss factor. This factor is the average difference between the minimum subcarrier SNR computed with it optimized pilot weight and the same subcarrier SNR computed with it respective pilot weight. Furthermore the channel capacity of a group of data subcarriers is also determinated based on the pilots ones. The figure 5.25 illustrates this factor loss. The dotted red lines represent the full CSI case and the blue ones are calculating using the pilot weights.

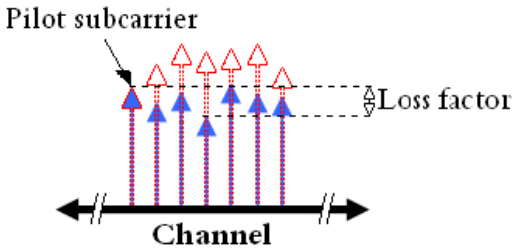

Figure 5.25: Illustration of the factor loss

After calculation over a large number of realizations we found that the mean value of the lost factor is equal to 9.5%. Thus to keep the simulations realistics this path loss factor of 9.5% will be applicated to the various groups of data subcarriers. As shown in figure 5.26 the loss factor of 9.5% permits to a good approximation of the values for the data subcarriers without CSI.

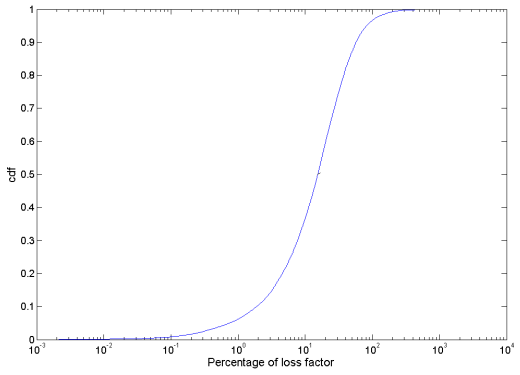

Figure 5.26: Cdf of the loss factor

As a conclusion we can say that we can use the pilot loss factor with the value of 9.5% and keep a realistic approach. Furthermore the computation time is greatly reduced.

5.4 Dropping of the users analysis

In order to achieve a better channel capacity for a multicast group, it is possible to drop the users which are in the worst conditions. As a matter of fact it is the user in the worst conditions that will lead to a decrease of the mean value of efficiency within the group. Therefore dropping the users in worst conditions should lead to an higher efficiency.

Two different ways to drop those users will be investigated:

- dropping the worst users for all the subcarriers,
- dropping the worst user for each subcarrier.

The analysis of the dropping of the users have been computed only for the beamforming *max-min* algorithm. The users are dropped before the application of the beamforming algorithm. This is due to our system model 4.1 which implies that the resulting optimized vector relies on the input channel vector $\mathbf{H} \in \mathbb{C}^{N \times M}$, where N is the number of users and M the number of transmitting antennas. Thus indeed the beamforming optimization depends on the size of the group.

It is also important to highlight the fact that the worst users are dropped based on the preprocessed SNR. Indeed it would have been possible to drop the users based on the results of the *max-min* algorithm processed for all the users. However to keep the processing time tolerable this solution was avoided.

In order to keep a respectable amount of users within the group, only the case where one and two users within a group will be dropped. All the plots presented below are based on various independent simulations of users moving through 10 positions. Different sizes of cell will also be investigated. Furthermore only the *max-min* algorithm will be investigate in this section since it is the algorithm achieving the best performances as explained in appendix 5.1.1. For the formulas used to obtain the results refer to section 3.4.

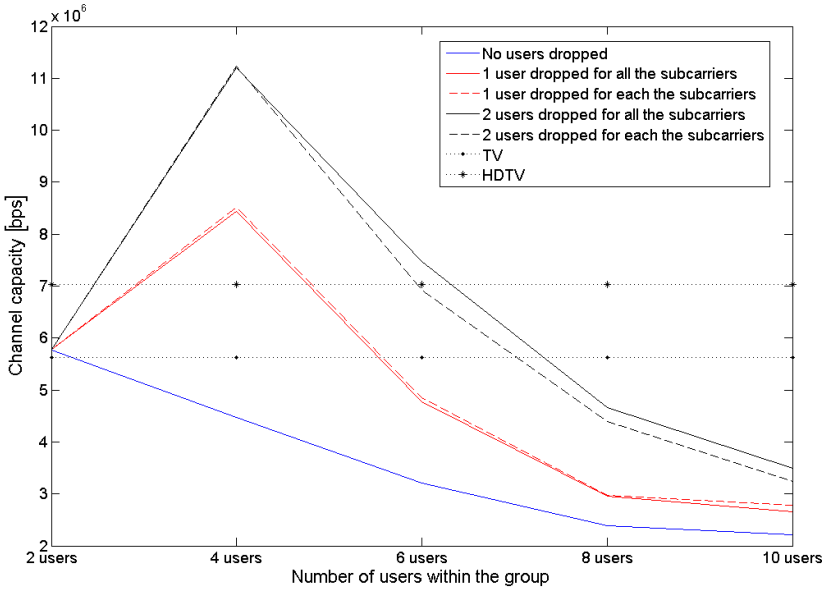

Figure 5.27: Channel capacity in a cell of 500m with users dropped

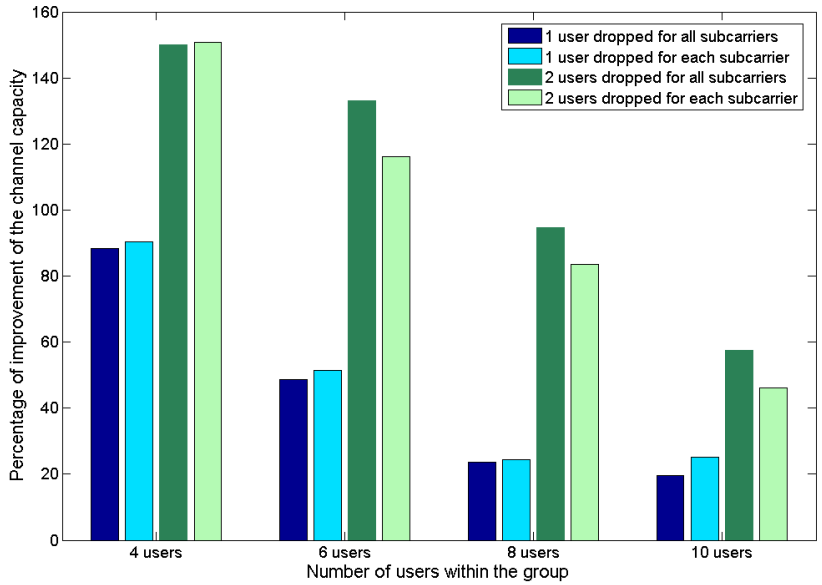

Figure 5.28: Percentage of the channel capacity improvement in a cell of 500m with users dropped

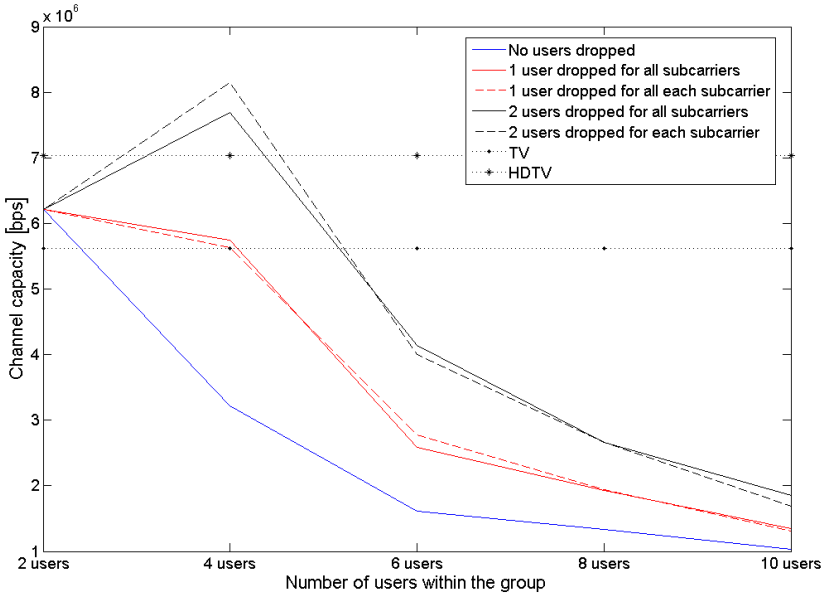

Figure 5.29: Channel capacity in a cell of 800m with users dropped

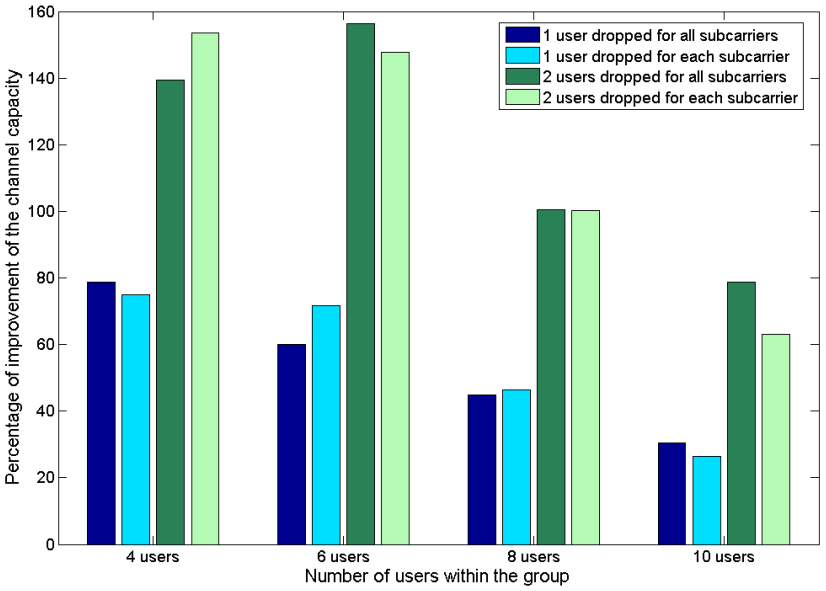

Figure 5.30: Percentage of the channel capacity improvement in a cell of 800m with users dropped

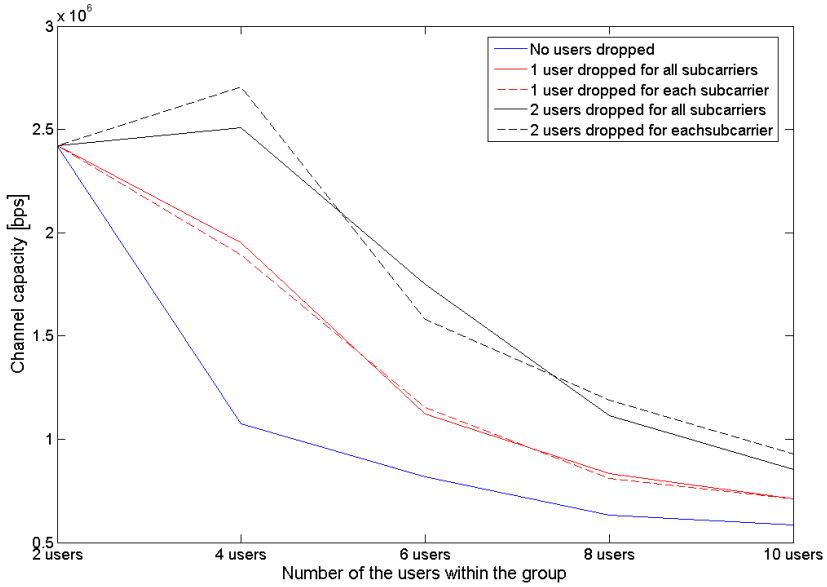

Figure 5.31: Channel capacity in a cell of 1400m with users dropped

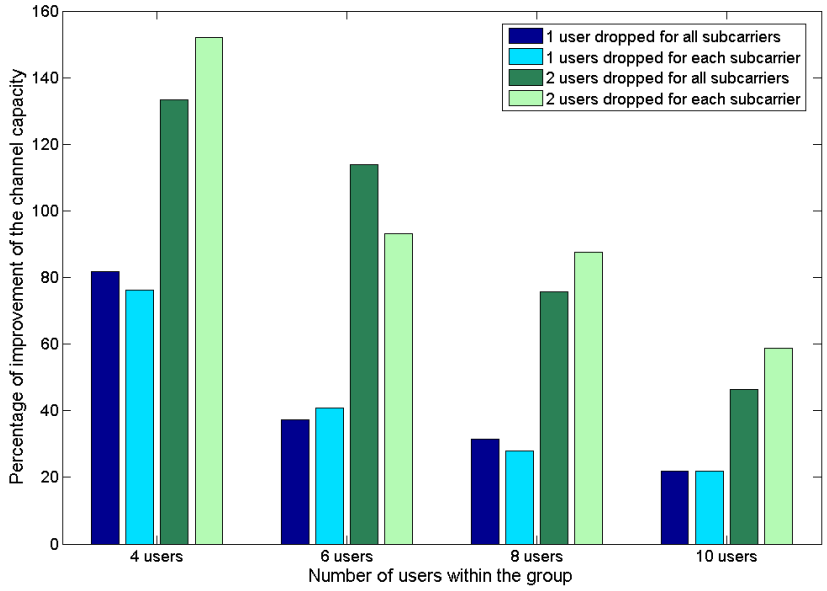

Figure 5.32: Percentage of the channel capacity improvement in a cell of 1400m with users dropped

It is apparent that to drop the worst users is increasing the efficiency of the system. Moreover dropping some users on each of the subcarriers or for all the subcarriers leads to quite the same results. Indeed it is usual situation that the user in the worst condition is the one in the worst conditions for all the subcarriers. Thus to make the results clearer further on in the report only the

case of the dropping for all the subcarriers will be considered.

Two main factors influence the improvement introduced by dropping users:

- **the size of the cell**. Indeed for a large cell size there is more probability to obtain users in bad conditions. Those users are the ones that have the most negative contribution to the channel capacity of the group. Furthermore for a large cell size, due to the nature of the path loss, the users in the worst conditions will likely be achieve a lower SNR than the users in the worst conditions in a smaller cell size. Thus the absolute improvement by dropping users in large cells is smaller then in small cells as shown in figures 5.27, 5.29 and 5.31. However the relative improvement is better for a small cell size.

- **the group size**. As a matter of fact the more users are part of a group the more possible it is to obtain a user in bad conditions. Moreover as explained in appendix 5.1.1 the efficiency of the *max-min* algorithm depends on the group size. Thus for an increasing group of users the absolute efficiency of dropping users is decreasing as shown in figures 5.28, 5.30 and 5.32.

An interesting result to study the impact of dropping users and the size of the cells on the channel capacity is to look at the Cdf of the channel capacity calculated on the minimum SNR within the group (equation 3.5).

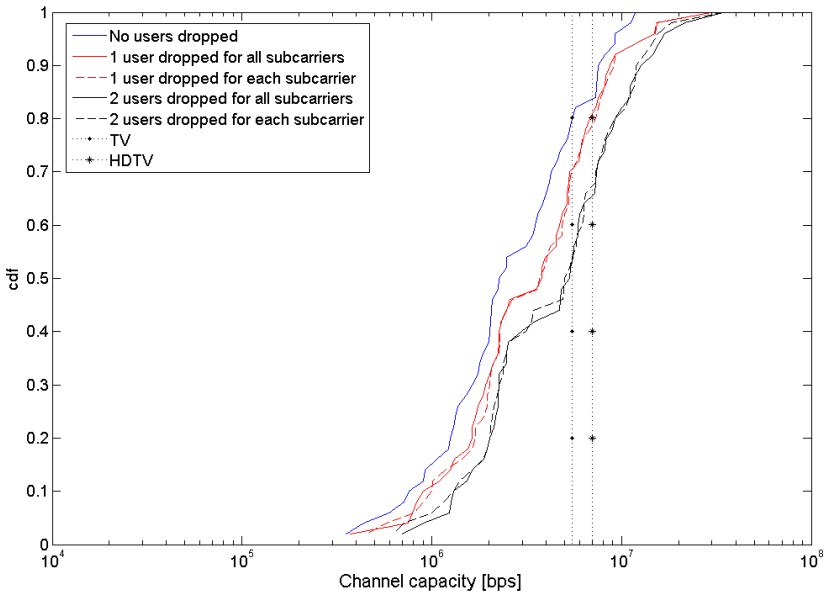

Figure 5.33: Cdf of the channel capacity with users dropped for a cell of 500m

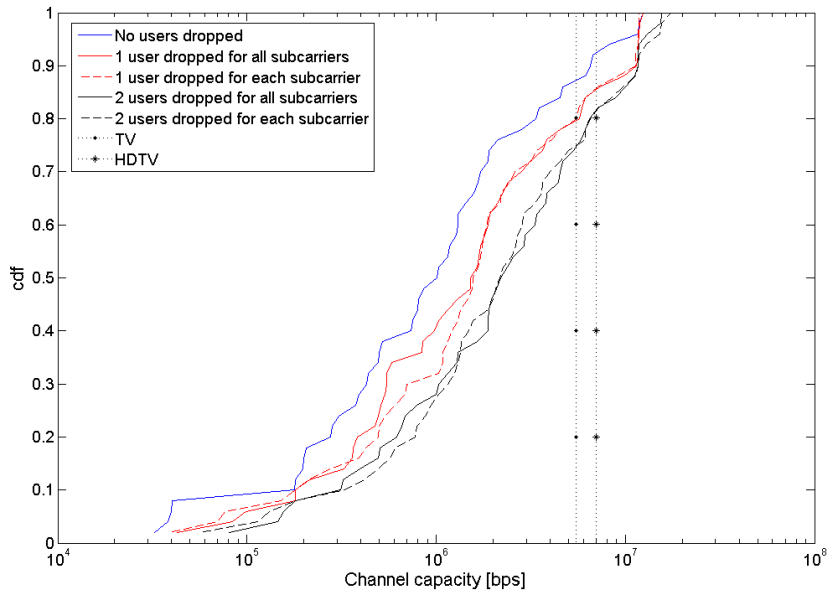

Figure 5.34: Cdf of the channel capacity with users dropped for a cell of 800m

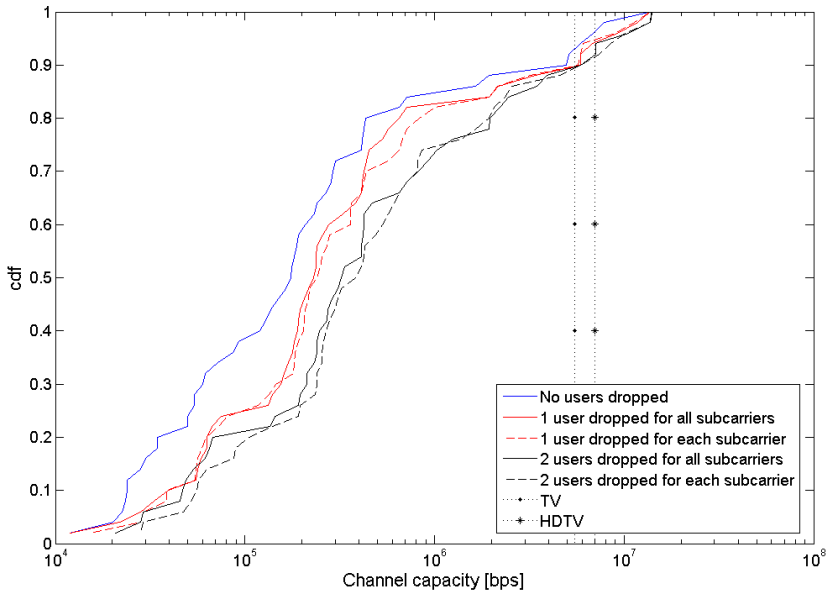

Figure 5.35: Cdf of the channel capacity with users dropped for a cell of 1400m

For the same reasons previously developed, it is clear that to drop some users permits to achieve a better channel capacity with higher probability. As shown in figure 5.33, for a cell size of 500m, dropping 2 users before applying the *max-min* algorithm, increases the probability to reach the necessary channel capacity for TV and HDTV by around 20%. This is one of the significant improvement coming out from our project proposal.

Furthermore the figures 5.33, 5.34 and 5.35 show that the efficiency of dropping users takes place at different channel capacity level depending on the cell size. Indeed as represented in picture 5.35, to drop some users in a cell of 1400m permits to achieve a better efficiency for a low channel capacity (around 20% of improvement around 0.1 Mbps and around 5% of improvement around 4 Mbps). Also as represented in picture 5.33, to drop some users in a cell of 500m permits to achieve a better efficiency for a high channel capacity (around 8% of improvement around 1 Mbps and around 17% of improvement around 10 Mbps). As previously explained this is due to the fact that for a large cell size there is, in our system, more probability to obtain users in bad conditions within a group.

5.4.1 Discussion

Dropping a user of a multimedia application influences his/her perception of the QoS. Two cases can be discussed:

- the user is never served. As soon as the user requests the application, if the BS declines the possibility to serve it based on its instantaneous SNR, the user is dropped from the multicast group. Since the user never has access to this application, he/she does not really suffer in term of QoS.
- the user is intermittently dropped from the application. During the transmission of the application to the user, due to the evolution of the SNR, the BS periodically drops the user from its services. Since the user is dropped sporadically it is rather annoying and thus the QoS of the user is decreasing.

Solutions to guarantee the QoS for the users can be:

- dropping the user from the multicast group at the beginning of the transmission. However due to the erratic behavior of our environment, the user can be in a good situation to receive the data the moment just after being dropped *e.g.* if the user is going trough a tunnel or stepping out of a basement. Thus this solution is not fair for the dropped user.
- changing the coding scheme across several frames at the BS to guarantee a certain QoS. Indeed based on the delay between the received packets it is possible to define a certain delay outage. Based on this outage the BS will change the coding scheme to guarantee the QoS of the user. This is more fair for the users dropped. However the BS equipments needs to take into account this adaptive coding scheme. This proposed solution implied interleaving and adaptive modulation and coding (AMC). However using this solution does not permit to reach the achievable throughput [38].

- multicast automatic repeat request (ARQ) can also be an alternative to the dropping problem. The idea of ARQ is that the BS, based on feedback from users regarding successfully received transmissions, adapts code weights for data packet linear combinations that are then sent. Each user exploits its previously received information in decoding the linearly combined packets [39]. This technique permits to achieve a higher throughput and increase the probability of a correct reception.

Based on this discussion it is possible to see that to drop users is possible while achieving a respectable QoS. Nonetheless an outage for the delay between the received packets need to be defined. Furthermore the BS equipments need to be adjust to this QoS requirements.

5.5 Comparison of the beamforming and MIMO results

In order to define which technique is better for multicast services, it is necessary to compare the results obtained by beamforming and MIMO techniques. Referring to the distributions of figures 5.13 and 5.20 it is easily possible to notice that the best performance is achieved by the MIMO techniques. Indeed the median values of the minimum SNR within a group for the beamforming *max-min* algorithm is $-8dB$. Whereas for the same analysis the MIMO 4x1 is achieving $2dB$; and for the MIMO 2x2, which implies the implementation of another antenna at the MS, it achieves almost $10dB$.

As a conclusion we can state that the MIMO techniques are achieving better performance for multicast services based on the results obtained from the analyzed beamforming and MIMO techniques. However this conclusion depends of the following fundamental parameters:

- **Group size:** it has been proved that the group size influences the performance of the algorithms. For the beamforming techniques, the group size is taken into account for the computation. Thus we noticed that the performance of the algorithms is decreasing while the group size is increasing. On the other hand for the MIMO techniques, the analysis shows us that they are achieving a good performance for a larger group of users.
- **Cell size:** as well as for the group size, the cell size has a different on the analyzed technologies. For the beamforming techniques, while the absolute achieved performance of the techniques are decreasing with an increasing cell size; the relative performance have a different behavior for the different techniques. Indeed the MIMO is performing better for a larger cell size whereas the relative performance of the beamforming are not changing with different cell sizes.
- **MS design:** the best MIMO technique, which is always better than the beamforming ones, is the 2x2. But this technique implies a radical change on the MS design by adding another antenna in the mobile station. This is an important for the manufacturer of mobile devices.

Chapter 6

Conclusion and future work

This project analyzed some beamforming and MIMO multicast solutions for Mobile WiMAX in order to increase the efficiency of the connection between a BS and a group of mobile users. Indeed nowadays an increasing number of users want to be able to access to multimedia applications while still using wireless mobility and this requires a high data rate connection. In order to optimize the wireless connection between BS and a group of MSs several beamforming and MIMO techniques have been investigated.

This report dealt with the 4G technology, which can be defined as the total convergence of wireless mobile and wireless access communications that permits to handle multimedia applications. The chosen 4G technology investigated had been the Mobile WiMAX. Basically this is a multi-carrier transmission technology which is using OFDM. Those two main characteristics permit to achieve a better performance while using the same bandwidth. Furthermore this technology is suitable to wireless multicast which permits to deliver the same data to a selected group of users. Using different algorithms for beamforming and MIMO it is possible to optimize the connection from the BS to the group of users in terms of requested QoS.

For the beamforming solution, the simulations started from the literature's proposed algorithms developed for the multicast services. First we checked the behavior of the algorithms and their respective influence on the performance of the group for a narrowband system. Afterward we applied the same algorithms developed for a narrowband channel to our wideband time varying channel. We noticed that the behavior of the algorithms simulated are the same for our model. Also that the existing *max-min* algorithm, which is maximizing the lowest SNR within a group, is achieving the best performance among the analyzed solutions.

For the MIMO solution, it is important to highlight that the implemented solutions does not require any computation at the BS side. The BS is only sending symbols following a certain procedure and the computation is made at the MS using the received symbols. It is possible to see that the various MIMO techniques discussed permit to achieve a better performance within the group. However it is necessary to discuss the price of such a device. Indeed implementing a second antenna in a MS, as needed for the MIMO 2×2, is a consequential

increase in the production cost. Moreover, the product cost is also raised by the need of microchip able to analyze the received symbols.

We also investigated the effect of the cell size on the possible achieved performances. It is important to note that the absolute improvement by dropping users in large cells is smaller than dropping users in small cells. Whereas the relative improvement of dropping users is better for a small cell size. Then the difference between using complete CSI and partial CSI have been investigated. We found out that the use of partial CSI, *i.e.* basing the optimization only on the pilot subcarriers, is a way to avoid the congestion of the feedback at the BS side while decreasing by a not significant percentage the overall efficiency. Finally, in order to achieve better performance from a group point of view, we proposed to drop some of the users that are in the worst conditions. The cases for one and two users have been investigated and the results show that this method permits to increase noticeably the group performance. However, in this case, it is necessary to take into account while design the BS the guarantee of the users' QoS *e.g.* AMC or ARQ.

As a conclusion it is possible to say that using solution as beamforming and MIMO for multicast services, it is possible to optimize the connection between a BS and a group of users. The choice of the technique depends on several parameters as cell size, group size or MS design as stated in the previous chapter.

6.1 Future work

This section will present the possible future works and field of investigations that can be further analyzed based on this project.

6.1.1 Discussion on the effect of the channel model

One of the possible system configuration not analyzed in this report, is the case of different taps delay in the channel model. The SUI-model analyzed (SUI-4 model) has its worst case of tap delay to be equal to 4 μs. The more delayed one, SUI-6 model, has its maximum delay at 20 μs. This channel model can cause frequency selective fading which produces inter-symbol interference at the receiver side. It's easy to understand why by looking at section 2.2.3 and comparing the values of taps delay with the guard interval of the WiMAX standard (table 2.4).

6.1.2 Channel interpolation based on the pilots

It is possible from the known pilots to apply interpolation methods. Those methods permit to derive the estimation of the channel knowledge at the data subcarriers positions [40]. Several methods have been investigated such as linear interpolation [41]. Those methods will not be developed further in this report. Nevertheless a basic description of pilot based linear interpolation will be explained in this section.

The first interpolation method is to obtain the values of the data subcarriers by taking them along the line formed by the two complex values from the surrounding pilot subcarriers. An example of such interpolation is shown in figure 6.1. P1 and P2 represent the pilot subcarriers. a, b, c, d represent the data subcarriers.

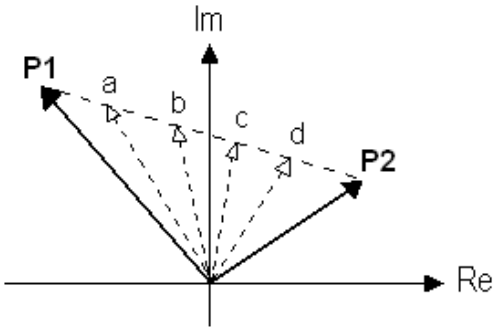

Figure 6.1: Interpolation based on a line between the pilots

Another method of interpolation which brings more accurate results is, instead of forming a line between the pilots, to form an arc between the pilot. The radius of this arc is interpolated based on the complex values of the pilots. An example of such interpolation is shown in figure 6.2. P1' and P2' represent the pilot subcarriers. a', b', c', d' represent the data subcarriers.

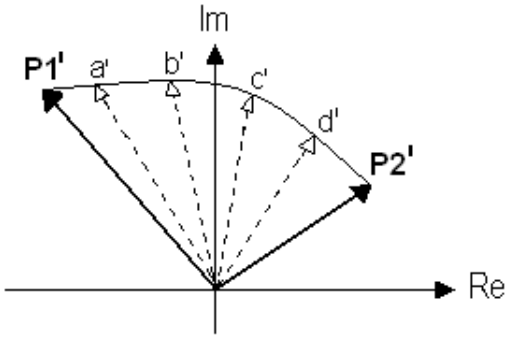

Figure 6.2: Interpolation based on an arc between the pilots

THIS PAGE IS INTENTIONALLY LEFT BLANK

Appendix A

OFDM

A.1 Mathematical approach

This section describes the mathematical aspect of OFDM. This approach is based on [42].

An OFDM signal consists of N orthogonal subcarriers modulated by N parallel data streams. Each baseband subcarrier can be expressed as

$$\phi_k(t) = e^{j2\pi f_k t} \tag{A.1}$$

with f_k the frequency of the k^{th} subcarrier. Without a cyclic prefix, one baseband OFDM symbol multiplexes N modulated carriers, thus is of the form

$$s(t) = \frac{1}{\sqrt{N}} \sum_{k=0}^{N-1} x_k \phi_k(t), \qquad 0 < t < NT_s \tag{A.2}$$

where x_k is the k^{th} complex data symbol, issued from a PSK or QAM modulation, and NT_s is the length of the OFDM symbol. The subcarrier frequencies f_k are equally spaced

$$f_k = \frac{k}{NT_s}$$

which provides orthogonality to the subcarriers $\phi_k(t)$ on $0 < t < NT_s$. The sampling in T_s of the in-phase and quadrature components of the OFDM leads to

$$s(nT) = \frac{1}{\sqrt{N}} \sum_{k=0}^{N-1} x_k e^{j2\pi \frac{nk}{N}}, \qquad 0 \leq t \leq N-1 \tag{A.3}$$

which is the inverse discrete Fourier transform (IDFT) of the constellation symbols x_k. The IDFT is typically implemented with an inverse fast Fourier transform (IFFT). The main difference between the IDFT and the IFFT is the complexity of implementation. Indeed, the complexity of the IDFT algorithm is, considering N number of samples, in N^2; whereas in the IFFT algorithm, the complexity is in $N.log(N)$. Nevertheless, the number of samples for an IFFT as to be in the power of two.

Extending the OFDM signal of equation A.2 over a period T_g *i.e.* adding the cyclic prefix, leads to

$$s(t) = \frac{1}{\sqrt{N}} \sum_{k=0}^{N-1} x_k e^{j2\pi f_k t}, \qquad -T_g < t < NT_s \tag{A.4}$$

After emission, the signal passes trough a channel which is modeled by a finite length impulse response limited to the interval $[0, \tau_{max}]$. If, as developed in A.2, the length of the cyclic prefix T_g is chosen such that $t_g > \tau_{max}$; the received OFDM symbol evaluated on the interval $[0, NT_s]$ is

$$r(t) = s(t) * h(t) + n_c(t) = \frac{1}{\sqrt{N}} \sum_{k=0}^{N-1} H_k x_k e^{j2\pi f_k t} + n_c(t), \qquad 0 < t < NT_s \tag{A.5}$$

with $n_c(t)$ is an additive white Gaussian noise (AWGN) due to the propagation through the channel and H_k is the Fourier transform of $h(t)$ evaluated at the frequency f_k. It is interesting to notice that, within this interval, the received signal is similar to the original signal except that $H_k x_k$ modulates the k^{th} subcarrier instead of x_k. Thus the cyclic prefix preserves the orthogonality of the subcarriers.

The OFDM signal can be demodulated taking a fast fourier transform (FFT) of the sampled data over the interval $[0, NT]$, ignoring the received signal before and after $0 < t \leq NT_s$. This leads to the following expression

$$y_k = H_k x_k + n_k, \qquad k = 0, ..., N-1, \tag{A.6}$$

where n_k is the FFT of the sampled noise terms $n_c(nT)$, $n = 0, ..., N-1$.

A.2 Basics

This section will investigate further the system structure, the advantages and disadvantages of OFDM technology.

A.2.1 OFDM signal design

Some parameters, such as the number of subcarriers N or the length of the cyclic prefix T_g, are very important in the design of an efficient OFDM system and are subjected to some restrictions.

Firstly, as stated in A.2, the cyclic prefix should be chosen to be greater than the maximum delay spread of the channel τ_{max}. At the same time, it should be a very small fraction of the OFDM symbol to minimize the loss of the signal energy *i.e.* $NT_s >> \tau_{max}$. If the bandwidth of the system is taken as $B \approx 1/T_s$, the condition presented can be applied to the number of subcarriers $N >> \tau_{max} B$.

If the OFDM symbol length NT_s is too long, the Doppler spreading can cause ICI and thus limite the performance of the system. Choosing the intercarrier spacing $1/NT_s$ much larger than the maximum Doppler frequency f_d, *i.e.* $f_d << 1/NT_s$ or $N << B/f_d$, allows us to avoid this problem.

A.2.2 OFDM transceiver system

As shown in figure A.1, the OFDM transceiver includes an *Error correction code* and an *Interleaver* part. Adding those parts permit to obtain more robustness on the signal transmitted. This topic will be developed further in the next section.

The next part consists of the *mapping* of the coded bit stream. Either phase shift keying (PSK) or quadrature amplitude modulation (QAM) is typically employed. After this part, the data is still serial and represented in complex numbers.

After mapping ,the serial data streams is converted to N parallel data streams. These N streams are then modulated onto N subcarriers using an *IFFT* of size N. After the IFFT, the *cyclic prefix* is inserted to every block of data. After the insertion, the transformed data are grouped again. Finally, after being summed, the digital data is converted to analog signals.

The OFDM signal get through the channel where it is subject to all sorts of fading and interference. After the reception, the signal is down-converted and carrier frequency synchronized. Then it is is convert to digital domain using an *Analog to Digital Converter*. This data is then demodulated using a *FFT*. Then the data streams are converted to serial data which are thereafter demodulated. Finally, the data get through a decoder and an interleaver which permits to recover the original bit stream.

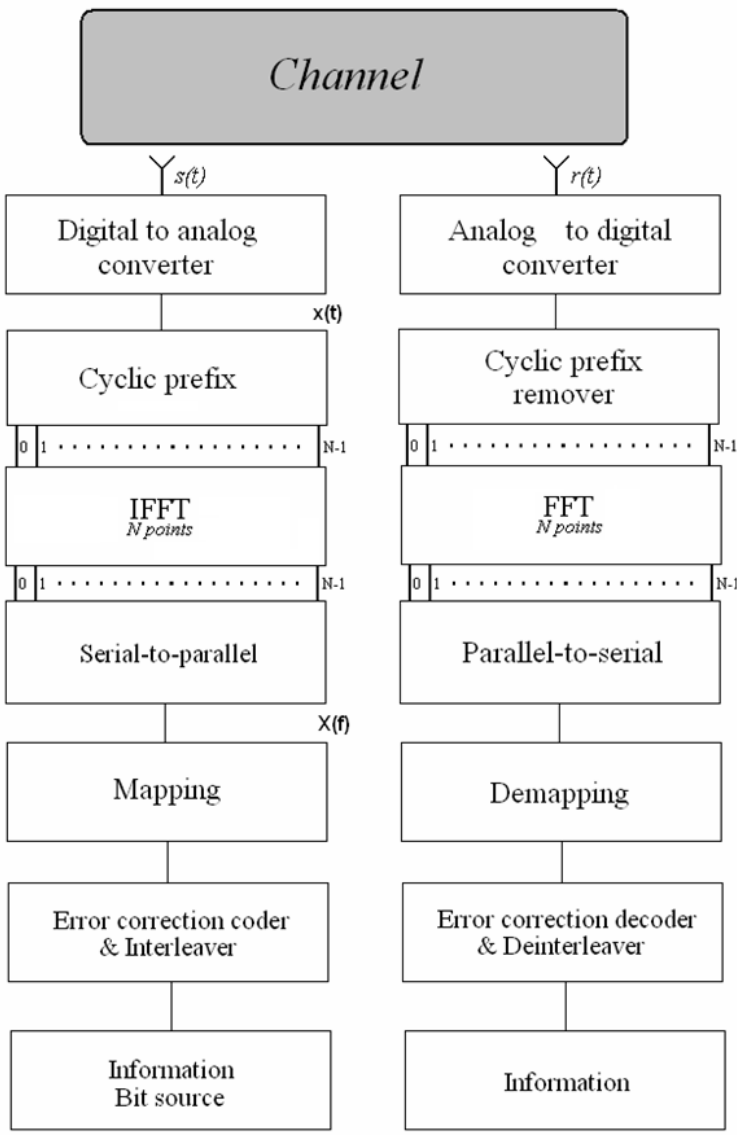

Figure A.1: OFDM system model

A.2.3 Orthogonality of carriers

The most important condition which differentiates OFDM from classic FDM is the orthogonality of carriers. Mathematically two functions $f(x)$ and $g(x)$ are said to be orthogonal in the period $[a, b]$ if

$$\int_a^b f(x)g^*(x)dx = 0 \tag{A.7}$$

OFDM carriers are sinusoidal so by considering two sinusoidal functions $e^{\frac{j2\pi mt}{T}}$ and $e^{\frac{j2\pi nt}{T}}$ the orthogonality property can be expressed as

$$\frac{1}{T}\int_0^T (e^{\frac{j2\pi mt}{T}})^*(e^{\frac{j2\pi nt}{T}})dt = \frac{1}{T}\int_0^T e^{\frac{j2\pi(n-m)t}{T}} = \delta_{mn} \tag{A.8}$$

with δ the Kronecker delta.

It permits to demonstrate that all harmonics of a sinusoid of frequency $f = 1/T$ are orthogonal to each other. This is the basic property of OFDM signals.

The **advantages** of the orthogonality are:

- high spectral efficiency near the Nyquist rate,
- efficient modulator and demodulator implementation using FFT algorithm (see section A.1),
- low cost of implementation of FFT components.

The **disadvantages** of the orthogonality are:

- very accurate frequency synchronization between transmitter and receiver is required,
- very sensitive to frequency shift (as Doppler effect).

A.2.4 Error correction coding and interleaving

OFDM uses a large number of narrow band subcarriers *i.e.* the subcarriers do not exceed the channel's coherence bandwidth and suffer from flat fading. It means that all the frequencies components of the signal will experience the same magnitude of fading. Because of this fading, it is common to use forward error coding (FEC) to protect the data transmitted on the various subcarriers. The modulation scheme is then referred to as coded OFDM (COFDM). The most common error correction coding used in COFDM is convolutional coding and the usual error control decoder is based on the Viterbi algorithm. This channel coding permits to obtain robustness again burst errors.

It is possible to also use frequency and/or time interleaving. Frequency interleaving is to make sure there is enough space, in term of frequency, between adjacent data. It permits to limit the risk of errors on consecutive bits by spreading the errors in the bit stream presented to the error correction decoder. Time interleaving is the same process, in term of time.

By using those two techniques, it is possible to obtain a more robust transmission and, as a consequence, achieve a smaller BER.

A.2.5 Guard interval and cyclic prefix

Another key principle in OFDM is the guard interval. Since the duration of each symbol is long, it is possible to insert a guard interval between the OFDM

symbols. This permits to eliminate ISI. A technique developed is consisting in adding a guard interval *i.e.* an empty space between two OFDM symbols as shown on picture A.2. The guard interval T_g must be chosen to be greater than the expected value of the delay spread τ_{max} *i.e.* $T_g > \tau_{max}$. As precise in 2.3.1, if $T_g < \tau_{max}$ symbols would suffer of ISI.

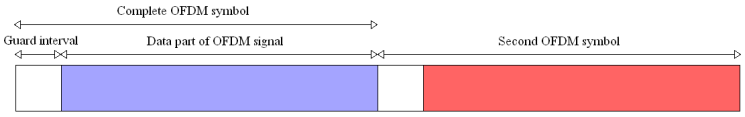

Figure A.2: OFDM symbol with guard interval

Figure A.3 shown an example of a signal with empty guard interval. This empty interval introduces inter carrier interferences (ICI). The lost of orthogonality of different subcarriers, due to time variation of the channel or loss of periodicity of the signal, results in power leakage among the subcarriers which is know as ICI [43].

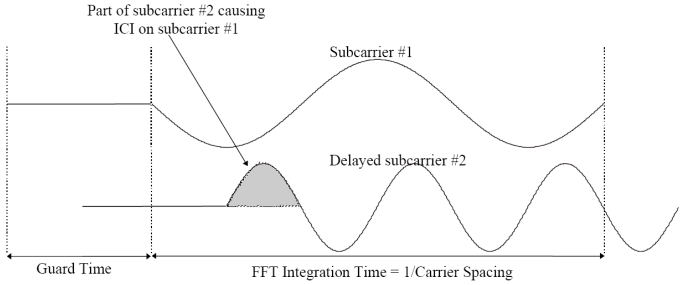

Figure A.3: Guard interval [11]

Figure A.4 (a), with no delay spread subcarriers are not suffering from ICI. In figure A.4 (b), it is possible to notice that the power of the subcarrier #2 at frequency f_1 is not null, which leads to interference on the subcarrier #1, which is ICI as defined previously.

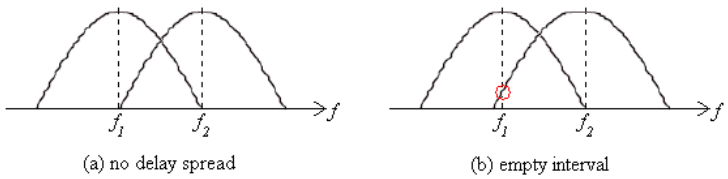

Figure A.4: Signal without empty guard interval (a) and with empty guard interval (b)

A way to avoid the ICI induced by the guard time is the cyclic prefix (CP).

The CP consists of the end of the OFDM symbol copied into the guard interval in front of the transmitted OFDM symbol. The reason that the end of the OFDM symbol is copied is to ensure that the receiver will integrate over an integer number of sinusoid cycles for each multipath when it performs OFDM demodulation with the FFT. Indeed after a Fourier transform all the resultant components of the original signal are orthogonal to each other. So, by keeping the periodicity of the signal, it is possible to make sure that all the subcarriers are orthogonal to each other. It is important to notice that the CP must be larger than the delay spread to ensure that the orthogonality is kept.

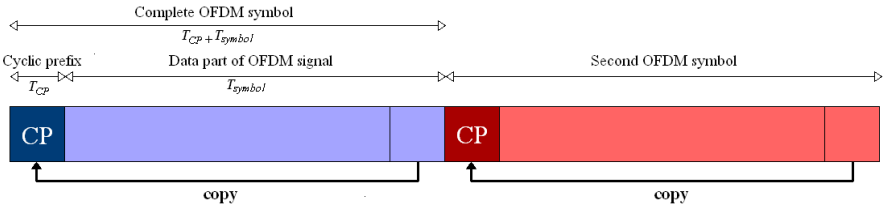

Figure A.5: OFDM symbol with cyclic prefix

Inserting a CP leads to a loss of the signal energy which is expressed as

$$SNR_{lossduetoCP} = -10log_{10}\left(1 - \frac{T_g}{T_s}\right) \tag{A.9}$$

with T_g the interval length of CP and T_s the OFDM symbol duration.[44]

Thus the CP permits to maintain the orthogonality between each of the subcarriers which permits to remove the ICI. But due to the use of some bandwidth to transmit a CP which did not contain any relevant information, an energy loss occurs. Nevertheless this loss is not so significant and permits to obtain the advantages described before.

A.2.6 Peak to average power ratio

According to [45], considering the block of data of length N, the number of subcarriers, as a vector, is $\mathbf{X}= [X_0, X_1, ..., X_{N-1}]^T$. Each symbol in $\mathbf{X}$ modulates one of a set of subcarriers, $f_n, n = 0, 1, ..., N-1$ and the duration of a symbol X_n in $\mathbf{X}$ is T_s. The N subcarriers are chosen to be orthogonal *i.e.* $f_n = n\Delta f$ with $\Delta f = \frac{1}{NT_s}$ and NT_s the duration of an OFDM data block $\mathbf{X}$. The complex envelope of the transmitted OFDM signal is given by

$$x(t) = \frac{1}{\sqrt{N}} \sum_{n=0}^{N-1} X_n e^{j2\pi f_n t}, 0 \leq t < NT_s \tag{A.10}$$

The peak to average power ratio (PAPR) of the transmitted signal expressed before is defined as

$$PAPR = \frac{\max\limits_{0 \leq t < NT_s} |x(t)|^2}{1/NT_s \cdot \int_0^{NT_s} |x(t)|^2 dt} \tag{A.11}$$

For the transmitted OFDM signal, this is one of the most important disadvantages. Indeed when the signals of all the subcarriers are constructively added, the peak power can be the product of number of subcarriers and the average power.

This factor leads to an increase in the complexity for the design of RF amplifier. In fact those amplifiers are really sensitive to high peaks of power and this often leads to their saturation. It also increases the complexity of the implementation of the digital-to-analog and analog-to-digital converters.

The techniques used most commonly to reduce the PAPR are Coding Techniques, Signal Distortion Techniques and Scrambling techniques. But this topic is not analyzed deeply within this report. More info can be found in the literature.

A.2.7 Bandwidth efficiency

Due to orthogonality of the carriers the guard band between each subcarrier is eliminated and brings to overlapping. This property permits to drastically improve the use of the bandwidth.

As shown in picture A.6 it is possible to compare normal FDM spectral efficiency to the one achieved with OFDM. Indeed in conventional multichannel system, the subchannels are separated by more than their two sided bandwidth; whereas, in an OFDM system, the subchannels are separated by half of their two sided bandwidth. A shown in picture A.7, it leads to a 50% overlap of adjacent channels.

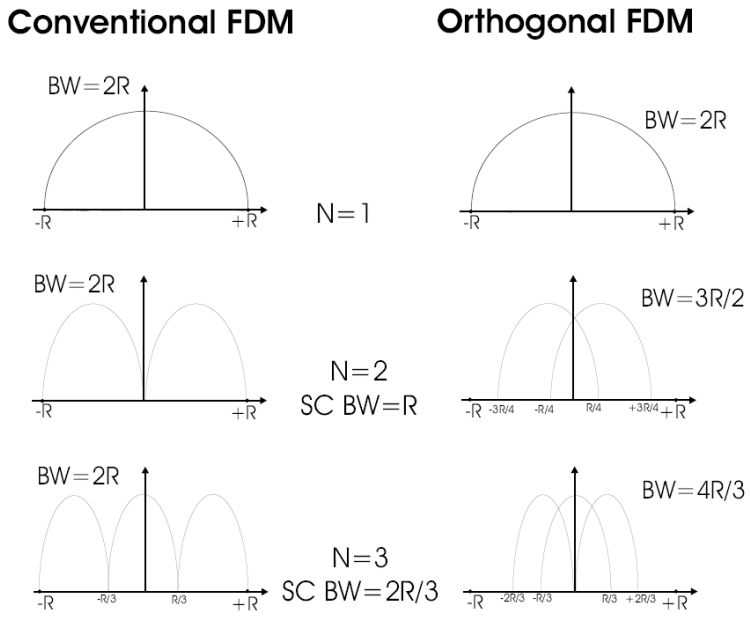

Figure A.6: Spectral efficiency [44]

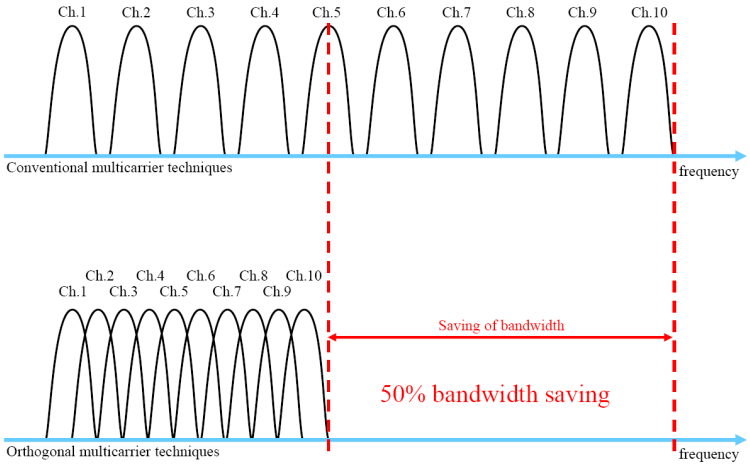

Figure A.7: Efficiency of OFDM versus FDM [44]

A.2.8 Synchronization in time and frequency

As shown in A.2 the subcarriers are spaced closer and closer in the frequency domain when the number of subcarriers is increasing. Thus to obtain an efficient demodulation at the receiver a strict synchronization is needed. This is a very critical topic of OFDM modulation.

Synchronization errors are divided in two topics:

- **frequency synchronization:** subcarrier frequency offset error between the transmitter and the receiver could cause some confusion in the OFDM reception. The main reasons are the channel Doppler shift and the frequency difference between the transmitter and the receiver. This scenario is shown in figure A.8. Figure A.8(a) shows the sampling frequency of the subcarrier f_n at the maximum frequency rate, resulting in a maximum signal amplitude and no ISI. If the frequency reference of the receiver is offset with respect to that of the transmitter by a frequency error of δf, then the received symbols suffer from ISI, as shown in figure A.8(b) [46]. For a normal Gaussian channel, the carrier frequency offset must be under 2% of the inter-carrier distance [47].

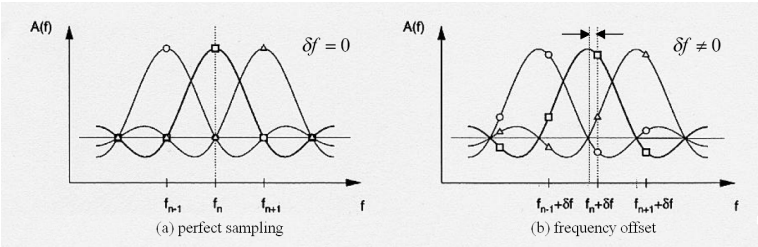

Figure A.8: Frequency synchronization [48]

- **timing synchronization:** the timing error could cause some problem to detect the beginning of a symbol. This is an important topic for the DFT used for the demodulation of the OFDM signal. It is also important to find the sampling clock frequency. Indeed it is important to estimate the frequency offset at the receiver to identify the start frame and the FFT window position for each OFDM.

It is also possible to divide the OFDM synchronization into data-aided and non-data-aided categories. The data-aided category uses a training sequence or some pilots symbols for the estimation which is very accurate. The non-data-aided categorie often uses the cyclic prefix correlation.

Appendix B

Test of the channel model

As described in section 4.3.1 the channel model used in this report is the SUI-Model. This model is used in order to calculate path-loss, shadowing and small scale fading within the scenario.

B.1 Path-loss

The first confirmation that the path-loss calculation is right, is coming from the plot of the calculated path-loss over a logarithmic distance. When plotting the path-loss on a logarithmic scale, based on the equation 4.30, the result is expected to be linear because of the path-loss behavior.

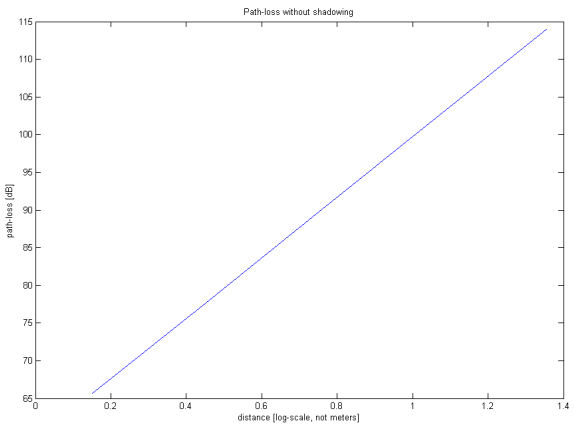

Figure B.1: Path-loss over log(d)

Figure B.1 shows that the behavior of the path-loss is as it was suppose to be: linear.

B.2 Shadowing

A test for the channel model is the analysis of path-loss and shadowing for a user moving on a circle around the BS. Because of its dependence on the distance, the path-loss calculated over a circle around the BS it is suppose to be constant. As shown in figure B.4 the pure path-loss is the same for all the users. However due to the nature of the shadowing, the values of the path-loss including the shadowing are different for the various users.

The following pictures show the shadowing map in figure B.2, the position of one single user moving 10 times around the BS in figure B.3, and its path-loss with and without the shadowing calculation in figure B.4.

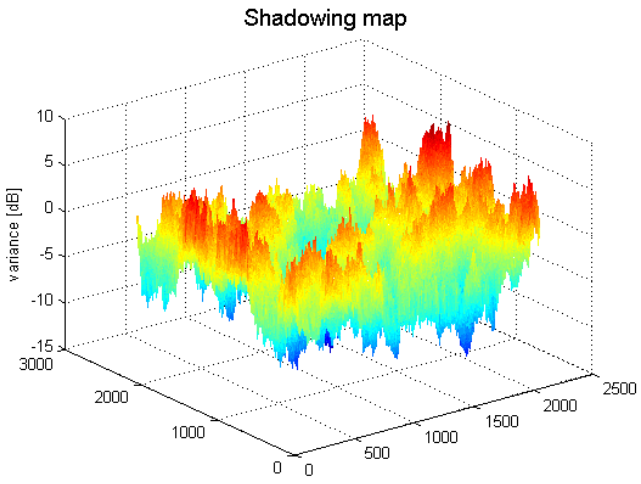

Figure B.2: Shadowing map

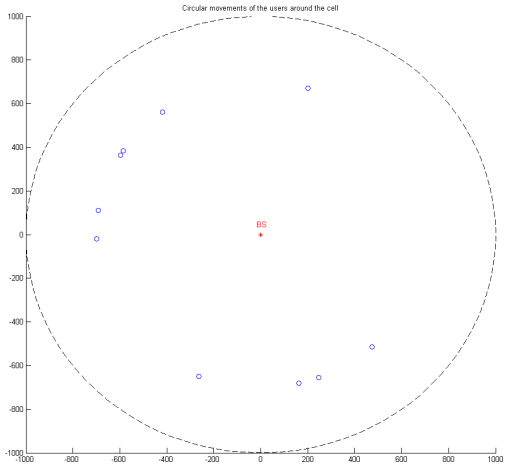

Figure B.3: User movements around the Base Station

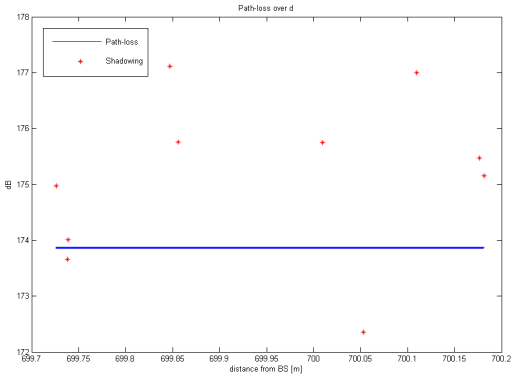

Figure B.4: Path-loss and shadowing calculation

B.3 Path-loss and shadowing

The next step is the simulation of the channel model plotting the variation of the path-loss with and without shadowing for a user moving from the Base Station to the cell's edge.

It is possible to see that there is a small variation between the two lines and this variation is coming from the analysis of the shadowing map. The shadowing map used for the simulation has 2050x2050 points and, in the picture, it is covering a cell with radius of 1000 meters. Further simulation will see different radius for the cell while keeping the same size for the shadowing map. This will lead to different approximations of the shadowing map where in the worst case almost 1 meter is the approximation for every single shadowing position.

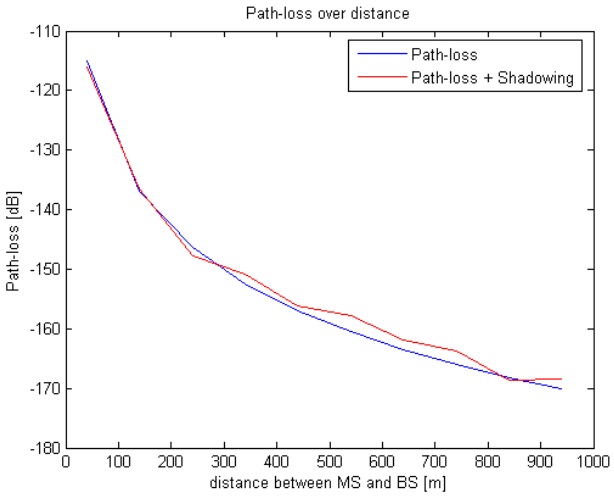

Figure B.5: Path-loss with and without shadowing

Anyway, the shadowing component is very small compared with the pure path-loss calculation therefore the main characteristic which changes a lot the value of channel gain is easily associated in the distance between MB and BS. The analysis will be then divided among different cell sizes in order to cover a larger number of scenarios.

The Cdf of the SNR of the path-loss and shadowing among users in a cell has been analyzed. The result in picture B.6 shows how the different cell size raises the SNR for the entire amount of users. The analysis has been done over a total number of 200users among 20 different cells having the same shadowing map but different sizes (500m and 1400m). The pictures shows an increase of the median SNR by almost 20dB for the same coverage of user's condition.

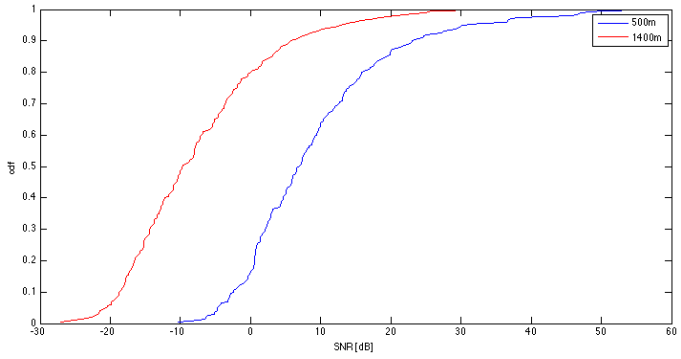

Figure B.6: Cdf of the SNR among different cell sizes

Appendix C

Different shadowing maps comparison

In order to analyze the influence of the shadowing map on the results of the model, the simulations have been computed in different shadowing maps and the results have been compared. Figure C.1 shows an example of a shadowing map used for those simulations. Those comparison have been made on 10 initial user placements in each shadowing map.

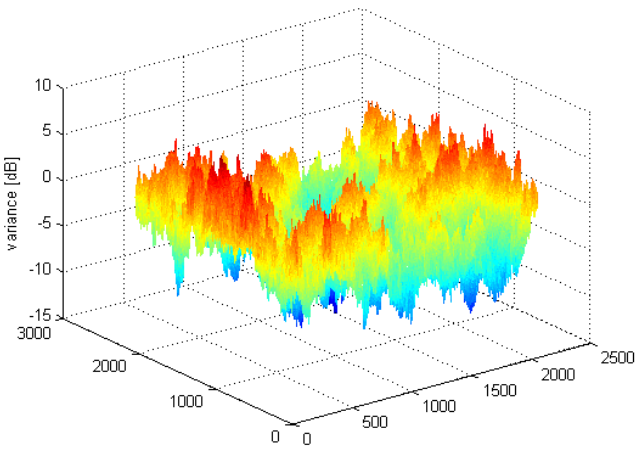

Figure C.1: Shadowing map

As a result, and to not show again all the results of chapter 5, only the Cdf of the channel capacity will be presented as a comparison in this section.

Figure C.2, as presented in section 5.4, shows the Cdf for the channel capacity for a cell of 500m. This result is based on a single shadowing map.

Using a different shadowing map and computing the results with the ones obtained with the previous shadowing map, we obtain figure C.3.

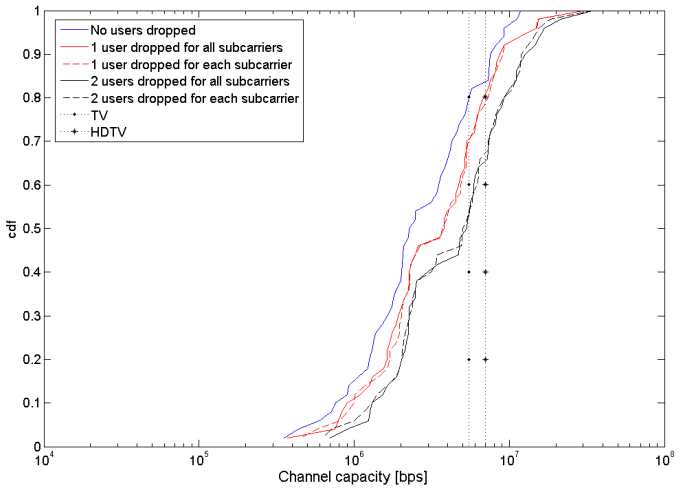

Figure C.2: Cdf of the channel capacity for a cell of 500m with results from a single shadowing map

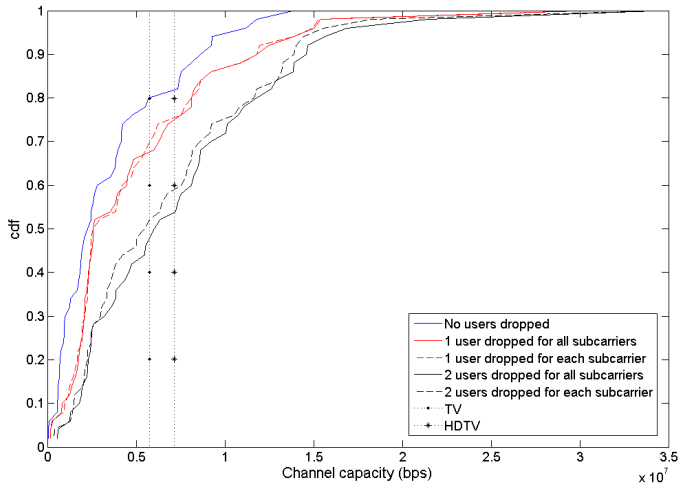

Figure C.3: Cdf of the channel capacity for a cell of 500m with results from two shadowing maps

It is possible to notice that the results are really close to each other. Thus working with a single shadowing map should be appropriate for the entire simulations.

It is important to highlight the fact that the most representative plot has been chosen. Other parameters and results have been compared and also found to be very similar.

Appendix D

Mobility Model

The mobility model can be divided in three parts: the initialization of the users, the movement and the bouncing of the users.

D.1 Initialization

In order to obtain a uniform distribution over the circular cell, it is necessary to follow a specific distribution. Assuming that the spatial user density is uniform and equal to ρ, the initial position as a function of the distance r between the user and the BS and a uniformly distributed angle φ. The distributions can be written as

$$p(r) = \int_0^{2\pi} \rho r d\varphi = 2\pi\rho r, p(\varphi) = \frac{1}{2\pi} \tag{D.1}$$

Figure D.2 shows an example of the initialization of the positions of 100 users for a cell size of 1000 meters. Figure D.1 shows the cumulative distribution function of the user distance from the cell center.

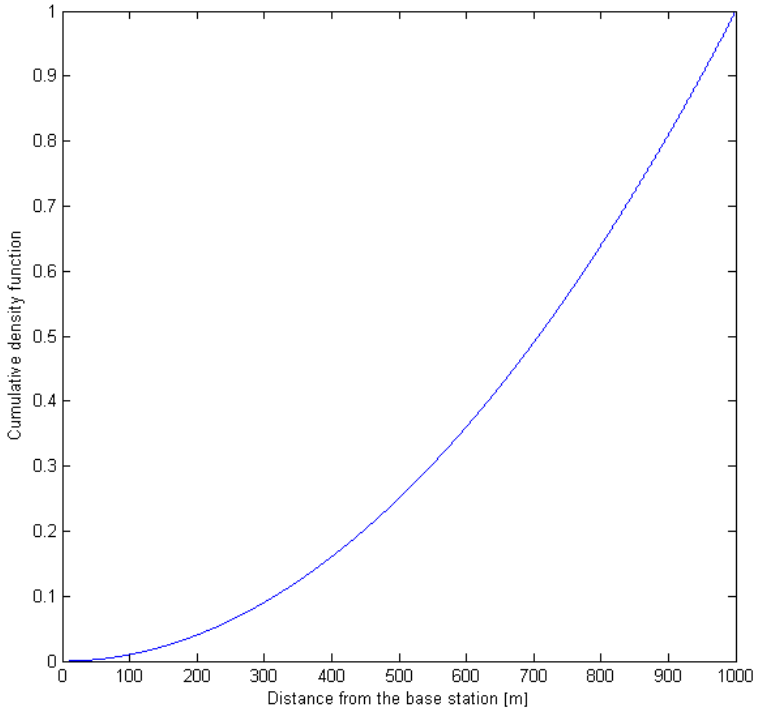

Figure D.1: Cdf of the users' initial positions

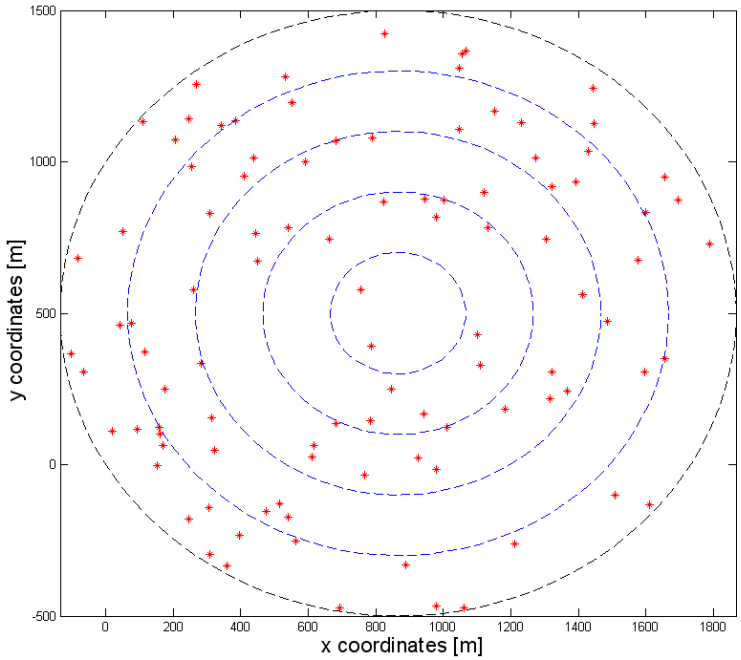

Figure D.2: Users position initialization

D.2 Movement

The users are moving in a smooth line with a constant velocity in order to keep a realistic correlation for the Doppler spectrum between the several movements. The movement section is based on a specific velocity and angle for each user. The initial angle determines the direction of movement. In order to obtain a movement that is not strictly linear it is necessary to add an angle at every movements. The value of this angle is taken between $\pm\frac{\pi}{36}$ radians. The mean velocity of the users is taken equal to $1.36m.s^{-1}$. A movement for 10 users and 100 repetitions is shown in figure D.3.

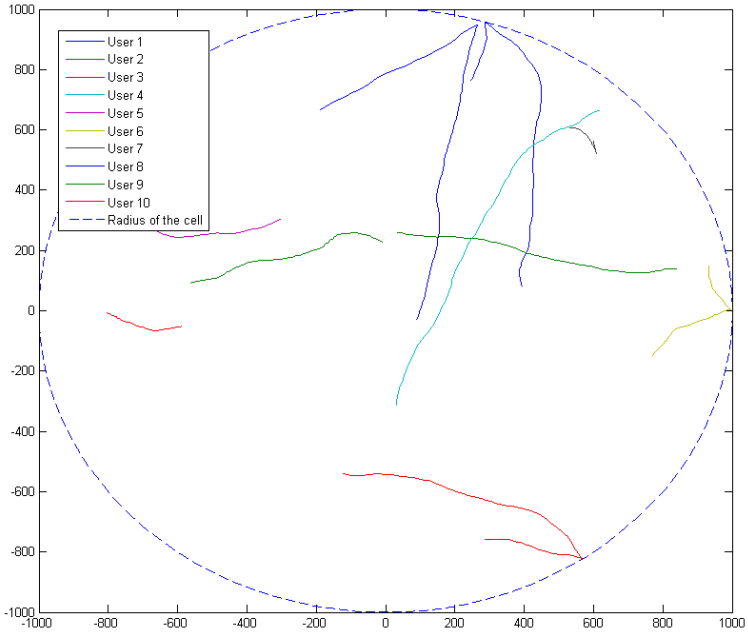

Figure D.3: Users moving around the cell

D.3 Bouncing

The analyzed scenario is based on a single cell network. To keep the same amount of users within the cell during the simulation it is necessary to limit the movements of the users inside the cell. To do so a bouncing function has been created which permits, for users trying to cross the edge of the cell, to bounce them back within the cell area. Such a bouncing on the edge case is shown in picture D.4 for 2 users. This figure is a zoomed in user 1 and 8 of the edge of figure D.3.

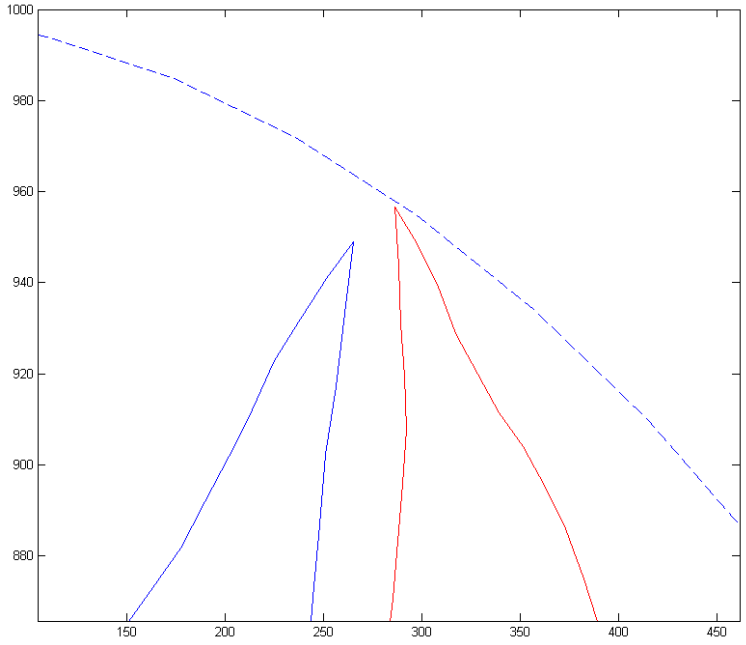

Figure D.4: Bouncing on the edge of the cell

Appendix E

Glossary

3GPP	Third Generation Partnership Project
4G	Fourth-Generation Communications System
AF	Array Factor
AMC	Adaptive Modulation and Coding
ARQ	Automatic Repeat request
AWGN	Additive White Gaussian Noise
bps	bits per second
BS	Base Station
CBT	Core-Based Tree
Cdf	Cumulative Distribution Function
CDMA	Code Division Multiple Access (CDMA)
COFDM	Coded Orthogonal Frequency Division Multiplexing
CP	Cyclic Prefix
DVB	Digital Video Broadcasting
EDGE	Enhanced Data rates for Global Evolution
FDM	Frequency Division Multiplexing
FDMA	Frequency Division Multiple Access
FEC	Forward Error Coding
FFT	Fast Fourier Transform
GPRS	General Packet Radio Service
GSM	Global System for Mobile communications

ICI	Inter Carrier Interference
IDFT	Inverse Discrete Fourier Transform
IEEE	Institute of Electrical and Electronics Engineers
IFFT	Inverse Fast Fourier Transform
IGMP	Internet Group Management Protocol
ISI	Inter-Symbol Interference
LOS	Line-of-sight,
MANET	Mobile Ad-hoc NETwork
MIMO	Multiple Input Multiple Output
MS	Mobile Station
OFDM	Orthogonal Frequency Division Multiplexing
OFDMA	Orthogonal Frequency Division Multiple Access
PAPR	Peak to Average Power Ratio
PIT-SM	Protocol Independent Multicast-Sparse Mode
PSK	Phase Shift Keying
QAM	Quadrature Amplitude Modulation
QoS	Quality of Service
RMS	Root Mean Square
RSVP	Resource reservation Protocol
SDP	SemiDefined Programming
sOFDMA	Scalable Orthogonal Frequency Division Multiple Access
SUI	Stanford University Interim
TDMA	Time Division Multiple Access
UMTS	Universal Mobile Telecommunications System
USMF	User Selective Matched Filter
WiMAX	Worldwide Interoperability for Microwave Access

Bibliography

[1] Willie W.Lu Bernhard H. Walke Xuemin Shen. *4G Mobile Communications: Toward Open Wireless Architecture*. www.IEEExplore.com, 1999.

[2] Wikipedia. *4G*. http://en.wikipedia.org.

[3] *Evolution of the Mobile Technology*. http://www.buzzle.com/editorials/.

[4] Dipl. Ing. Ralf Dieter Wölfle. *Ausbreitungs-Modellrechnungen*. 2007. Eletrosmoginfo1of2.pdf.

[5] Mahmood M. Zonoozi and Prem Dassanayake. *Shadow Fading in Mobile Radio Channel*. IEEE, 1996.

[6] J.D. Parsons. *The Mobile Radio Propagation Channel*. Second Edition.

[7] Amoroso F. *The Bandwidth of Digital Data Signals*. November 1980. IEEE Communications Magazine.

[8] Paolo Barsocchi. *Channel Models For Terresterial Wireless Communications: A Survey*. National Research Council.

[9] Tom Henderson. *The Physics Classroom Tutorial*. 1996-2007. Lesson 3: Behavior of waves.

[10] M. Jankiraman. 2002.

[11] Muhammad Imadur Rahman. *Fundamentals of multi-carrier (OFDM) systems*. Department of Electronics Systems, Fall 2007. Aalborg University.

[12] G.Gong. *Multicarrier Modulation and OFDM*. E&CE 411, Spring 2006. Handout 4.

[13] Joseph C. Pasquale and George C. Polyzos. *The Multimedia Multicasting Problem*. ACM Multimedia Systems, 1998.

[14] Upkar Varshney. *Multicast Over Wireless Networks*.

[15] Dr M.P.Sebastian M.Phani Vijaya Krishna. *HMAODV: History aware on Multicast Ad Hoc On Demand Distance Vector Routing*.

[16] Praveen Kumar and Heshan El Gamal. *On The Throughput-Delay Tradeoff in Cellular Multicast*. IEEE, 2005.

[17] Constantine A. Balanis. *Antennas theory - Analysis and design*. John Wiley and sons, Inc., 1997. Second edition.

[18] Benjamin Friedlander. *Using MIMO to Increase the Range of Wireless Systems*. IEEE, 2005.

[19] George Lawton. *Is MIMO the future of wireless communications*. Technology news, 2004.

[20] Helmut Bolcskei. *MIMO-OFDM Wireless Systems*. ETH Zurich, August 2006.

[21] *IEEE 802.16*. Wikipedia, 2007.

[22] *WiMAX Physical Layer*. Tutorial Point. www.tutorialspoint.com/wimax/wimax_physical_layer.htm.

[23] *Channel Models for Fixed Wireless Applications*. IEEE 802.16 Broadband Wireless Access Working Group, 2003-06-27.

[24] *Mobile WiMAX Part I: A Technical Overview and Performance Evaluation*. WiMAX forum. www.wimaxforum.org/news/downloads/Mobile_WiMAX_Part1_Overview_and_Performance.pdf.

[25] Kardi Teknomo. *Microscopic Pedestrian Flow Characteristics: Development of an Image Processing Data Collection and Simulation Model*. Department of Human Social Information Sciences, Graduate School of Information Science, 2002. Ph.D. Dissertation.

[26] Egon Schulz. *Real-Time Experiments with a Scalable MIMO-OFDM Air-Interface - Outdoor Measurements in Typical Urban Environments*. 2007. Special seminar in Ålborg University.

[27] Nihar Jindal and Zhi-Quan Luo. *Capacity Limits of Multiple Antenna Multicast*. IEEE.

[28] Daniel V.P. Figueiredo, Nicolas Marchetti Muhammad Imadur Rahman, Marcos D. Katz Frank H.P. Fitzek, Youngkwon Cho, and Ramjee Prasad. *Transmit Diversity Vs Beamforming for Multi-User OFDM Systems*. Ålborg University, 2004.

[29] Yuri C.B. Silva and Anja Klein. *Adaptive Beamforming and Spatial Multiplexing of Unicast and Multicast services*. 17th IEEE International Symposium on Personal, Indoor and Mobile Radio Communications, 2006.

[30] Yuri C.B. Silva and Anja Klein. *Downlink Beamforming and SINR Balancing for the Simulataneous Provision of Unicast/Multicast services*. Dramstadt University of Technology, Commuications Engineering Lab, July 2007.

[31] J. F. Sturn. *Using SeDuMi 1.02, a MATLAB toolbox for optimization over symmetric cones*. Optim. Meth. Softw, 1999. vol. 11-12, pp. 625-653.

[32] Timothy N. Dividson Nicholas D. Sidiropoulos and Shi-Quan (Tom) Luo. *Transmit Beamforming for Physical-Layer Multicasting*. IEEE, 2006. 1053-587X.

[33] C.F. Mecklenbrauker M. Rupp. *On Extended Alamouti Schemes for Space-Time Coding*. IEEE, 2002.

[34] WiMAX Forum. *WiMAX's technology for LOS and NLOS environments*. WiMAX Forum. Main contributors: Eugene Crozier and Allan Klein.

[35] Mahmood M; Zonoozi and Prem Dassanayake. *Shadow fading in mobile radio channel*. Mobile communcations and signal processing group, Departement of Electrical & Electronic Engineering, Victoria University of Technology, 1996.

[36] I-Kang Fu, David Chen Wandy C. Wong, Mike Hart, and Peter Wang. *Path-Loss and shadow fading models for IEEE 802.16j relay task group*. IEEE, 18/07/2006.

[37] V. Erceg L.J. Greenstein, S. Ghassemzadeh and D.G. Michelson. *Ricean K-factors in narrowband fixed wireless channels: Theory, experiments and statistical models*. WPMC' 99 Conference Proceedings, September 1999. Amsterdam.

[38] Sebastian Caban Christian Mehlführer and Markus Rupp. *Experimental Evaluation of Adaptive Modulation and Coding in MIMO WiMAX with Limited Feedback*. Hidawi Publishing Coporation - EURASIP Journal on Advances in Signal Processing, 2008. Volume 2008, Article ID 837102.

[39] Peter Larsson. *Multicast Multiuser ARQ*. IEEE, 2008. 1525-3511/09.

[40] Wu-Sheng Lu Xiaodai Dong and Anthony C.K. Soong. *Linear Interpolation in Pilot Symbol Assisted Channel Estimation for OFDM*. IEEE, 2007. 1536-1276/07.

[41] Meng-Han Hsieh and Che-Ho Wei. *Channel estimation for OFDM systems based on comb-type pilot arrangement in frequency selective fading channels*. IEEE, 1998. 0098-3063/98.

[42] S.K. Wilson J.J. van de Beek, P. Ödling and P.O. Börjesson. *Orthogonal Frequency-Division Multiplexing (OFDM)*.

[43] John G. Proakis Tiejun Ronald Wang and James R. Zeidler. *Techniques for Supression of Intercarrier Interference in OFDM Systems*. IEEE, 2005. ISBN 0-7803-8966-2.

[44] Frank H.P. Fitzek Muhammad Imadur Rahman, Suvra Skhar Das. *Center for TeleInFrastruktur (CTiF)*. Department of Electronics Systems, 18 February 2005. ISBN 87-90834-43-7.

[45] Seung Hee Han and Jae Hong Lee. *Peak-to-Average Power Ratio Reduction of an OFDM Signal by Signal Set Expansion*. Seoul National University.

[46] Lei Wei and Christian Schlegel. *Synchonization Requirements for Multi-user OFDM on satellite Mobile and Two-path Rayleigh Fading Channels*. IEEE Transacitons on communications, April 1995. Vol. 43 No. 2/3/4.

[47] Paul H. Moose. *A Technique for Orthogonal Frequency Division Multiplexing Frequency Offset Correction*. IEEE Transacitons on communications, October 1994. Vol. 42 No. 10.

[48] L. Hanzo and T. Keller. *OFDM and MC-CDMA - A Primer*. IEEE, 2006. ISBN-13 978-0-470-03007-3.

[49] E. Lawrey. *Multiuser OFDM*. Fifth International Symposium on Signal Processing and its Applications, 1999.

[50] Cheong Yui wong, Khaled Ben Letaif Roger S. Cheng, and Ross D. Murch. *Multiuser OFDM with Adaptive Subcarrier, Bit, and Power Allocation*. IEEE Transacitons on communications, 1999. 0733-8716/99.

[51] Dr. A. Reza Hedayat, Karthik Rangarajan Li Guo, Paul Sergeant Dr. Hang Jin, and Sai Subramanian. *Smart WIMAX - Delivering personal broadband*. Navini, July 2007.

[52] Per Lehne and Magne Pettersen. *An Overview Of Smart Antenna Technology For Mobile Communications Systems*. IEEE, Fourth Quarter 1999. vol. 2 no. 4.

[53] M.D. Trott A. Narula, M.J. Lopez and G.W. Wornell. *Efficient use of side information in multiple-antenna data transmission over fading channels*. IEEE JSAC, Oct. 1998. Vol. 16, pp. 1423-1436.

[54] Timothy Neame Milosh Ivanovich, Jonathan Li, Jackson Yin, and Paul Fritzpatrick. *GPRS data traffic modeling*. Telstra resarch laboraties, 0. 23.pdf.

List of Figures

THIS PAGE IS INTENTIONALLY LEFT BLANK

List of Tables